Publication No. U-1658

INTERIM REPORT

ON

FACSIMILE AND ACCELEROMETER

SYSTEMS INTEGRATION STUDY

TASK I

OF

JPL CONTRACT LC-950267

15 MAY 1962

AERONUTRONIC DIVISION
FORD MOTOR COMPANY

CONTENTS

CONTENTS (Continued)

CONTENTS (Continued)

INTRODUCTION

Aeronutronic Publication No. 10162(U), dated 5 February, 1962, describes the general features of two lunar vehicles capable of returning detailed data from the lunar surface at an early date using the Ranger delivery system. The first of these vehicles is a Facsimile System, or Lunar Surface Photoreconnaissance Capsule (LSPC), intended to reproduce on earth a photograph showing in fine detail a panoramic view of the lunar landscape. The second vehicle is an Accelerometer System, or Lunar Surface Measurement Capsule (SURMEC), intended to measure directly the lunar surface strength characteristics at a number of dispersed points on the surface.

Task I of JPL Letter Contract No. 950267 authorizes Aeronutronic to perform a Systems Integration Study of these two systems. This interim report presents, for each capsule, sections covering Mission Objectives and Design Criteria, System Design Characteristics and Restraints, and a brief discussion of analytical and design effort on system tradeoffs.

The sections on Mission Objectives and Design Criteria provide ground rules, guidelines, and definitions of the general design philosophy; they also establish an order of priority among competing criteria. The material includes only design criteria that have been established at least on a preliminary basis, rather than a discussion of alternate methods.

The sections on Design Characteristics and Restraints explain in general terms how the design objectives will be met, and in sufficient detail that functions of the systems and subsystems

can be identified. All design restraints are covered in these sections, such as those resulting from the vehicle, packaging, environment, and scientific experiments.

FACSIMILE SYSTEM (LSPC)

MISSION OBJECTIVES AND DESIGN CRITERIA

1.0 INTRODUCTION

The primary purpose of the Lunar Surface Photoreconnaissance Capsule (LSPC) is to obtain high-resolution facsimile pictures of the lunar surface at the earliest possible date. The systems and techniques developed in the first five Ranger flights will be fully utilized in meeting this objective.

It will be a design objective to require no changes in the Ranger RA-3, 4, 5 system for delivering a lunar landing sphere. The landing sphere itself shall utilize Ranger components and techniques wherever applicable.

Any margins in weight and volume will be employed to ensure the achievement of the primary objective of obtaining surface facsimile pictures.

2.0 MISSION OBJECTIVES

The LSPC lunar rough landing capsules are planned for a series of repeated attempts to acquire, process, and transmit to earth facsimile picture data corresponding to a portion of the lunar terrain surrounding the landing sphere assembly's resting place. This picture is to be taken from an elevation of a few feet above the lunar surface. The facsimile picture data shall be obtained (1) with sufficient quality and content that it materially contributes to the knowledge of lunar surface topography and texture, (2) with definition sufficient to aid in the design of manned lunar landing vehicles, and (3) at a date early enough to be effective in this design.

3.0 DESIGN CRITERIA

Design criteria applicable to the launch vehicle, spacecraft bus, and LSPC are described in the following subparagraphs.

3.1 Launch Vehicle and Spacecraft Bus Criteria

Other than mandatory engineering change orders resulting from RA-3, 4, 5 experience, no changes will be required for the LSPC mission on either the Atlas and Agena B boosters or the Ranger RA-3, 4, 5 spacecraft bus.

3.2 Capsule Assembly Criteria

The LSPC consists of a Landing Sphere Assembly, which impacts on the lunar surface, and a Retro System Assembly, which includes those subsystems necessary to slow the Landing Sphere Assembly to an acceptable impact velocity.

3.2.1 Retro System Assembly

Other than mandatory engineering change orders resulting from RA-3, 4, 5 experience, no changes will be required in the altimeter, spin motor, retro rocket motor and other subassemblies of the complete RA-3, 4, 5 retro system assembly.

3.2.2 Landing Sphere Assembly

Components and techniques developed for the RA-3, 4, 5 landing sphere assembly will be employed with minimum modification in the LSPC Landing Sphere Assembly wherever applicable. To make maximum use of previous work, the design of the optical scanning, sensing and data handling portions of the Landing Sphere Assembly will generally conform to the designs already developed during the feasibility study conducted under Contract N-21453, Task II.

3.2.2.1 Competing Characteristics. Competing characteristics shall be treated in the following order:

(a) Reliability of landing sphere operation on the lunar surface.

(b) Picture resolution and general quality.

(c) Schedule.

(d) Biological sterility.

(e) Ease of fabrication and producibility of system.

(f) Pre-flight checkout simplicity and shelf lifetime.

(g) Picture area coverage. Only that coverage in excess of a minimum requirement equivalent to two 90-degree azimuth sectors with 50-degree elevation scanning shall be considered to be a competing characteristic.

3.2.2.2 Defined Characteristics. Defined characteristics are as follows:

(a) Weight. The weight of the landing sphere assembly is fixed at 89.3 pounds by the selected trajectory and available launch vehicle performance and especially by the available impulse of the RA-3, 4, 5 retro motor. This design weight must be maintained to achieve maximum impact survival probability. If an excess design weight problem exists, the solution will be to reduce the extent of the picture area coverage. If the landed sphere with all of its desired components is underweight, additional steps to increase (1) the reliability of the mission, and (2) the calibration of distance in the picture will be considered the best uses of the additional weight allowance.

(b) Impact Environment. The RA-3, 4, 5 lunar impact environment specification (Master List of Environmental Requirements, Section II, Aeronutronic Publication No. U-902-1, dated 15 April 1961) shall be used for design purposes.

(c) Effect on Spacecraft Bus and Retro Assembly. The interfaces between the landing sphere assembly, the retro assembly, and the spacecraft bus shall remain as designated for RA-3, 4, 5.

3.2.2.3 Reliability Philosophy Affecting Design. Design techniques employed insofar as possible to achieve a high reliability shall include the following:

(a) Minimization of required functions.

(b) Simplification of functions.

(c) Use of proved components.

(d) Use of passive rather than active components.

(e) Arrangement of functions in parallel rather than in series.

(f) Minimization of dependence on lunar terrain.

(g) Redundancy.

After all elements of the system are adequately ruggedized, redundancy shall be employed to the extent permitted within the weight limitation.

3.2.2.4 Experimental Philosophy Affecting Design

(a) Pre-launch Environmental Control. The landing sphere assembly and its components shall not be subjected to environments beyond flight-acceptance levels, and the burden of protection from overexposure shall be on operators and facilities rather than on the landing sphere assembly itself. Clean, air-conditioned working areas, special handling fixture, air transport, electrical overload protection, and other such measures external to the landing sphere assembly shall be used to the extent practicable, and the landing sphere assembly design shall be based primarily on environments expected from the time of final mating onward through launching and flight. Wherever possible, biological sterility shall be achieved by external measures without the requirement for access into sealed components, so that the adverse effect of the sterility requirement on equipment design, reliability, and schedule is minimized.

(b) Operating Condition at Launch. The design criterion should be to attain a high mission reliability without dependence on checkout instrumentation, control, and

correction of deficiencies in the landing sphere assembly after completion of assembly. Subsystems must be designed to maintain full operating ability and to hold calibration from the time of assembly to flight. Provisions for checkout testing after completion of assembly of the landing sphere shall only be provided to the extent that they can be demonstrated to increase the net probability of success for the mission when the added complexity to provide checkout testing is considered.

(c) In-flight Failure Detection. Failure detection methods shall be employed only to the extent that they do not detract from the reliability of achieving the primary mission objective.

(d) Function After In-flight Failure. Interdependence between subsystems shall be minimized, but will necessarily exist to a large extent. The general design criterion is that no subsystem is required to function after failures of subsystems on which it depends, except where this can be achieved without complicating the design or diverting effort from the main objectives of the flight.

3.2.2.5 Test Philosophy Affecting Design

The objective is to obtain reliability by design rather than by extensive development. In general, designs shall not be compromised to accommodate testing. However, when subsystem acceptance tests are the only way of determining readiness for assembly and flight, the design must, of course, incorporate the necessary test provisions. Moreover, a test of the complete spacecraft assembly is considered essential to verify the compatibility between the capsule and the spacecraft bus.

In system tests, the purpose is primarily to simulate flight and lunar operation. The burden of simulation shall, as far as possible, fall on equipment external to the landing sphere assembly.

SYSTEM DESIGN CHARACTERISTICS

1.0 OPERATIONAL DESCRIPTION

The primary functional operations of the Lunar Surface Photoreconnaissance Capsule include terminal flight control, retro propulsion, semi-rough landing, survival, event sequencing, power supply, obtaining a facsimile picture of the moonscape in the vicinity of the landing site, electronic processing and transmission of the electrical facsimile signals to earth, thermal control, and mechanical support.

Upon receipt of a signal from the spacecraft bus at the terminal end of the flight, the altimeter is deployed and the thermal radiation shield retracted. When the altimeter detects that the spacecraft is at fuzing altitude, the retro motor and landing sphere assembly are freed from the bus. The solid propellant spin rocket motor imparts rotation about the longitudinal axis for attitude stabilization, followed by a retro impulse from the solid propellant retro rocket motor to reduce the descent velocity to zero at a specified altitude above the lunar surface. After retro rocket burnout, the spent motor case is separated from the landing sphere. To survive the semi-rough landing from the free fall, the instrument package (called the payload) is protected by an envelope of crushable shock-absorbing material capable of limiting the landing deceleration and absorbing the impact energy.

Subsequent to impact the spherical inner payload establishes its alignment with the local vertical. A porting mechanism produces a hole in the shell of the landing sphere through which the antenna is erected and a portion of the electrical/optical/mechanical facsimile system

is extended. The facsimile system then commences to view the surrounding lunar terrain through vertical scanning while slowly rotating in azimuth. The photo-facsimile data is transmitted in real time to earth until depletion of the capsule power supply.

2.0 CONFIGURATION DESCRIPTION (Figures 2-1 through 2-4)

An Atlas first-stage booster, Agena B second stage, and Ranger RA-3, 4, 5 spacecraft bus are utilized to deliver the LSPC. The basic configuration of the LSPC consists of the payload cushioned in a spherical impact limiter and mounted to the forward end of the solid propellant retro rocket motor, which in turn is mounted to the bus through the motor support structure. A cylindrical radiation shield of flexible laminated material surrounds this assembly. The spin rocket motor is attached to a plug rigidly supported in the retro nozzle throat, and the altimeter assembly is mounted on the top of the bus hexagonal frame. The capsule assembly is capped by the bus-controlled omnidirectional antenna.

Two separation clamps with appropriate explosive bolt cutters are to be used to temporarily bond equipment together. The upper one holds the landing sphere assembly to the retro motor, and in a small cavity located between these two is the power and sequencing assembly (P&SA) containing the pre-impact timing mechanism. The lower clamp binds the retro motor to the motor support structure. The motor support structure is attached to the top of the bus hexagonal frame and provides accurate bus/capsule alignment. Located around the periphery of the landing sphere/retro motor interface are damping devices which limit the motions produced by vibrational excitations. The lower end of the radiation shield is tied to the base of the retro support structure. The shield is held under tension by retractors attached to its opposite end. The altimeter and its support and deployment mechanism are located outside of, and at the base of, the shield envelope. The altimeter support structure is clamped firmly to the bus.

Within the impact limiter is the payload sphere suspended at neutral buoyancy in flotation fluid. The center of gravity of the sphere is located below the center of buoyancy so that after impact the payload erects and self-aligns with the local vertical. A caging mechanism is located on the bottom of the outside surface of the payload sphere. This cages the payload from the time of final assembly until retro braking

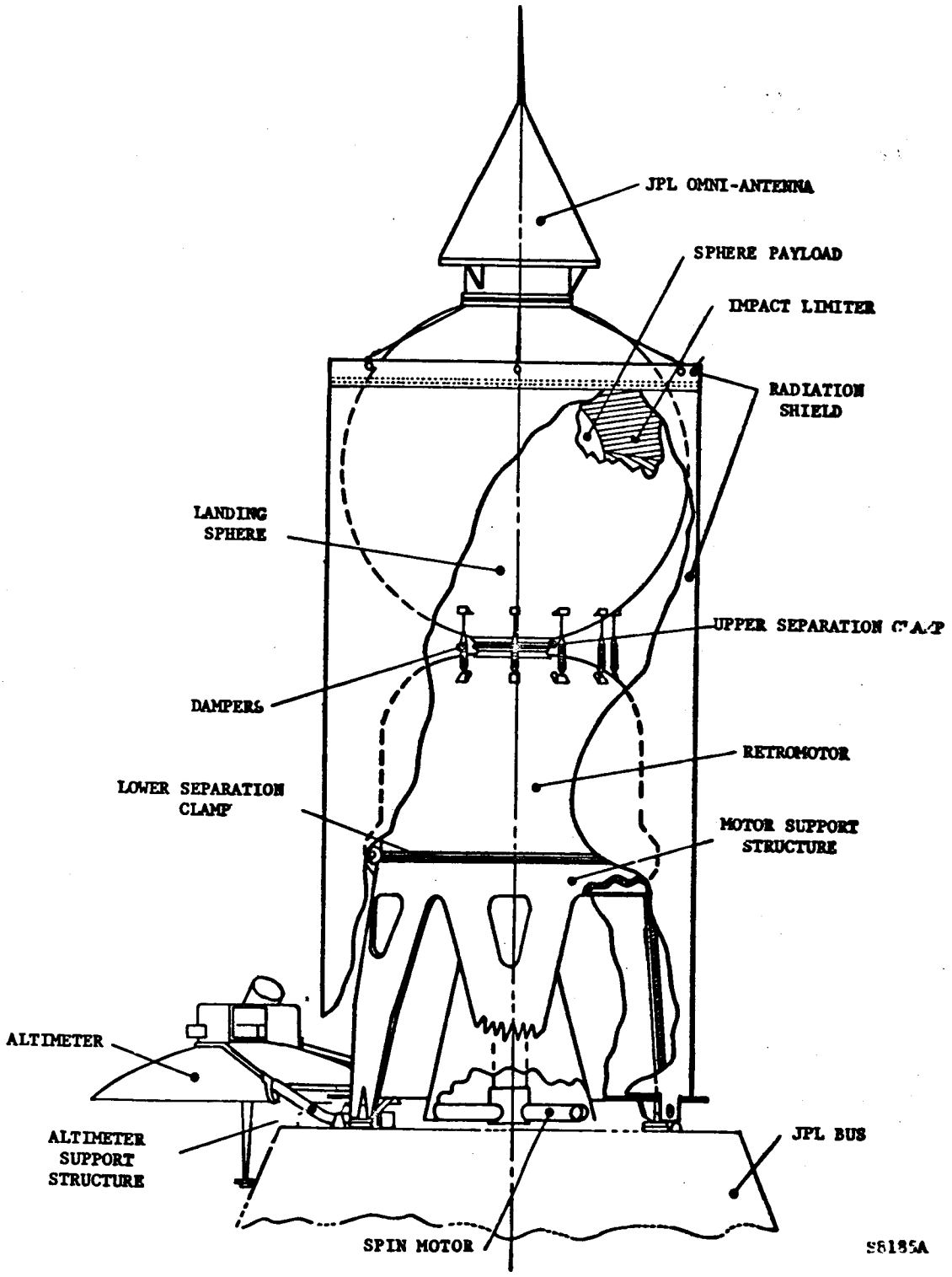

FIGURE 2-1. LUNAR SURFACE PHOTORECONNAISSANCE CAPSULE

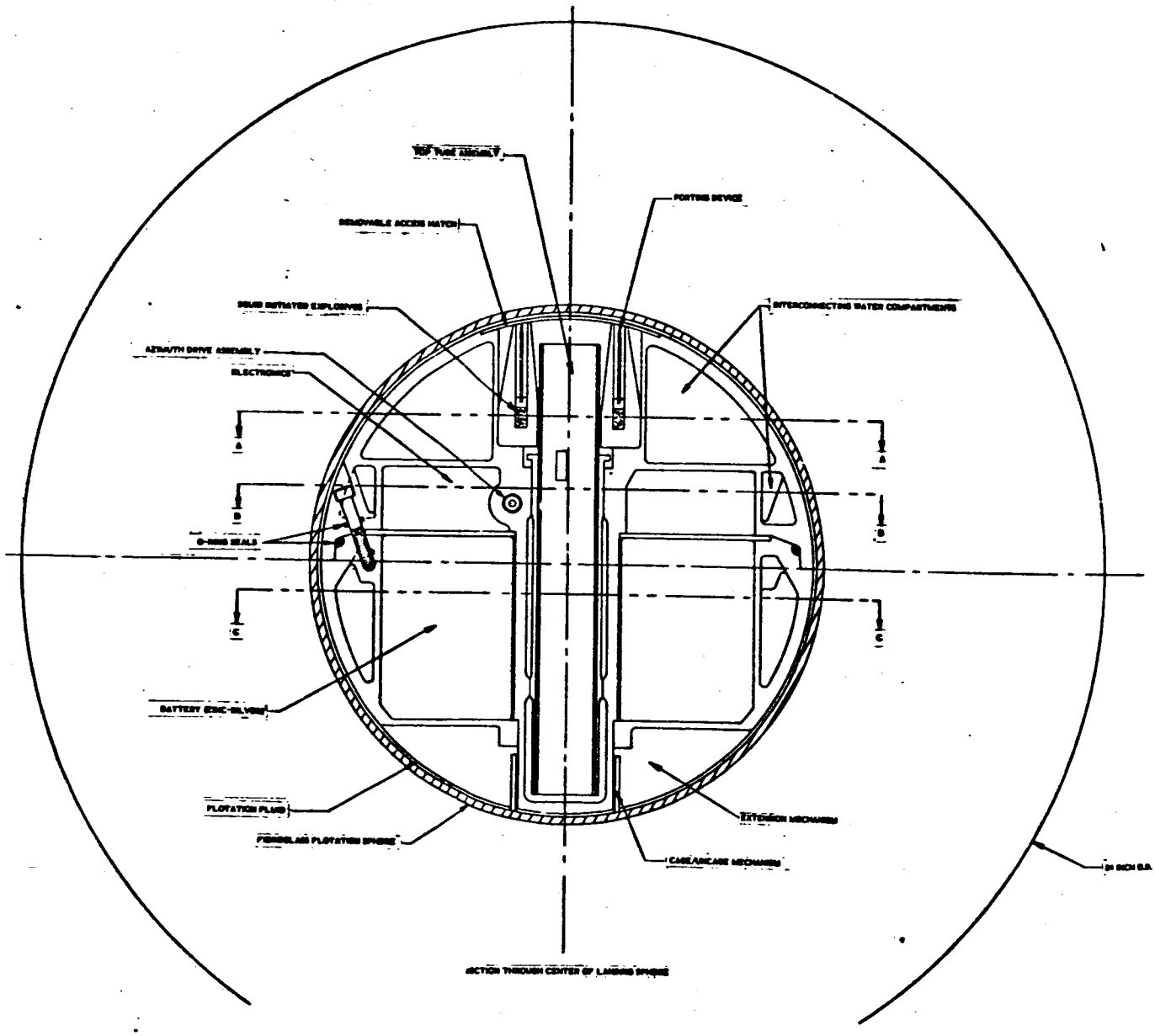
REMOVABLE ACCESS HATCH
PORTING DEVICE
INTERCONNECTING WATER COMPARTMENTS
AZIMUTH DRIVE ASSEMBLY
ELECTRONICS
A
B
C
O-RING SEALS
BATTERY (ZINC-SILVER)
FLOTATION FLUID
FIBERGLASS FLOTATION SPHERE
EXTENSION MECHANISM
CASE/ARCASE MECHANISM
SECTION THROUGH CENTER OF LANDING SPHERE

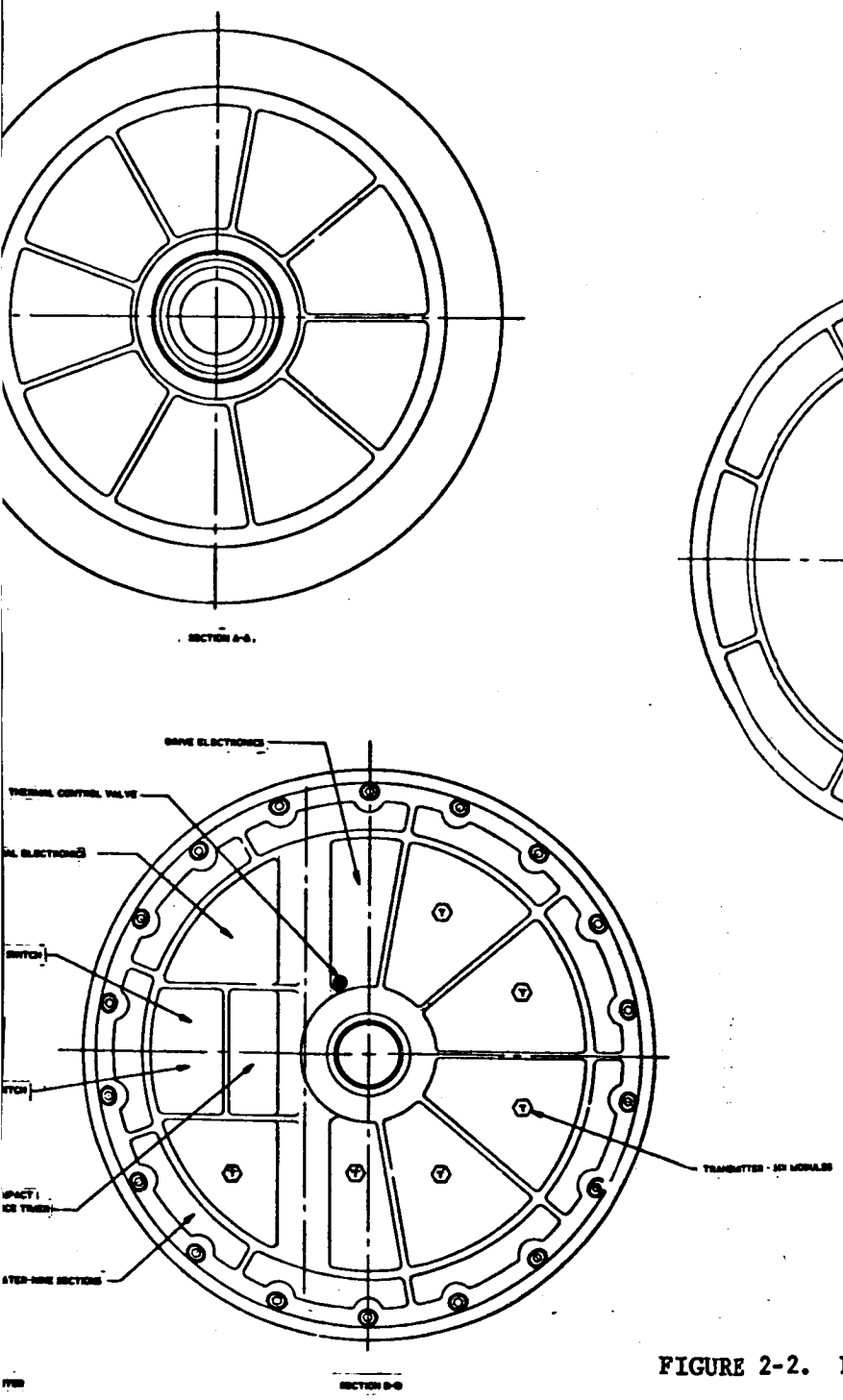

FIGURE 2-2. LANDING SPHERE ASSEMBLY

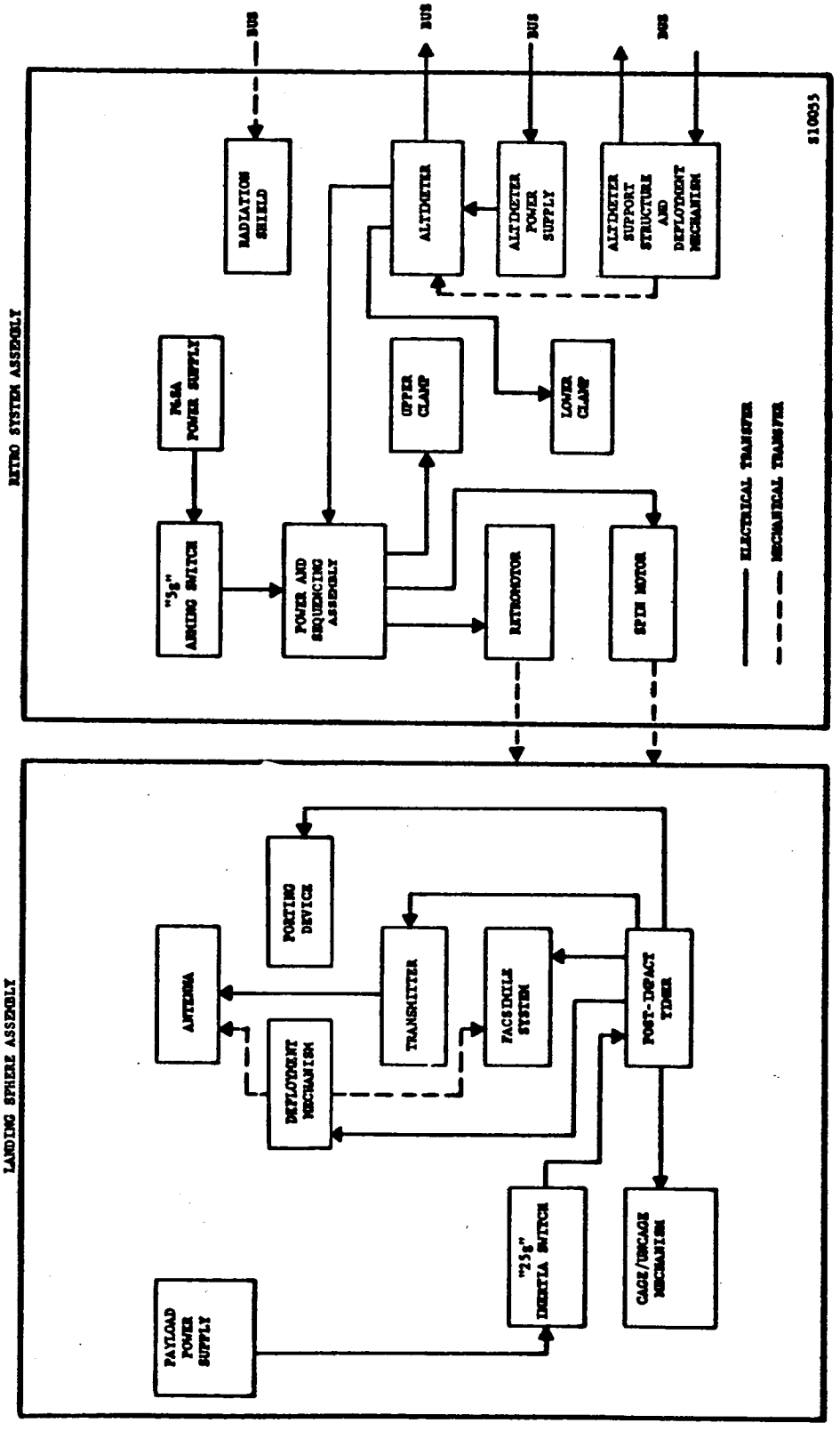

FIGURE 2-3. LSPC BLOCK DIAGRAM

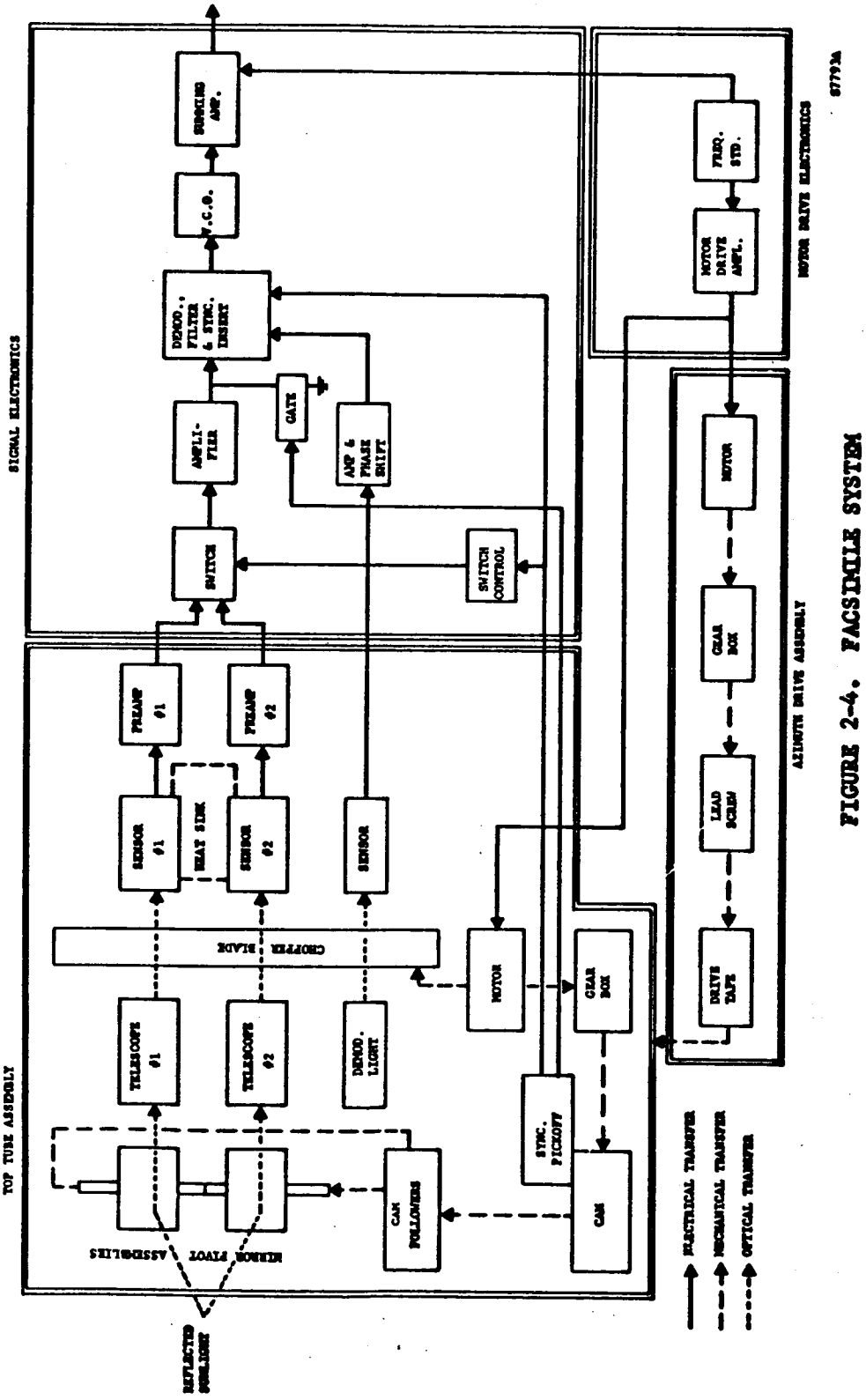

FIGURE 2-4. FACSIMILE SYSTEM

just prior to impact at which time the caging foot is retracted. After impact and alignment to the vertical another caging foot is extended to again cage the sphere. An explosive hole-cutter or porting mechanism is located at the top of the erected payload sphere and is positioned to fire upward, providing a hole through which the top tube assembly (which includes the inflatible antenna and a portion of the facsimile system) is extended by means of a deployment mechanism. The facsimile system is composed of the azimuth drive assembly, motor drive electronics, signal electronics, and an electrical/optical/mechanical top tube assembly. Only the latter top tube assembly portion of the facsimile system is extended through the hole provided by the porting mechanism. The payload structure also contains the required 960 mc telemetry transmitter, power supply, post-impact timer, inertia switches, water tanks for evaporative cooling, and a thermal control valve.

3.0 SEQUENCES

3.1 General Description

3.1.1 Operation Modes

3.1.1.1 Launch. When launch acceleration exceeds 5g for 1.5 seconds, a switch arms the P&SA in the retro system assembly. This arming procedure is inserted as a safety feature to isolate the P&SA power supply from the rocket motor squib circuitry until after launch.

3.1.1.2 Descent. Completion of the spacecraft terminal maneuver aligns the capsule assembly roll axis with the predicted relative velocity vector. At approximately 40 minutes prior to impact a command signal, which is timed and powered from the bus, fires a bolt cutter which releases the altimeter and its parabolic antenna from the stowed position such that the boresight of the antenna is aligned parallel to the capsule roll axis. Following this, the bus releases a clamp and the omnidirectional antenna is deployed away from the capsule by means of a boom. This also releases the radiation shield retraction mechanism so that the flexible shield collapses to the base of the retro motor support structure.

At approximately 60 seconds before unbraked impact the bus again provides power to actuate a switch which turns on the altimeter. This turn-on allows for a 15-second warmup time and a 25-second uncertainty time in bus impact prior to 180,000 ft altitude (20.6 seconds

before bus impact). At fuzing altitude (approximately 70,000 feet), the altimeter closes a relay which in turn connects bus power to four redundant lower separation clamp bolt cutters on the retromotor support structure. Simultaneously, bus power fires two parallel squib switches which activate the P&SA.

The P&SA contains three electrical timers which are started simultaneously. The first of these is a spin motor timer which provides a nominal delay of 215 milliseconds. The delay of spin motor ignition is 20 milliseconds and the lower clamp opening is completed in less than 200 milliseconds. Lower bound tolerances assure that the spin motor ignition always occurs after clamp opening. Spin motor burning time does not exceed 1.3 seconds.

The second P&SA timer accomplishes firing of the retromotor. The nominal delay (from altimeter fuzing) of this circuit is 2 seconds and varies up to $\pm$ 0.3 seconds depending upon the measured mean temperature of the propellant. The retromotor burns for about 9.6 seconds. Nominal burn-out altitude is 1,000 feet at which time the descent velocity is nominally zero. The dispersions in burnout altitude are such that burnout occurs prior to impact for approximately 99 percent of the cases.

The third P&SA timer is used to fire two upper clamp bolt cutters which separate the empty retromotor case from the landing sphere. It has a nominal delay of 12.5 seconds after P&SA initiation.

3.1.1.3 Post-Impact

In order to initiate the remaining sequence of functions, a squib switch in the payload is closed during retrobraking when a 25g inertia switch is closed for more than 1 second. This switch initiates (with essentially no delay) pre-impact uncaging and also activates a sequence timer which

(a) after 10 minutes accomplishes post-impact caging,

(b) after 11 minutes fires the porting device which cuts a hole through the flotation fluid shell and impact limiter to permit venting of the flotation fluid and coolant systems.

(c) after 12 minutes extends the top tube assembly and antenna through the hole by means of a deployment mechanism, and

(d) after 13 minutes turns on the motor drive electronics (which activates vertical scanning and azimuth drive), the signal electronics, and the transmitter and turns off the sequence timer.

3.1.2 Tabular Resume

The sequential events which occur during the terminal and post-impact phases are summarized in Table 3.1.2-1 and illustrated in Figure 3.1.2-1.

3.1.3 Peripheral Support

3.1.2.1 Bus. In order to satisfactorily complete all events, it is necessary for the bus to

(a) align the capsule assembly roll axis with the predicted relative velocity vector,

(b) provide command signals which are both timed and powered from the bus to

(1) release the altimeter deployment mechanism,

(2) release the omni-directional antenna and radiation shield,

(3) actuate a thermal switch to turn on the altimeter,

(c) provide power to

(1) activate the four bolt cutters on the lower separation clamp, and

(2) activate two squib switches which start the P&SA timers.

3.1.3.2 Capsule

Other than those operations mentioned above which require bus energy, all timers, inertia and squib switches, power supplies, pyrotechnic and propulsion systems required to adequately perform the sequencing operations will be supplied by either the LSPC retrosystem assembly or landing sphere assembly.

TABLE 3.1.2-1

TERMINAL AND POST-IMPACT SEQUENCE OF EVENTS

Nominal Time	Event	Initiated By
T_1* - 40 min	Deploy altimeter Deploy omni-antenna Retract radiation shield	bus
T_1 - 60 sec	Turn on altimeter	bus
T_1 - 45 sec	Altimeter warmed up	-
T_1 - 8.1 sec = T_2	Fuzing altitude Fire P&SA squib switches Fire lower clamp bolt cutters	Altimeter
T_2 + 6 msec	P&SA timers started	Squib switch
T_2 + 175 msec	Lower clamp separation completed	-
T_2 + 221 msec	Signal spin motor ignition	P&SA timer
T_2 + 2 sec	Start retromotor ignition	P&SA timer
T_2 + 5.2 sec = T_3	Start post-impact timer Pre-impact uncaging	25-g switch
T_2 + 11.6 sec	Retromotor burnout	-
T_2 + 12.5 sec	Upper clamp separation	P&SA timer
T_2 + 32 sec	Landing sphere impact	-
T_3 + 10 min	Post-impact caging	Post-impact timer
T_3 + 11 min	Activate porting device	Post-impact timer
T_3 + 12 min	Deploy and inflate antenna Deploy top tube assembly	Post-impact timer
T_3 + 13 min	Activate electronics	Post-impact timer

*T_1 is the time of bus unbraked impact.

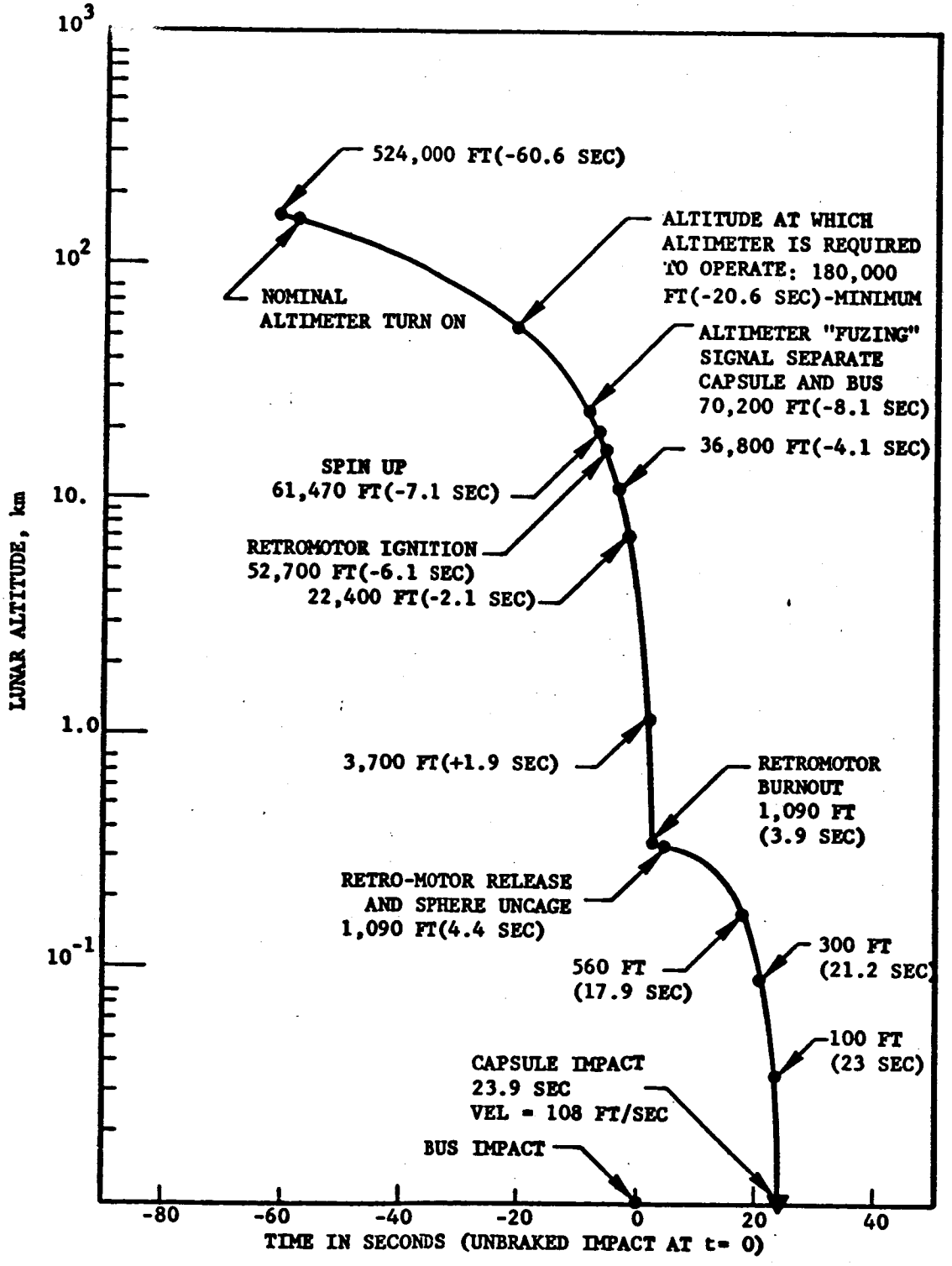

FIGURE 3.1.2-1. TERMINAL SEQUENCE OF EVENTS

3.2 Engineering Data

3.2.1 Commands

After release from the spacecraft bus, that portion of the capsule assembly which undergoes the retromaneuver is autonomous, requiring no additional command inputs to perform its assigned functions. Subsequent major events are conducted sequentially by series and parallel timing mechanisms in the P&SA and within the landing sphere assembly.

3.2.2. Measurements (excluding the scientific experiment)

3.2.2.1 Retrosystem Assembly. When the altimeter is fully deployed, an electrical microswitch on the altimeter support structure is closed which provides a signal to the bus telemetry system confirming this event. Also, during altimeter operation a means of generating a dc signal that is indicative of the reflected power received by the altimeter is provided to the bus for the purpose of telemetering this information to earth. The bus also monitors the altimeter fuzing signal and spin motor separation from the spacecraft.

3.2.2.2 Landing Sphere Assembly. The payload antenna is not effective until after impact, preventing any detection of failure during impact from transmitted signal characteristics. Direct post-impact failure detection is limited to monitoring the internal thermal environment. The voltage-controlled oscillator which controls the data subcarrier and the crystal-controlled oscillator which controls the carrier are both temperature sensitive and are calibrated prior to launch. Detection of failure modes other than this must be indirectly deduced from a relative diagnosis of signal magnitude and content.

4.0 FLIGHT CONTROL

4.1.1 General

After bus initiation of the terminal sequence the retrosystem assembly, with the aid of those inputs from the bus described in 3.1.3.1, delivers the landing sphere assembly to a nominal altitude of 1,000 feet above the lunar surface at zero descent velocity. There shall be no electrical connections between the landing sphere assembly and the retrosystem assembly.

4.1.2 Altimeter

A radio altimeter is required which radiates energy to and receives its own reflected radiation from the lunar surface for the purpose of determining when the bus has reached the correct altitude for separation of the lunar capsule. The altimeter shall be the only means for initiating this separation from the bus. A means of generating a dc signal which is indicative of the received reflected energy will be provided for the purpose of telemetering this information to earth. The altimeter shall be capable of being deployed from a stowed position so as to point at the lunar surface along the spacecraft roll axis. Although the altimeter is deployed and activated by command from the bus, it shall contain its own power supply.

4.1.3 Spin Rocket Motor

A solid propellant spin motor assembly is required to develop and deliver axial rotation to stabilize the retromotor/landing sphere assembly. Its exhaust nozzles will be canted to deliver a forward impulse to the assembly as well as torque. Spin motor ignition is initiated by a command from the P&SA.

4.1.4 Retrorocket Motor

A solid propellant retromotor assembly shall be capable of braking the total landing sphere weight from the nominal bus impact velocity. This velocity is completely removed at a nominal altitude of 1,000 feet above the lunar surface. Retromotor ignition is initiated by a command from the P&SA.

4.1.5 Power and Sequencing Assembly (P&SA)

A P&SA is required to initiate and control the timing of sequential events prior to impact. Its operation is initiated by the altimeter fuzing signal. It will contain its own source of power.

4.1.6 Separation System

Two clamps are used to temporarily mate the landing sphere to the retromotor and the retromotor to its support structure. Lower clamp separation is initiated by the altimeter fuzing signal, and upper clamp separation is initiated by the P&SA.

4.1.7 Support Structure

A support structure capable of supporting the weight of the entire capsule assembly under all prelaunch, boost and transit environmental conditions must be provided. The structure will also contain all necessary wiring and a mechanism for attachment to and release of the retromotor, and must be compatible with the bus structures.

4.2 Post-Impact Orientation

4.2.1 Erection Method

The payload is floated at neutral buoyancy within the impact limiter. Its cg shall be offset from the center of buoyancy so that the payload axis will be aligned with the local vertical and can be caged in this position after impact.

4.2.2 Porting Mechanism

Subsequent to erection, a porting mechanism shall produce a hole in the flotation fluid shell and impact limiter above the folded antenna and top tube assembly. This hole shall be of sufficient diameter to allow the top tube assembly to move freely through it.

4.2.3 Antenna and Top Tube Development Mechanism

Subsequent to porting, the antenna and top tube must be permanently deployed vertically by the deployment mechanism.

4.3 Communication

4.3.1 Antenna

The inflatable antenna shall be capable of pneumatic inflation and shall approximate omni-directional coverage over a hemisphere for data transmission.

4.3.2 Transmitter

The L-band transmitter located within the payload operates at approximately 960 mc and shall have a power output of not less than 2 w and an information bandwidth of not less than 65 cps.

4.4 Scientific Experiment

The facsimile system shall be capable of taking pictures of the lunar surface surrounding the landing sphere's resting place. Picture scanning in elevation is employed and is combined with a slow rotation of the top tube assembly about the azimuth axis. The vertical scan line separation shall not be greater than 0.1 degree, and the system angular resolution shall be compatible with this scanning for object distances greater than 45 inches. The facsimile picture area coverage shall equal or exceed the equivalent of two 90-degree azimuth sectors with 50-degree elevation scanning.

4.5 Environmental Control

4.5.1 Impact Limiter

The impact limiter shall be capable of protecting the payload from damage after a lunar gravity free-fall of nominally 1,000 feet with no initial velocity. The impact limiter shall remain intact after the fall.

4.5.2 Thermal Controls

Passive temperature control shall be provided to insure mission success under direct solar radiation. A radiation shield shall contribute to this protection during earth-to-moon transit, and a water boil-off thermal control system contained within the payload sphere shall maintain allowable payload temperatures during lunar operation.

SYSTEM DESIGN RESTRAINTS

1.0 ENVIRONMENT

The capsule components must be designed to survive and operate satisfactorily through the environmental stages listed in Table 1-1. These are designated as:

(a) Condition I: ground handling through lunar flight

(b) Condition II: ground handling through spin-up

(c) Condition III: ground handling through retrothrust

(d) Condition IV: ground handling through impact and lunar operation

The expected environmental levels are listed in Tables 1-2 through 1-5.

2.0 VEHICLES

2.1 General

2.1.1 Weight

The total weight of the capsule system shall not exceed 333 pounds.

2.1.2 Center of Gravity

The center of gravity of the entire capsule system as installed (altimeter in stowed position) on the bus shall lie within 30 inches of the bus/capsule support structure interface. The misalignment of the

TABLE 1-1

Condition	Events	Major Equipment
I	Ground Handling, Launch and Lunar Flight	Altimeter and support and deployment mechanism Radiation shield and retraction mechanism Lower separation clamp Retromotor support structure Wiring harness and junction box
II	Condition I plus Spacecraft Separation and Spin-up	Spin motor
III	Condition II plus Retrothrust	P&SA Vibration dampers Upper separation clamp Retromotor
IV	Condition III plus Impact and Lunar Operation	Landing sphere

TABLE 1-2

VIBRATION ENVIRONMENT

(Applies to all defined conditions)

	Sinusoidal		White Noise		Combined Sine	Combined Noise
Thrust Axis						
Magnitude	± 3"*	± 2.5 g	7.5 g**	5 g	2.25 g	2.25 g
Bandwidth, cps	1-2	2-40	15-1500	15-1500	40-1500	15-1500
Duration	8 min; COSR***		6 sec	3 min	3 times, 2 min each; COSR for sinusoid	
Pitch Axis						
Magnitude	± 3"	± 1.25 g	3.75 g	2.25 g	1.125 g	1.125 g
Bandwidth, cps	[----------same as thrust----------]					
Duration	[same as thrust]		12 sec		[--same as thrust--]	
Yaw Axis						
Magnitude	[					]
Bandwidth, cps	----------same as pitch----------					
Duration	[					]

* Where "±" is shown, peak values are implied.

** Where "±" is not shown, rms values are implied.

*** Constant Octave Sweep Rate

TABLE 1-3

THRUST-GENERATED ACCELERATION AND SPIN ENVIRONMENT

	Linear Acceleration (g)	Angular Acceleration (rad/sec^2)	Spin Rate (rpm)
Condition I			
Thrust Axis	+ 7, - 2	-	-
Yaw and Pitch Axes	± 2	-	-
Condition II			
Thrust Axis	[same as Condition I]	30	287
Yaw and Pitch Axes		-	-
Conditions III, IV			
Thrust Axis	+ 65, - 2	[----same as Condition II----]	
Yaw and Pitch Axes	± 2		

TABLE 1-4

IMPULSIVE SHOCK ENVIRONMENT

Condition I, II, III	Amplitude*	Duration
Thrust Axis	20 g peak	3 millisec
Yaw and Pitch Axes	6 g peak	3 millisec
Condition IV (any direction)	3,000 g peak (Integral up to 200 ft/sec)	4 millisec

TABLE 1-5

TEMPERATURE, PRESSURE AND HUMIDITY ENVIRONMENT

	Temperature (^{o}F)	Pressure (mm Hg)	Humidity (% RH)
Condition I, II, III			
Pre-launch	+ 20 to + 125 plus solar radiation	774	100
Space flight	Direct solar radiation where exposed; radiation to 0^{o}R where shaded	0	-
Condition IV	+ 260 max	10^{-12}	

* 1/2 sine wave

thrust axis of the rocket motor and the bus longitudinal axis (as defined by the bolt circle surface) shall not exceed 0.1 degree. The center of gravity of the separated capsule assembly shall not be displaced more than 0.03 inch from the nominal retrothrust axis.

2.2 Power System

2.2.1 Power and Sequencing Assembly

A sealed battery pack is to be used as the sole source of power for the pre-impact sequencing unit and must be small enough to be completely contained within the P&SA unit. It shall provide for an operating period of 16.5 seconds. At no time during operation shall the open circuit voltage be greater than 28 volts nor the terminal voltage less than 14 volts. It shall be capable of providing a continuous current drain of 30 milliamperes plus three (non-simultaneous) current pulses: two 3-ampere pulses each of 1-second duration and one 4-ampere pulse of 100-milliseconds duration. The battery pack should be rechargeable through 5 cycles.

2.2.2 Altimeter

A power supply, including a sealed battery pack, converters and regulators, shall be an integral part of the altimeter system. It shall provide for an operating time of 2 minutes. At no time during operation shall terminal voltage be less than 6 volts nor more than 9 volts. It shall be capable of providing a maximum peak current drain of 5 amperes. The battery pack should be rechargeable through 5 charge/recharge cycles.

2.2.3 Landing Sphere

A sealed battery pack shall be located in and used as the sole source of power for the payload.

2.3 Flight Control

2.3.1 Retrorocket Motor

The retrorocket motor is required to serve as the braking device for a vehicle weighing approximately 308 pounds including the motor weight. The motor with suitable attach devices shall serve as a primary structural member of the capsule system in such a way as to permit separation from the spacecraft structure and separation from the landing sphere assembly.

The retromotor shall decelerate the landing sphere in gravity-free vacuum space by approximately 8816 feet per second, and shall provide reasonable assurance that burnout will occur at an altitude between 0 and 2000 feet above the lunar surface. The motor shall be of nearly symmetrical configuration so that a condition of dynamic balance may be achieved. The motor shall support the approximately 93-pound weight of the landing sphere plus attachings mounted along the thrust axis on the head end of the motor. The retromotor shall also serve as the structural support for the spin system in such a way as to permit jettisoning of the spin system during retromotor ignition.

2.3.2 Spin Rocket Motor

The spin motor assembly shall be required to develop and deliver to the retromotor/landing sphere assembly a torque to accelerate this assembly to a spin rate of approximately 285 rpm. The spin axis is to be coincident with the retromotor thrust axis. The torque vector shall not be misaligned from the retrorocket centerline by more than 0.010 radian. The spin motor is to be mounted so that the spent motor case can be jettisoned shortly after retromotor ignition. The spin unit ignition shall be sequenced by a signal from the P&SA. The unit must ignite promptly and reliably upon receipt of the signal with a desired minimum probability of ignition of 0.995. It shall be of symmetrical configuration so that a condition of dynamic balance may be achieved.

2.3.3 Support and Separation

The support and separation assembly serves as the primary structural member for transmitting loads from the bus to the capsule. The forward end of the support assembly is attached to the rocket motor case continuously about the circumference of the case. Separation must occur at this plane on receipt of a command signal from the altimeter assembly. The misalignment of the bus longitudinal axis (as defined by the bolt-circle of the bus) and the thrust axis of the rocket motor shall not exceed 0.1 degree. Exposure to the launch environment shall not produce an additional misalignment which exceeds 0.1 degree. The complete separation process shall not produce a capsule angular rate which exceeds 0.04 radian/second.

2.3.4 Altimeter

Erection of the altimeter shall be accomplished in no less than 5.2 seconds. The delay between the bus-generated commands for deployment of the altimeter and the omni-antenna shall be no less than 5 seconds.

The antenna is to be erected at the beginning of spacecraft terminal maneuver (one hour before landing). The erection mechanism will attach to the bus structure. When the antenna is in the operating position, it will project over the side of the bus, and its beam axis must be parallel to the roll axis of the spacecraft. The antenna beam axis shall be within 0.25 degree of normal to a reference plane defined by three points on the antenna structure.

The altimeter is to start operation upon receipt of a command signal and deliver a single output signal (designated "fuzing signal") at a prescribed altitude (designated "fuzing altitude"). The altimeter will not be separated from the bus. The altimeter shall start within 1 second after receiving a start signal voltage step of 18 to 30 volts. The altimeter shall not cause any interference with other r-f equipment on the bus operating in the vicinity of 890 and 960 mc. The altimeter is to be started at a time before bus impact such that warm-up will be complete at an altitude of not less than 180,000 feet. The pulse repetition frequency shall be between 500 and 600 pps, and warm-up time shall not exceed 15 seconds. To prevent false fuzing under these conditions, warm-up shall not begin at an altitude in excess of 820,000 feet. During the time of operation of the altimeter, the approach velocity to the moon will be between 8400 and 9400 feet per second. The fuzing altitude shall be set at a point between 61,800 and 81,800 feet. The altimeter shall provide a range resolution accuracy such that the cumulative errors, from all effects (range measurement, antenna boresighting errors, switching time, etc.) shall result in a measurement error of no greater than 500 feet at the fuzing altitude. The altimeter shall operate and shall be capable of delivering a fuzing signal for a period of not less than 120 seconds following warm-up. The altimeter shall have a probability of false fuzing, from maximum starting altitude, of not greater than 1 percent.

2.3.5 Impact Limiter

The impact limiter shall be nominally transparent to radio frequency energy. It shall be adequate to sustain impact normal with the lunar surface at velocities up to 200 feet per second. An interconnect member, adequate to attach the sphere to the retromotor throughout the flight environment, shall be attached at one end (along the thrust axis) and shall provide a means of separating the landing sphere from the rocket after rocket motor burnout. A similar clamp device and attach fitting shall be provided on the opposite end, along the thrust axis to support the spacecraft omni-antenna.

2.3.6 P&SA

The P&SA shall consist of equipment and circuitry for sequencing the terminal events just prior to lunar impact. It shall possess a means for isolating the battery supply from the timers and squib circuits until after launch acceleration exceeds a nominal value of 5 g for 1.5 seconds. The sequencing unit and the batteries shall be self-contained.

3.0 SCIENTIFIC EXPERIMENT

For shadow contrast and prevention of the main sensors from being damaged by direct solar radiation, at no time during the experiment should the lighting angle be less than 20 degrees nor greater than 70 degrees. (The lighting angle is defined as the angle between the sun-moon line and the lunar local vertical.)

4.0 COMMUNICATIONS

4.1 Antenna

The facsimile data are to be transmitted from the moon to DSIF in real time. The antenna shall be compatible with communication angles of from 0 to 45 degrees. (The communication angle is defined as the angle between the earth-moon line and the lunar local vertical.)

4.2 Transmitter

Subsequent to mounting the capsule on the bus, the transmitter shall not be operative until after impact. The carrier shall be 960 mc in the L-band and shall be phase-modulated. If subcarriers are employed, they shall be standard IRIG channels.

5.0 OPERATIONS AND TEST PLAN (EFFECT ON CAPSULE DESIGN)

The landing sphere assembly design shall be based primarily on environments expected from the time of final mating onward through launching and flight. Its components shall not be subjected to environments beyond flight-acceptance levels, and the burden of protection from overexposure shall be on operators and facilities rather than on the landing sphere assembly itself.

High mission reliability must be attained without dependence on checkout instrumentation, control, and correction of deficiencies in the landing sphere assembly after completion of assembly. Subsystems must be designed to maintain operating ability and to hold calibration from the time of assembly to flight.

Except for gross system checkout and tests to verify the compatibility between the capsule and the spacecraft bus, design constraints do not permit testing, trouble-shooting, nor component replacement beyond final assembly.

All elements of deliverable capsules which can be tested non-destructively must pass acceptance tests. Acceptance tests are environmental and functional tests of the specific components, subsystems and systems which are scheduled for flight. These tests demonstrate that the flight units satisfy the designs and specifications.

6.0 PACKAGING AND WIRING

All electrical, electronic, and electromechanical parts in the capsule will be procured to Minuteman, Space Parts Working Group, or equivalent Aeronutronic-generated high-reliability specifications. To the extent practicable modular scheme of packaging of electronic equipment shall be used. The external wiring system for the capsule is used for transmission of electrical signals for controlling terminal events prior to lunar impact. A portion of the system shall also be used to provide telemetry information to the bus telemetry system.

7.0 STERILIZATION

Direct action shall be taken to deliver the capsule system in a bacteriologically sterile condition. To do this, all feasible and reasonable engineering precautions shall be exercised by subjecting the various system elements to one or more of the following:

(a) heat-soaking components and subassemblies at 257°F for 24 hours,

(b) using sporicidal resin systems,

(c) using liquid sterilizing additives to non-metallic components,

(d) using surface sterilizing agents during interfacing operations, or

(e) exposing to ethylene oxide/Freon 12 gas mixture,

and conducting assembly operations, where required, in a sterile environment.

8.0 INTERFACE PROBLEMS

Mechanical mating of the capsule system to the bus is limited to the landing sphere/JPL omni-antenna interface, the retrosupport structure/bus interface, and the altimeter/bus interface. These operations shall be accomplished within tolerances which conform to Sections 2.1.2, 2.3.3, and 2.3.4. The design of the capsule should be such that it will not interfere with the shroud envelope.

A junction box capable of exchanging all signals necessary to meet the capsule/bus electrical interface shall be provided.

EVOLUTION OF SYSTEM DESIGN CHARACTERISTICS

Early in 1961, under a series of studies of possible Ranger extensions, it was realized that high resolution photography from a hard landed capsule would provide most useful engineering information for later missions. The difficulty with conventional means of obtaining such pictures is that they are very complex, require too much power, and would require extensive ruggedization in order to withstand a 3,000 g landing.

The capsule extension studies were then directed toward defining the feasibility and possible configuration for obtaining lunar surface photographs within the constraints of the hard-landing capsule. It was assumed that the functional sequence of landing and the systems involved would be identical to RA-3,4,5. Thus the mission would have to be accomplished after a 3,000 g, 3 millisecond impact, and from within the geometry of a 12-inch sphere, and a weight limit of approximately 50 pounds. It was concluded that orientation to the local vertical would be accomplished by flotation, as in the Seismometer Capsule; and that, in order to view the lunar surroundings, it would be necessary to remove at least a section of the shell and impact limiter to provide access to the outside.

The large information content inherent in a photographic mission, combined with the low available data rate from the size, weight, and power-limited lunar capsule, would tend to indicate the need for some data storage. The overriding desire to avoid such data storage led, in February, 1961, to the decision to limit further studies to a slow-scan facsimile type photographic mission. The facsimile scheme appeared to be particularly well-suited to meet the capsule limitations and the slow-scan was permissible due to the unique conditions of the lunar surface. Within the few-hour time span considered

appropriate to the mission, the lunar scene exhibits essentially constant lighting and a very small probability of terrain feature change. The mission time limitation was defined primarily by DSIF considerations and secondarily by capsule thermal control considerations.

The major question areas at the initiation of the study included battery/power/weight trade-offs, the availability of an adequate RF transmitter, the feasibility of impact limiter and outer flotation shell cutting, capsule stability on the lunar surface, difficulties of thermal control with a fairly large payload section exposed to the harsh lunar environment, and optical and mechanical configuration feasibility.

The initial configuration of the photoreconnaissance capsule evolved along the following lines. It was decided that a relatively slight geometrical variation of the Seismometer Capsule battery would provide adequate power for the photoreconnaissance mission. Initial battery weight estimates were set at 15 pounds, and an energy/weight ratio of 50 watt hours per pound was assumed. The structural proof test of the Seismometer battery, as accomplished on the Ranger program, was considered adequate to demonstrate its feasibility for the photoreconnaissance mission. The effective radiated power output for the r-f communication link was of the order of 3 watts compared to the 50 milliwatts of the Seismometer Capsule transmitter. The battery requirements were based on the use of a three to five watt output power transmitter working into an "omnidirectional" antenna. Initial development in the transmitter area was concerned with obtaining higher power from all solid-state devices, and with the possible ruggedization of ceramic tube power amplifiers. A considerable development program conducted at Aeronutronic resulted in the fabrication of a three watt all-solid-state transmitter, which required less than the allowed 100 watts input power. Critical components of the transmitter were tested under the impact environment, and survived.

An early demonstration of the feasibility of cutting a hole in the residual impact limiter and shell was made. Analysis has continued, particularly in the area of defining the relationship between hole cutter dynamics and capsule static stability on the lunar surface. It appears that an arrangement of hemispherical bumps cemented on the impact limiter, or their equivalent, and careful control of the pyrotechnics of the hole cutter, will result in a high confidence in capsule stability during this operation.

Definition of the High Resolution Facsimile mechanical and optical configuration of this system occupied most of the (HRF) Feasibility Program (Task II, Contract N-21453). It was decided that data handling from the optical system should be similar to that of the Seismometer Capsule. Bandwidths up to 250 cycles per second were considered in relation to the optical and mechanical scanning rates. It was initially deemed desirable that no moving parts be used in the extended assembly. As a result of uncertainty in the terrain at the landing site, a field of view of 360 degrees in azimuth was considered to be desirable.

Initially, several configurations were considered which depended upon placing an erectible antenna on top of an extendable periscope-like tube, and used various mirror segments to form virtual images of the lunar scene in a position where they could be scanned by optical systems located within the survival sphere. On March 23, 1961, a spherical convex mirror segment configuration was formalized. It proposed the use of a double pinhole scanning telescope located within the survival sphere, and set a resolution objective of 2.4×10^7 image points with a grey scale of 10 and 55 degree vertical view field. The donut geometry of the extended mirror lent itself well to the inclusion of an inflatable antenna on top of the periscope, and had the advantage that no moving parts were used outside of the survival sphere. However, the configuration was based upon erroneous photometric assumptions, in that the energy on the photocell was assumed to be equal to the brightness of the scene; also the pinhole scan proposed was inconsistent with the diffraction criteria. The virtual image formed by the convex mirror was to be scanned in a spiral geometry (similar to a phonograph record groove pattern) by a small telescope-photocell assembly. This early system provided an object space angular resolution of 6×10^{-4} radians.

On March 27, 1961 a detailed study of the optical aspects of the above convex mirror system was completed. This study showed a requirement for including lenses in the telescope-sensor scan assembly at the base of the tube due to a resolution requirment of 1.3×10^{-5} radians. This resolution capability was implicit in the desire to limit the spherical mirror radius to approximately one inch. The depth of focus of the telescope-mirror system was shown to be satisfactory, primarily as a result of the extremely small aperture ratio then considered adequate. The principal aberrations of the optical system were also calculated and found acceptable, again due to the small aperture ratio; however, the Rayleigh criteria of

resolution was not met at 1.3×10^{-5} radians for the three millimeter telescope objective which at that time was included in the design. These design considerations took place still under the incorrect assumption of high illumination levels.

On March 30, 1961, a revision of the calculations on the communication system limitations (transmitter power of approximately five watts) required a reduction in the number of image points from a value of 2.4×10^7 to 1.4×10^7. At this time, an eight-hour total mission limitation was set as a compromise between constant lighting versus low data rate, and to permit all data to be received at a single DSIF station. The system specifications then included a 500 bit per second data rate and an object field resolution of 0.7×10^{-3} radians, and the original 50 degree by 360 degree view field; however, the photometry calculations were at this time still based upon erroneous illumination assumptions. On April 5, 1961, a proposal for Lunar Capsule extensions (Aeronutronic Publication No. P-10631(U)) was submitted to JPL which embodied most of the geometrical and configuration limitations developed to that date. This system consisted of a small telescope located near the bottom of the survival sphere. The telescope was to be driven in a spiral scan as mentioned above; however, the photo-sensitive surface was changed to two inch diameter circular annulus which remained stationary during the scanning process. Complete coverage of the entire virtual image formed by the convex mirror occupied an eight-hour period. A flexible light shield was to be used to protect the stationary photo sensitive surface from stray exposure. The technical memos written during the program to this date were included as appendices to this proposal. Two fundamental errors were still in the design at this time:

(1) The resolution capability of this small telescope failed to meet the Rayleigh criteria for diffraction by a factor of eight.

(2) The assumptions and calculations of photometric levels were incorrect.

On May 8, 1961, a review of the design analysis on the Facsimile Capsule was completed. It was at this point that the diffraction limitations on the system were definitized and the need for a larger aperture telescope became apparent. The desire to avoid moving parts outside the capsule had to be sacrificed in the interests of keeping the porting hole to a reasonable diameter. Rather than reduce

the number of image points or final print quality, various mechanizations involving moving mirrors external to the shell were investigated. Although recalculation of the photometric relationships in relationship to S-1 and S-4 cesium photocells was made, the available sensor illumination level was still assumed at an incorrect level. Photometric calculations were even more optimistic at this time because of the move toward larger apertures.

As a result of the change in concept to that of using external moving mirrors, three new mechanizations were considered. In these the Rayleigh criteria was discarded in favor of a more restrictive limitation. The new mechanizations were:

(1) A radial strip of spherical mirror with a radius of 6.5 inches rotated in azimuth only with the telescope contained within the survival sphere as before. Diffraction limitations had thus forced a change to a spherical mirror radius of 6.5 inches from 1 inch. The telescope in this configuration would require either slip-ring feedout of the spiral type scan (with a telescope-mounted sensor) or stepped motion with a large diameter photocell. The configuration required a three-inch port cut in the shell and impact limiter.

(2) A strip of spherical mirror such that it required only smooth circular motion of the telescope to effect the scan. This configuration embodied the first mention of two alternately blanked telescopes and a time-shared data handling system which thus eliminated fly-back time losses. However, the system did have overlap losses, as opposed to fly-back, and these amounted to 13 percent with the best scheme of this type.

(3) Nodding telescope directly scanning the lunar landscape without the interposition of a spherical convex mirror. This scheme was considered more desirable if a plane mirror was nodded instead of the telescope proper

Also considered was a scheme which eliminated both the convex mirror and the telescope, by use of a nodding concave active optical element, thus eliminating the need for lenses. All of the above systems envisioned an angular resolution of 7×10^{-4} radians with 1.4×10^{7} image points. It may be seen that the system described in (3) is approaching the final HRF configuration.

Between May and the end of July, 1961, informal studies directed toward optimizing the facsimile configuration continued. Several systems involving the use of multi-sided flat mirrors in the top tube assembly were proposed in an effort to reduce fly-back problems, and to allow scanning the lunar scene with pure rotary motion. It should be noted that up to this time no detailed system mechanical configurations had been developed; such as choice of motor drives, gear ratios, and cam mechanizations.

Toward the end of July, 1961, under the HRF contract, a more detailed photometric analysis led to the discovery of the error in previous photometric calculations. It was demonstrated that an increase in signal-to-noise ratio at the detector output, by a factor of 100, would be required for satisfactory system operation. Three alternative methods of obtaining this increase were considered:

(1) With the retention of the angular resolution of $.7 \times 10^{-3}$ radians, an increase in objective lens diameter of the telescope would be made by a factor of ten. This system would require a variable focus scheme correlated to the instantaneous vertical view angle, plus the assumption that the viewed terrain was relatively flat. Neither consideration was attractive.

(2) Again, within the framework of the design objective angular resolution, a reduction in the total picture view field could be made. With a fixed mission time, the data bandwidth could be reduced and reduce correspondingly the noise proportional to the square root of the reduction in total image points. This solution was clearly inadmissible as an only means of increasing signal-to-noise ratio.

(3) By decreasing angular resolution and taking advantage of the relaxed optical tolerances thus afforded, it is possible to obtain an overall increase in

signal-to-noise ratio of 100 with only nominal loss of picture quality. This approach was adopted in the system evolution because of the powerful (and favorable) effect on signal-to-noise ratio of the resolution decrease. Quantitatively, a decrease in resolution results in squared increase in light output per image point (proportional to geometrical area); an allowable proportional increase in objective diameter while remaining in focus (this results in an increase of sensor light levels proportional to the square of the resolution decrease); and a reduction in data bandwidth requirement due to reduced number of image points in a fixed eight-hour scan time. To obtain a factor of 100 increase in signal-to-noise, the angular resolution was decreased to 1.7×10^{-3} radians, i.e., a factor of 2.5, which, when raised to the fifth power results in the needed factor of 100. The use of many-sided mirrors and pure rotation, as well as the limitation to motion only within the survival sphere, were precluded by the increase in size of the telescope objective.

Since photometry (specifically, sufficient light delivered to the sensor) appeared as the major system problem, the month of August, 1961, was primarily devoted to studies of various available sensors and sensor/preamplifier combinations. The basic signal electronic problem was to design a low-noise transistor preamplifier capable of working with the high impedance sensors. Instrumentation was developed to facilitate comparison of various sensor systems, both in the laboratory and in direct viewing of the moon. The final choice of the silicon duodiode type of sensor was made at this time principally because of its higher sensitivity despite the fact that thermal control of the sensor is required. The Gallium Arsenide and the deep base silicon type sensors, although more tolerant of high temperatures, were less sensitive and hence less attractive.

Completion of the sensor studies signaled the solution of the last major functional problem in the HRF configuration. Detailed system design studies then proceeded and evolved a system with angular resolution design objective of 1.745×10^{-3} radians, an objective diameter of 5 millimeters, and a focal length of 8.2 centimeters. Mechanically, a return was made to the nodding mirror and telescope configuration primarily for reasons of optical simplicity and because such a

configuration could be implemented to eliminate fly-back time losses. Two telescope-mirror systems were combined back-to-back within the top tube. These systems alternately scanned diametrically opposed portions of the scene in two vertical sweeps each of eight seconds during the entire tube assembly was rotated 180 degrees in azimuth during the eight-hour mission time.

In order to confine the extended assembly to a one-inch tube, it was necessary that the vertical and azimuth scans be driven by separate motors. By September 8, 1961, specific choices had been made for motor and gear box combinations for the two drives, and for the majority of other purchased systems parts. Detailed design continued throughout September and October, and fabrication of the HRF prototype demonstration model occupied October and November, 1961.

Although some small changes in the system were introduced subsequently, October 26, 1961 was, in effect, the design freeze date for the demonstration system. This system first functioned as an entity on December 23, 1961, and the scheduled system demonstration was successfully conducted on December 28, 1961, completing the HRF Feasibility program.

Continued system tradeoff studies conducted since April 1962 under Task I of JPL Contract LC-950267 have not resulted in any significant changes in the basic design. While a reduced transmitter minimum output power of two watts was adopted at JPL suggestion to assure a high transmitter reliability, a more detailed analysis of the communications link still indicated a satisfactory margin in signal-to-noise ratio and phase-lock probability.

An analytical investigation was conducted on the possibility of payload tip-over due to a misaligned reaction from the explosive hole-cutter device. Complete removal of the balsa limiter prior to cutting through the flotation shell was considered as a means of reducing the reaction force. However, the force reduction was not large and this method adds several series events to the capsule sequence with a resultant potential loss in reliability. With small protuberances added to the exterior of the impact limiter to stabilize the landed sphere on the lunar surface, the tip-over probability on a reasonable range of expected slopes is reduced to a desirable low level.

ACCELEROMETER SYSTEM (SURMEC)

MISSION OBJECTIVES AND DESIGN CRITERIA

1.0 INTRODUCTION

The primary purpose of the Surface Measurement Capsule (SURMEC) is to obtain representative data on the lunar surface strength characteristics at the earliest possible date. The systems and techniques developed in the first five Ranger flights will be fully utilized in meeting this objective.

It will be a design objective to require no changes in the Ranger RA-3, 4, 5 system for delivering a lunar landing sphere. The landing sphere itself shall utilize Ranger components and techniques wherever applicable.

Any margins in weight and volume will first be employed to ensure the achievement of the primary objective of surface strength measurement. Only then will additional scientific experiments, selected to contribute to the design of manned lunar vehicles, be incorporated on a strict noninterference basis.

2.0 MISSION OBJECTIVES

The SURMEC lunar rough landing capsules are planned for a series of repeated attempts to obtain data on the lunar surface penetration resistance and compressive strength at dispersed points over a significant sampling area. This data shall be obtained (1) with definition sufficient to aid in the design of manned lunar landing vehicles, and (2) at a date early enough to be effective in said design. Other experiments which expand this primary objective or measure additional lunar properties shall be included in this capsule on a noninterference basis.

3.0 DESIGN CRITERIA

Design criteria applicable to the launch vehicle, spacecraft bus, and Surface Measurement Capsule are described in the following subparagraphs.

3.1 Launch Vehicle and Spacecraft Bus Criteria

Other than mandatory engineering change orders resulting from RA-3, 4, 5 experience, no changes shall be required for the SURMEC mission on either the Atlas and Agena B boosters or the Ranger RA-3, 4, 5 spacecraft bus.

3.2 Capsule Assembly Criteria

The SURMEC consists of a Landing Sphere Assembly, which impacts on the lunar surface, and a Retro System Assembly, which includes those subsystems necessary to slow the Landing Sphere Assembly to an acceptable impact velocity.

3.2.1 Retro System Assembly

Other than mandatory engineering change orders resulting from RA-3, 4, 5 experience, no changes shall be required in the altimeter, spin motor, retrorocket motor and other subassemblies of the complete RA-3, 4, 5 retrosystem assembly.

3.2.2 Landing Sphere Assembly

Components and techniques developed for the RA-3, 4, 5 landing sphere assembly will be employed with minimum modification in the SURMEC landing sphere assembly wherever applicable.

3.2.2.1 Competing Characteristics. Competing characteristics shall be treated in the following order:

(a) Reliability of landing sphere operation on the lunar surface.

(b) Correlation of data with actual surface characteristics.

(c) Schedule.

(d) Biological sterility.

(e) Ease of fabrication and producibility of system.

(f) Pre-flight checkout simplicity and shelf lifetime.

(g) Performance of secondary experiments.

3.2.2.2 Defined Characteristics. Defined characteristics are as follows:

(a) Weight. The weight of the landing sphere assembly is fixed at 89.3 pounds by the selected trajectory and available launch vehicle performance and especially by the available impulse of the RA-3, 4, 5 retromotor. This design weight must be maintained to achieve maximum impact survival probability.

(b) Impact Environment. The RA-3, 4, 5 lunar impact environment specification (Master List of Environmental Requirements, Section II, Aeronutronic Publication No. U-902-1, dated 15 April 1961) shall be used for design purposes.

(c) Effect on Spacecraft Bus and Retroassembly. The interfaces between the landing sphere assembly, the retroassembly, and the spacecraft bus shall remain as designed for RA-3, 4, 5.

3.2.2.3 Reliability Philosophy Affecting Design. Design techniques employed insofar as possible to achieve a high reliability shall include the following:

(a) Minimization of required functions.

(b) Simplification of functions.

(c) Use of proved components.

(d) Use of passive rather than active components.

(e) Arrangement of functions in parallel rather than in series.

(f) Minimization of dependence on lunar terrain.

(g) Redundancy.

After all elements of the system are adequately ruggedized, redundancy shall be employed to the extent permitted within the weight limitation.

3.2.2.4 Experimental Philosophy Affecting Design.

(a) Pre-launch Environmental Control. The landing sphere assembly and its components shall not be subjected to environments beyond flight-acceptance levels, and the burden of protection from overexposure shall be on operators and facilities rather than on the landing sphere assembly itself. Clean, air-conditioned working areas, special handling fixtures, air transport, electrical overload protection, and other such measures external to the landing sphere assembly shall be used to the extent practical, and the landing sphere assembly design shall be based primarily on environments expected from the time of final mating onward through launching and flight. Wherever possible, biological sterility shall be achieved by external measures without the requirement for access into sealed components, so that the adverse effect of the sterility requirement on equipment design, reliability, and schedule is minimized.

(b) Operating Condition at Launch. The design criterion should be to attain a high mission reliability without dependence on checkout instrumentation, control, and correction of deficiencies in the landing sphere assembly after completion of assembly. Subsystems must be designed to maintain operating ability and to hold calibration from the time of assembly to flight. Provisions for checkout testing after completion of assembly of the landing sphere shall only be provided to the extent that they can be demonstrated to increase the net probability of success for the mission when the added complexity to provide checkout testing is considered.

(c) In-flight Failure Detection. Failure detection methods shall be employed only to the extent that they do not detract from the reliability of achieving the primary mission objective.

(d) Function After In-flight Failure. Interdependence between subsystems shall be minimized, but will necessarily exist to a large extent. The general design criterion is that no subsystem is required to function after failures of subsystems on which it depends, except insofar as can be achieved without complicating the design or diverting effort from the main objectives of the flight.

3.2.2.5 Test Philosophy Affecting Design

The objective is to obtain reliability by design rather than by extensive development. In general, designs shall not be compromised to accommodate testing. However, when subsystem acceptance tests are the only way of determining readiness for assembly and flight, the design must, of course, incorporate the necessary test provisions. Moreover, a test of the complete spacecraft assembly is considered essential to verify the compatibility between the capsule and the spacecraft bus.

In system tests, the purpose is primarily to simulate flight and lunar operation. The burden of simulation shall, as far as possible, fall on equipment external to the landing sphere assembly.

SYSTEM DESIGN CHARACTERISTICS

1.0 OPERATIONAL DESCRIPTION

The primary functional operations of the Lunar Surface Measurement Capsule (SURMEC) include terminal flight control, retro-propulsion, semi-rough landing, survival, event sequencing, power supply, obtaining surface strength data in the vicinity of the landing site, electronic processing and transmission of the data to earth, thermal control, and mechanical support.

Upon receipt of a signal from the spacecraft bus at the terminal end of the flight the altimeter is deployed and the thermal radiation shield retracted. When the altimeter detects that the spacecraft is at fuzing altitude, the retromotor and landing sphere assembly is freed from the bus. The solid propellant spin rocket motor imparts rotation about the longitudinal axis for attitude stabilization, followed by a retro-impulse from the solid propellant retrorocket motor to reduce the descent velocity to zero at a specified altitude above the lunar surface. The high acceleration of the retromotor switches on the payload electronics. After retrorocket burnout, the spent motorcase is separated from the landing sphere. To survive the semi-rough landing from the free fall, the instrument package (called the payload) is protected by an envelope of crushable shock-absorbing material capable of limiting the landing deceleration and absorbing the impact energy.

Following impact and removal of the outer impact limiter material, the spherical inner payload establishes its alignment with the local vertical. A shell cutter produces a hole in the flotation-fluid shell through which the antenna is erected. The stored acceleration data from the lunar impact are then transmitted to earth.

Sensor spheres are deployed at spaced intervals and the resulting impact acceleration data are transmitted to earth in both real and delayed time. As secondary experiments, penetrometer data and acoustic reflection data are also transmitted.

2.0 CONFIGURATION DESCRIPTION (FIGURES 2-1 THROUGH 2-3)

An Atlas first-stage booster, Agena-B second stage, and Ranger RA-3, 4, 5 spacecraft bus are utilized to deliver the SURMEC. The basic configuration of the SURMEC consists of the payload cushioned in a spherical impact limiter and mounted to the forward end of the solid propellant retrorocket motor, which in turn is mounted to the bus through the motor support structure. A cylindrical radiation shield of flexible laminated material surrounds this assembly. The spin rocket motor is attached to a plug rigidly supported in the retronozzle throat, and the altimeter assembly is mounted on the top of the bus hexagonal frame. The capsule assembly is capped by the bus-controlled omni-directional antenna.

Two separation clamps with appropriate explosive bolt cutters are to be used to temporarily bond equipment together. The upper one holds the landing sphere assembly to the retromotor, and in a small cavity located between these two is the power and sequencing assembly (P&SA) containing the pre-impact timing mechanism. The lower clamp binds the retromotor to the motor support structure. The motor support structure is attached to the top of the bus hexagonal frame and provides accurate bus/capsule alignment. Located around the periphery of the landing sphere/retromotor interface are damping devices which limit the motions produced by vibrational excitations. The lower end of the radiation shield is tied to the base of the retrosupport structure. The shield is held under tension by retractors attached to its opposite end along with ties attached to the omni antenna separation clamp. The altimeter and its support and deployment mechanism are located outside of, and at the base of, the shield envelope. The altimeter support structure is clamped firmly to the bus.

The impact limiter surrounding the payload is designed for explosive removal from the flotation sphere. Within the flotation-fluid shell is the payload sphere suspended at neutral buoyancy in flotation fluid. The center of gravity of the sphere is located below the center of buoyancy so that after impact the payload erects and self-aligns with the local vertical. A caging mechanism is located on the bottom of the outside surface of the payload sphere for caging the payload from the time of final assembly until just prior to impact. An explosive shell-

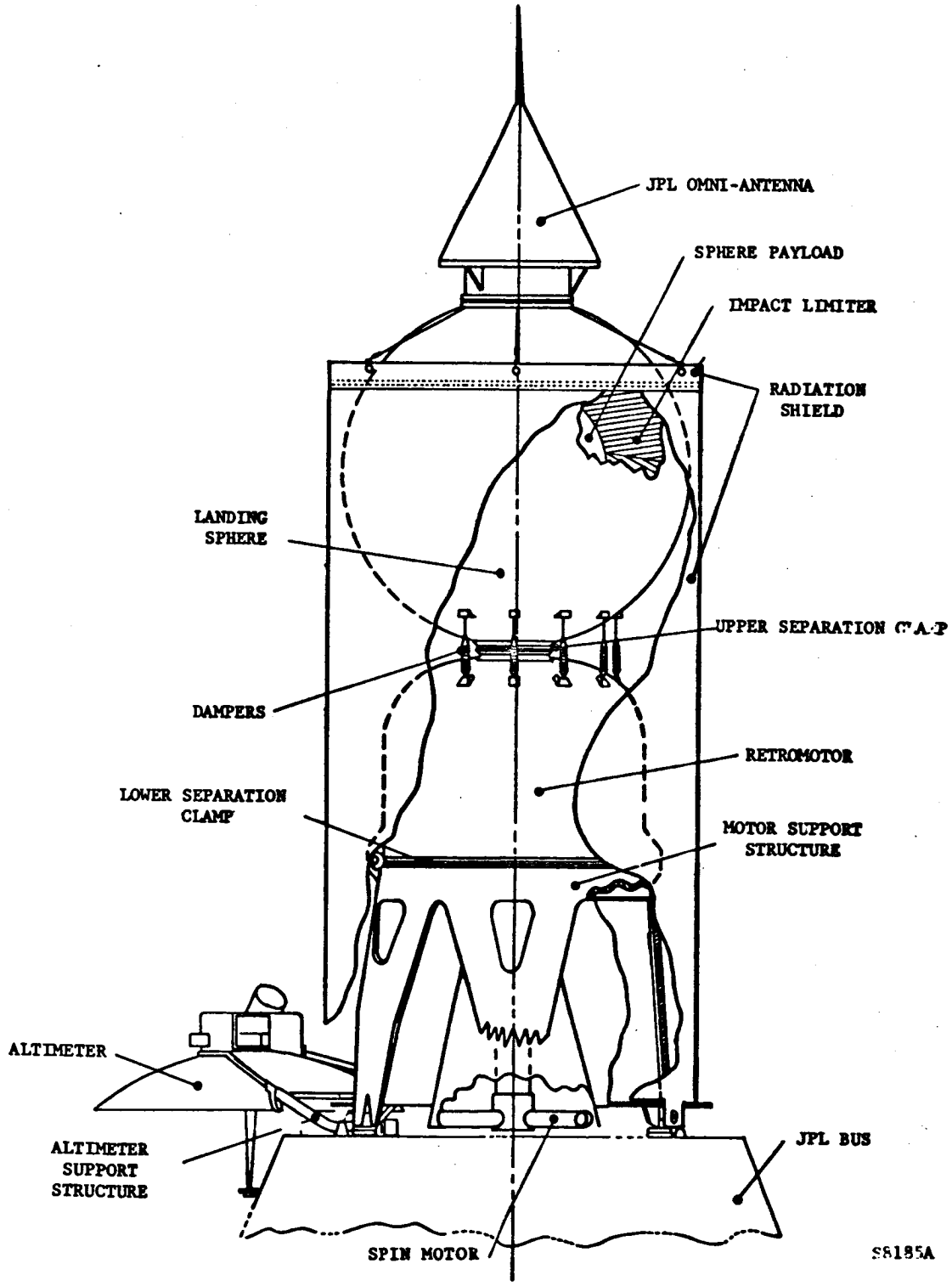

FIGURE 2-1. LUNAR SURFACE MEASUREMENT CAPSULE

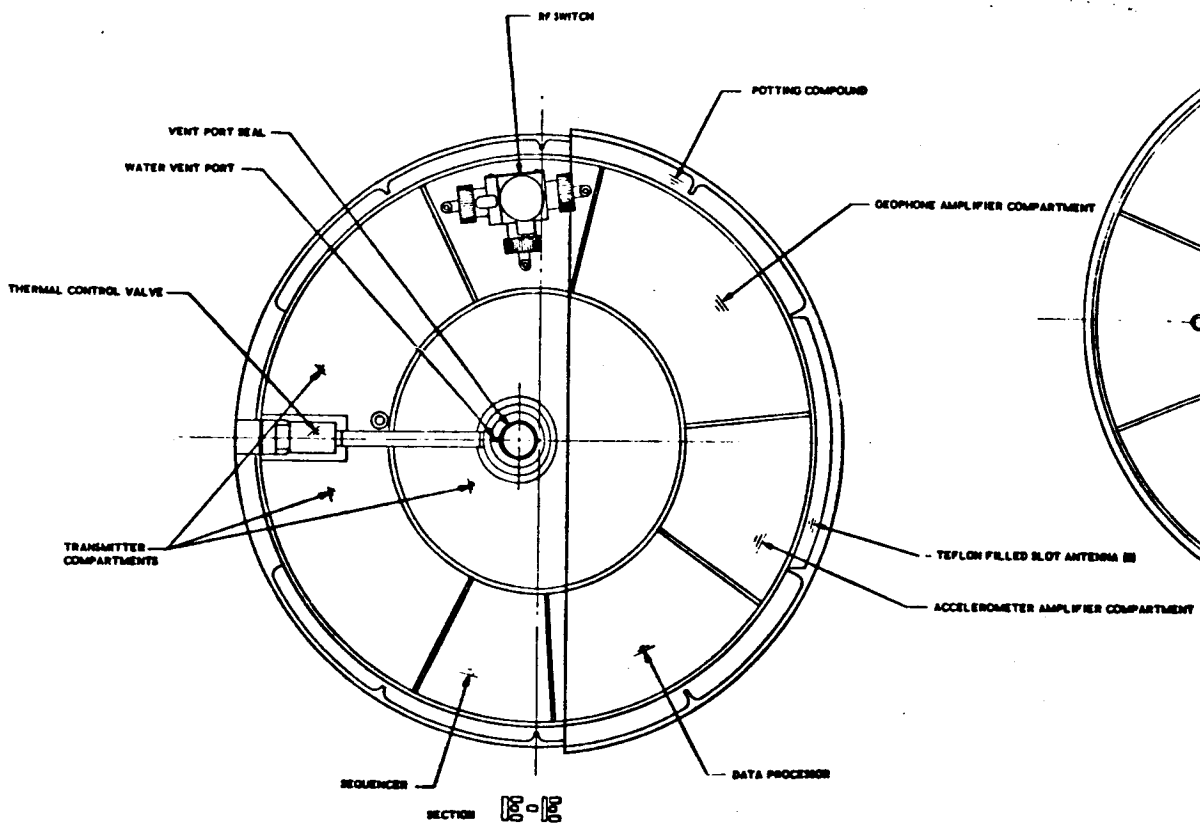

UPPER WATER COMPARTME

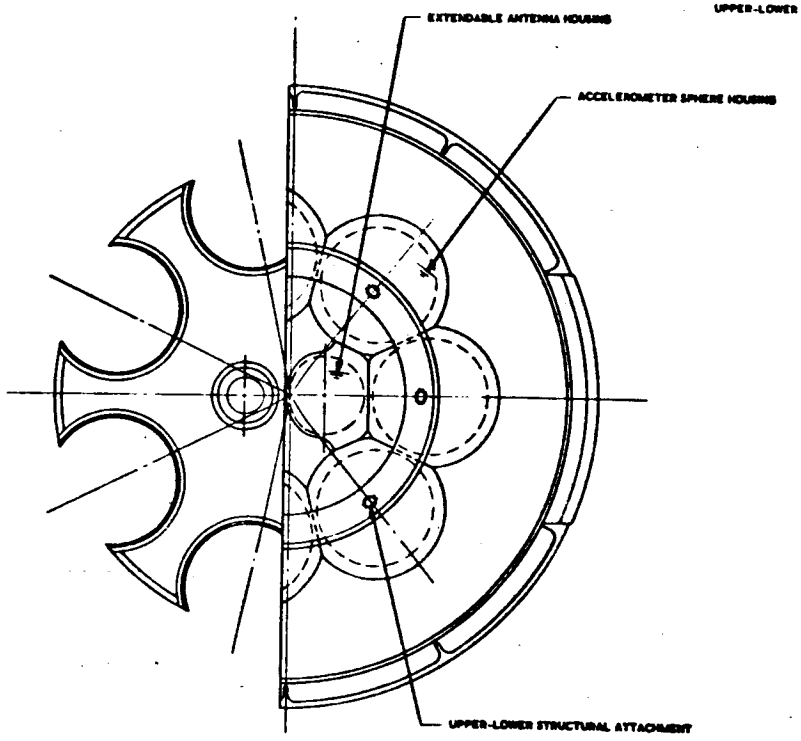

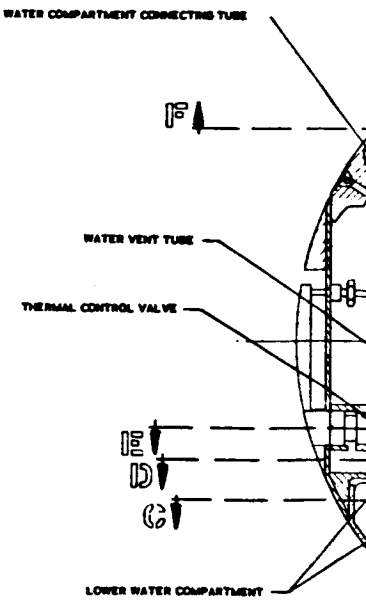

RE-ORDER No. 62-155

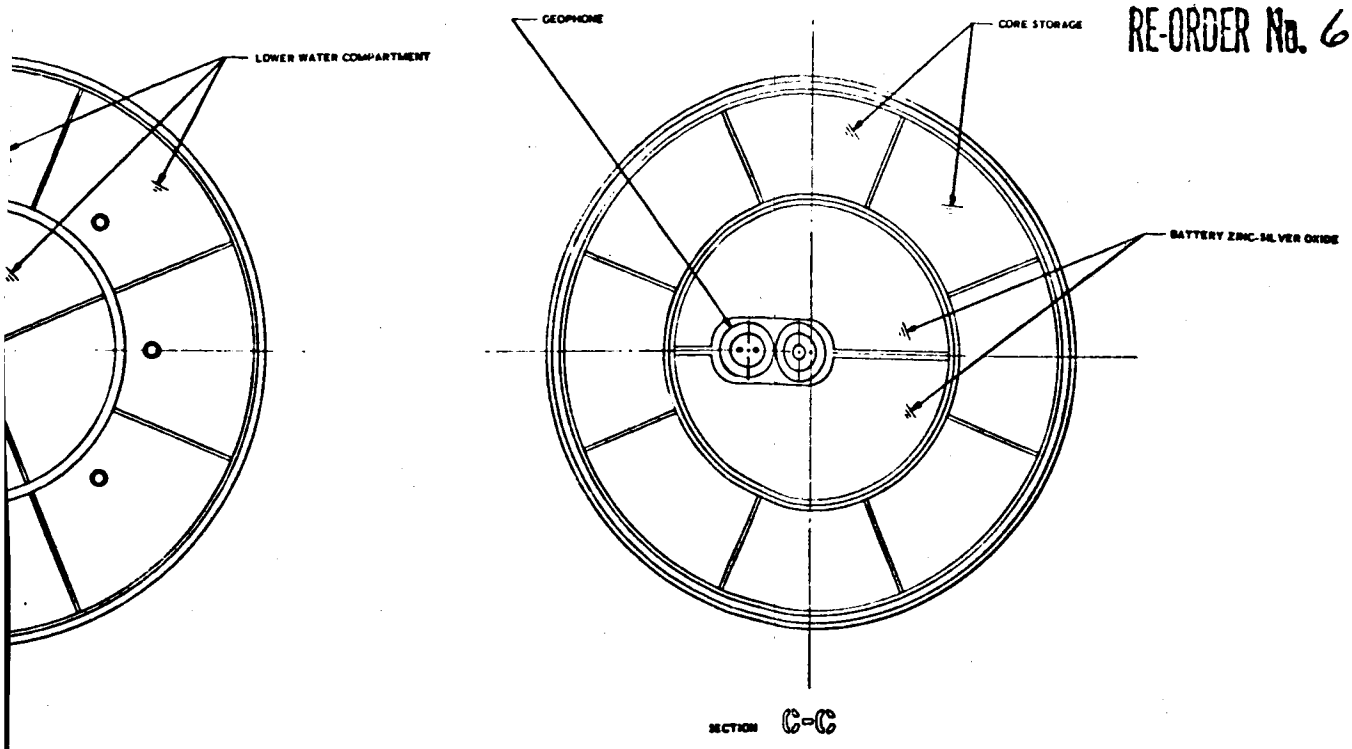

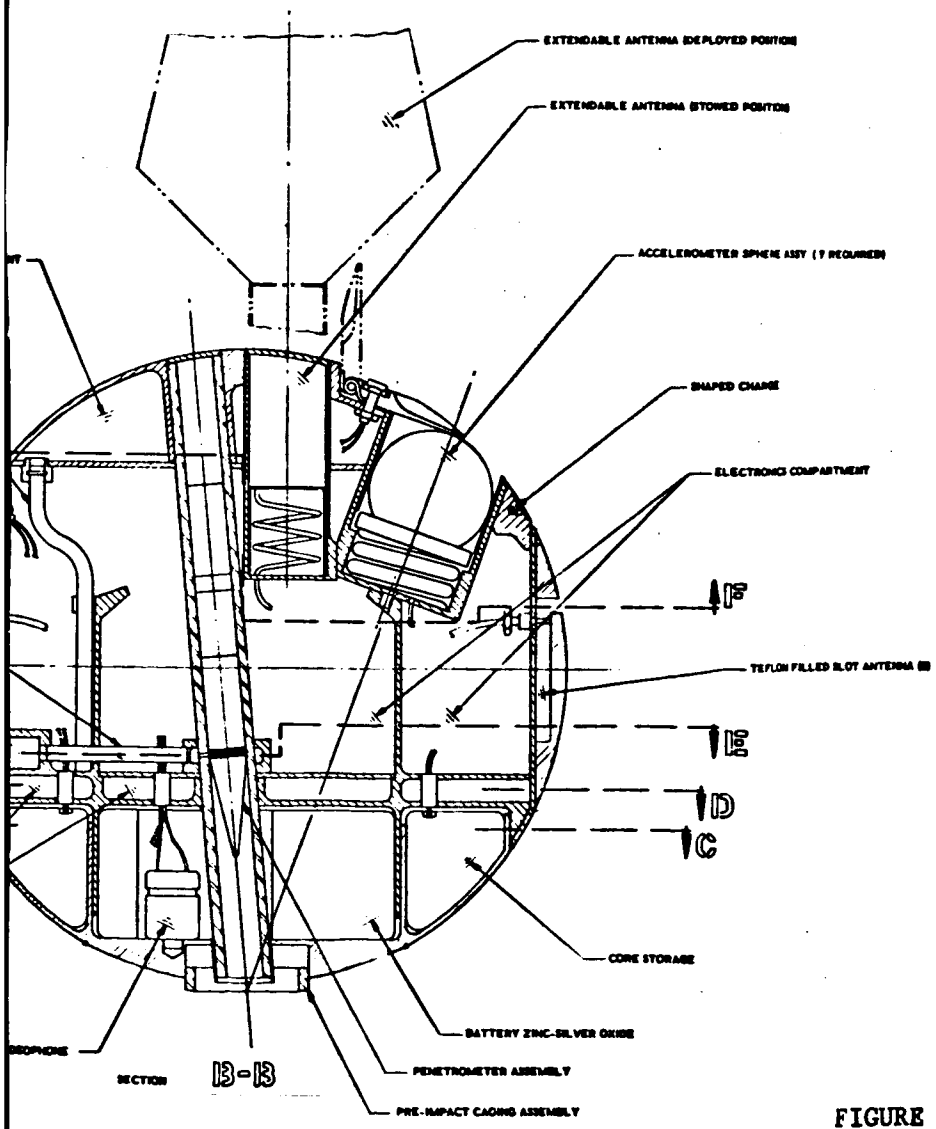

S7528-1

FIGURE 2-2A. LANDING SPHERE ASSEMBLY

2

54

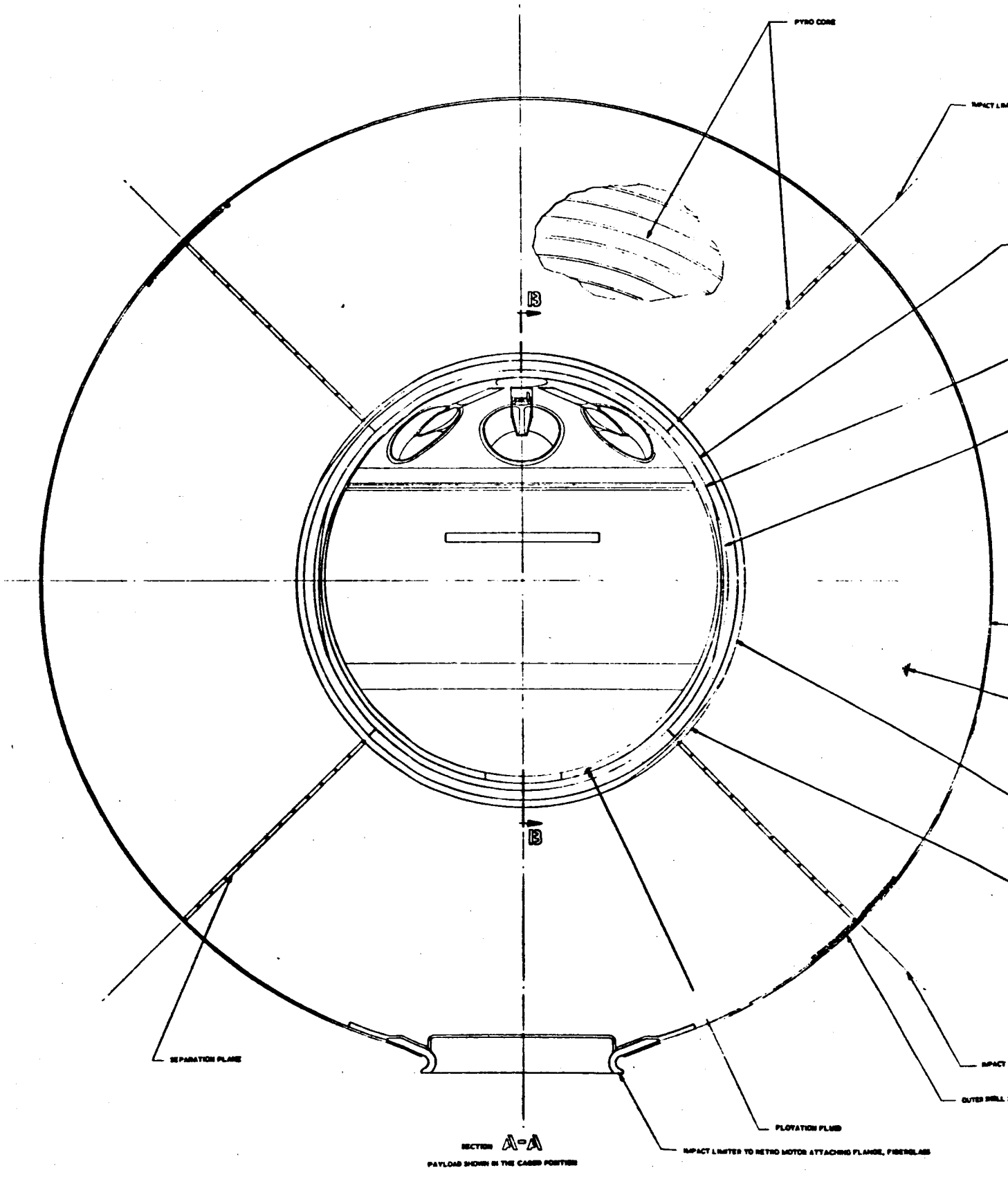

SECTION A-A

PAYLOAD SHOWN IN THE CASED POSITION

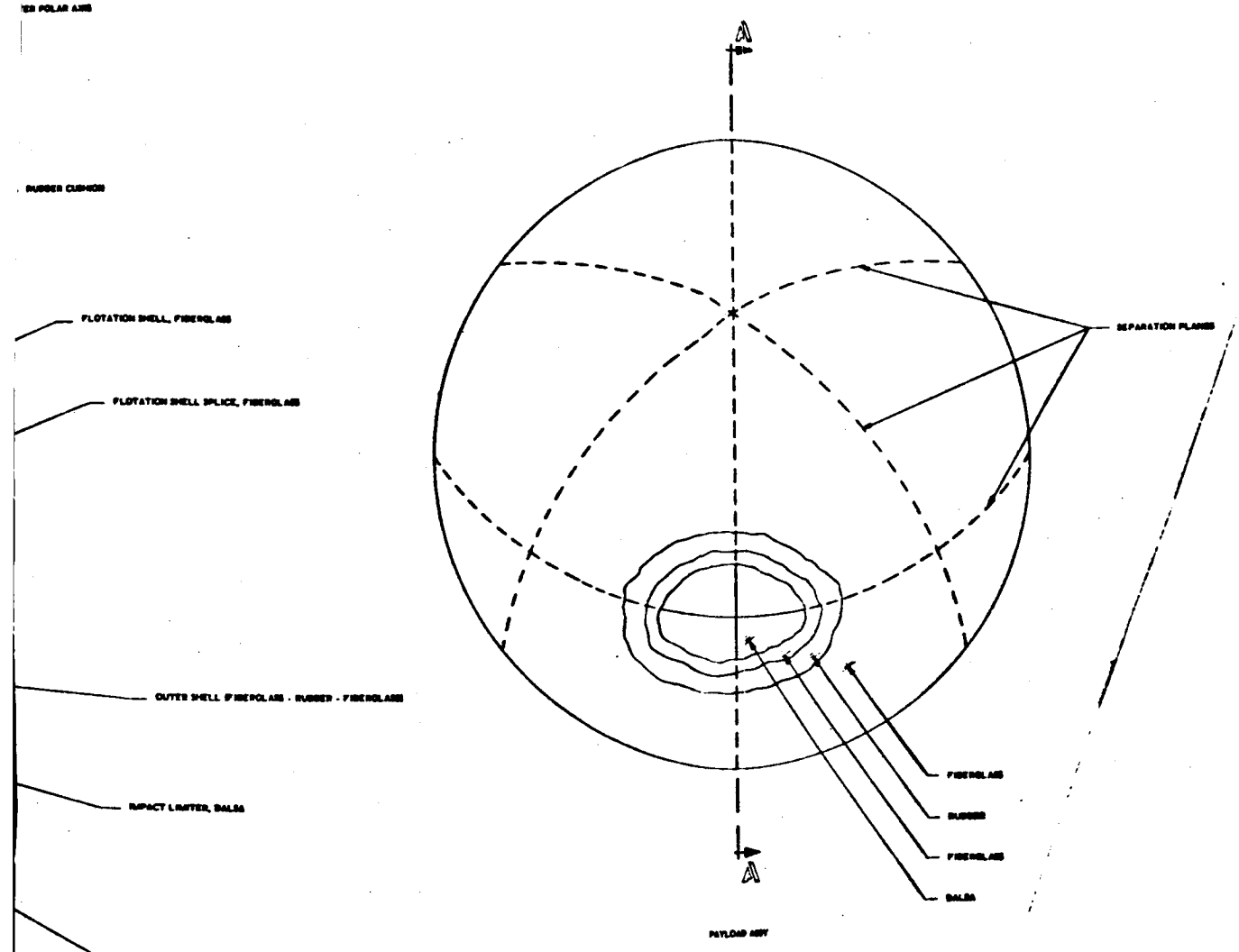

87528-2

FIGURE 2-2B. LANDING SPHERE ASSEMBLY

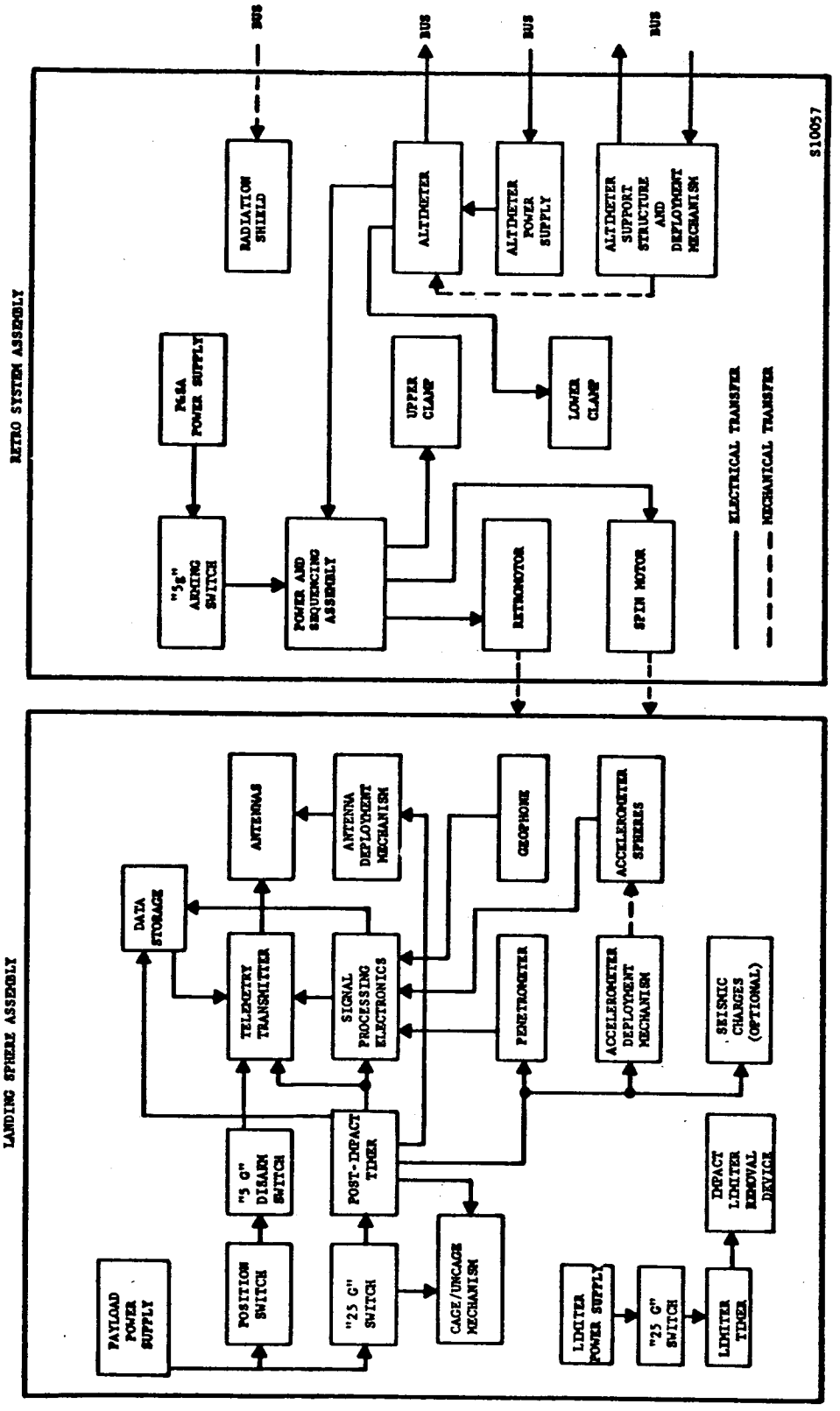

FIGURE 2-3. SURMEC BLOCK DIAGRAM

cutter is located on the erected payload sphere and is positioned to fire upward for removal of the upper portion of the flotation shell. The inflatable antenna and the accelerometer sensor spheres are positioned for deployment through this opening. The payload structure also contains the required sensor deployment mechanisms, signal electronics, data storage unit, 960 mc telemetry transmitter, power supply, post-impact timer, inertia switches, water tanks for evaporative cooling, thermal control valve, penetrometer, geophone, and a fixed backup antenna.

3.0 SEQUENCES

3.1 General Description

3.1.1 Operational Modes

3.1.1.1 Launch

When launch acceleration exceeds 5g for 1.5 seconds a switch arms the P&SA in the retrosystem assembly. This arming procedure is inserted as a safety feature to isolate the P&SA power supply from the rocket motor squib circuitry until after launch.

3.1.1.2 Descent

Completion of the spacecraft terminal maneuver aligns the capsule assembly roll axis with the predicted relative velocity vector. At approximately 40 minutes prior to impact a command signal, which is timed and powered from the bus, fires a b[illegible]utter which releases the altimeter and its parabolic antenna from the stowed position so that the boresight of the antenna is aligned parallel to the capsule roll axis. Following this the bus releases a clamp and the omni-directional antenna is deployed away from the capsule by means of a boom. This also releases the radiation shield retraction mechanism so that the flexible shield collapses to the base of the retromotor support structure.

At approximately 60 seconds before unbraked impact the bus again provides power to actuate a switch which turns on the altimeter. This turn-on allows for a 15-second warmup time and a 25-second uncertainty time in bus impact prior to 180,000 feet altitude (20.6 seconds before bus impact). At fuzing altitude (approximately 70,000 feet)

the altimeter closes a relay which in turn connects bus power to four redundant lower separation clamp bolt cutters on the retromotor support structure. Simultaneously, bus power fires two parallel squib switches which activate the P&SA.

The P&SA contains three electrical timers which are started simultaneously. The first of these is a spin motor timer which provides a nominal delay of 215 milliseconds. The delay of spin motor ignition is 20 milliseconds. Lower bound tolerances assure that the spin motor ignition always occurs after clamp opening. Spin motor burning time does not exceed 1.3 seconds.

The second P&SA timer accomplishes firing of the retromotor. The nominal delay (from altimeter fuzing) of this circuit is 2 seconds and varies up to $\pm$ 0.3 seconds depending upon the measured mean temperature of the propellant. The retromotor burns for about 9.6 seconds. Nominal burnout altitude is 1,000 feet at which time the descent velocity is nominally zero. The dispersions in burnout altitude are such that burnout occurs prior to impact for approximately 99 percent of the cases.

The third P&SA timer is used to fire two upper clamp bolt cutters which separate the empty retromotor case from the landing sphere. It has a nominal delay of 12.5 seconds after P&SA initiation.

3.1.1.3 Post Impact

In order to initiate the remaining sequence of functions, two separate timer and inertia switch assemblies are required. One is located in the payload and the other within the impact limiter. A squib switch in the impact limiter is closed during retrobraking when the 25g inertia switch is closed for more than 1 second. This activates the timer which after 3 minutes provides a signal to remove the impact limiter.

A squib switch in the payload is closed during retrobraking when a 25g inertia switch is closed for more than 1 second. This switch initiates (with essentially no delay) pre-impact uncaging, turns on the payload electronics, and also activates a sequence timer which:

(a) After 13 minutes fires the penetrometer, which also serves to vent the flotation fluid and coolant system, and fires the shell cutter device which removes the upper portion of the flotation fluid shell, permitting the inflatable antenna to erect.

(b) After 28 minutes initiates data transmission from the data storage unit (failure of the high-gain antenna to erect leaves the transmitter coupled to the fixed backup antenna and data readout set at a low level).

(c) After 29 minutes fires the release device to launch the first accelerometer sensor sphere, whose impact data is transmitted in real time as well as stored.

(d) After 30 minutes and again after 31 minutes transmits the data in the data storage unit.

(e) After 32 minutes and at succeeding 3 minute intervals repeats the cycle of (d) and (e) above with each of the remaining accelerometer sensor spheres.

(f) After launch of the last sphere, continues to transmit the data contained in the data storage unit at one-minute intervals until expiration of the power supply.

3.1.2 Tabular Resume

The sequential events which occur during the terminal and post-impact phases are summarized in Table 3.1.2.-1 and illustrated in Figure 3.1.2-1.

3.1.3 Peripheral Support

In order to satisfactorily complete all events it is necessary for the bus to:

TABLE 3.1.2-1

TERMINAL AND POST-IMPACT SEQUENCE OF EVENTS

Nominal Time	Event	Initiated by
T_1* - 40 min	Deploy altimeter Deploy omni antenna Retract radiation shield	bus
T_1 - 60 sec	Turn on altimeter	bus
T_1 - 45 sec	Altimeter warmed up	-
T_1 - 8.1 sec = T_2	Fuzing altitude Fire P&SA squib switches Fire lower clamp bolt cutters	Altimeter
T_2 + 6 msec	Start P&SA timers	Squib switches
T_2 + 175 msec	Lower clamp separation completed	
T_2 + 221 msec	Signal spin motor ignition	P&SA timer
T_2 + 2 sec	Start retromotor ignition	P&SA timer
T_2 + 5.2 sec = T_3	Start post-impact timer Pre-impact uncaging Turn on Payload electronics Start impact limiter timer	Payload 25g switch Limiter 25g switch
T_2 + 11.6 sec	Retromotor burnout	-
T_2 + 12.5 sec	Upper clamp separation	P&SA
T_2 + 32 sec	Landing sphere impact	-
T_3 + 3 min	Remove impact limiter	Limiter timer
T_3 + 3 to 13 min	Erect to vertical	Post-impact timer

TABLE 3.1.2-1 (Continued)

Nominal Time	Event	Initiated by
T_3 + 13 min	Activate shell cutter Deploy penetrometer, store data Erect High-gain antenna	Post-impact timer
T_3 + 13 to 28 min	DSIF acquisition	-
T_3 + 28 min	Transmit stored data (uses fixed antenna and low data rate if high-gain antenna has not erected)	Post-impact timer
T_3 + 29 min	Launch first sensor sphere Transmit data, real time Store data	Post-impact timer
T_3 + 30 min	Retransmit stored data	Post-impact timer
T_3 + 31 min	Retransmit stored data	Post-impact timer
T_3 + 32 min	Repeat cycle of launch-transmit-store-retransmit at 3 min intervals	Post-impact timer
	Repeat last data transmission to end of battery life	Post-impact timer

*T_1 is the time of bus unbraked impact.

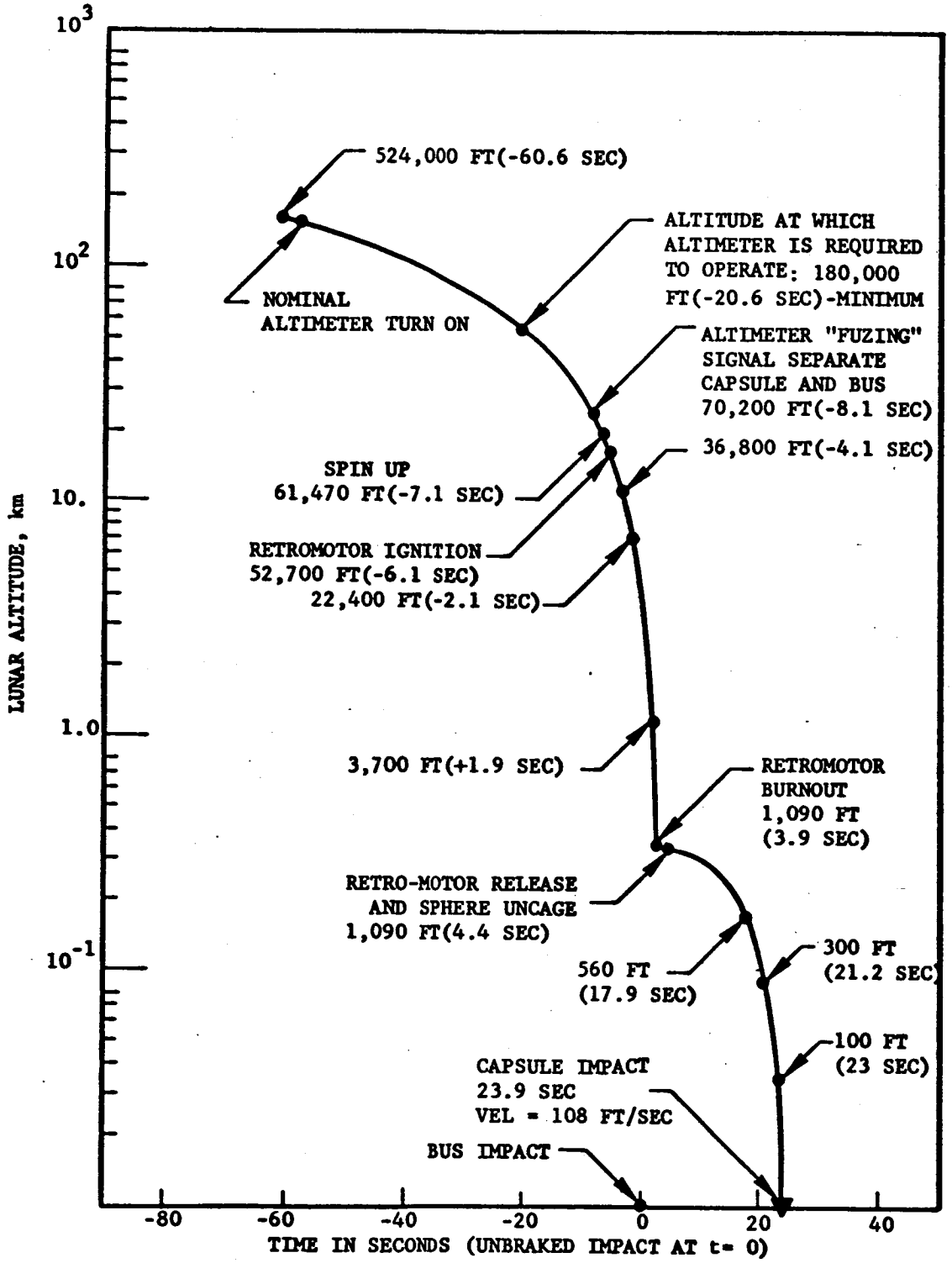

FIGURE 3.1.2-1. TERMINAL SEQUENCE OF EVENTS

(a) Align the capsule assembly roll axis with the predicted relative velocity vector

(b) Provide command signals which are both timed and powered from the bus to:

(1) Release the altimeter deployment mechanism

(2) Release the omni-directional antenna and radiation shield

(3) Actuate a thermal switch to turn on the altimeter

(c) Provide power to:

(1) Activate the four bolt cutters on the lower separation clamp, and

(2) Activate two squib switches which start the P&SA timers.

3.1.3.2 Capsule

Other than those operations mentioned above which require bus energy, all timers, inertia and squib switches, power supplies, pyrotechnic and propulsion systems required to adequately perform the sequencing operations will be supplied by either the SURMEC retrosystem assembly or landing sphere assembly.

3.2 Engineering Data

3.2.1 Commands

After release from the spacecraft bus, that portion of the capsule assembly which undergoes the retromaneuver is autonomous, requiring no additional command inputs to perform its assigned functions. Subsequent major events are conducted sequentially by series and parallel timing mechanisms in the P&SA and within the landing sphere assembly.

3.2.2 Measurements (excluding the scientific experiment)

3.2.2.1 Retrosystem Assembly

When the altimeter is fully deployed an electrical microswitch on the altimeter support structure is

closed, which provides a signal to the bus telemetry system confirming this event. Also, during altimeter operation a means of generating a dc signal that is indicative of the reflected power received by the altimeter is provided to the bus for the purpose of telemetering this information to earth. The bus also monitors the altimeter fuzing signal and spin motor separation from the spacecraft.

3.2.2.2 Landing Sphere Assembly

The payload transmitter coupled to the fixed antenna is activated just prior to impact. Immediate signal acquisition by DSIF would permit a gross detection of failure during impact. After impact, the transmitted signal characteristics will also be altered significantly during removal of the impact limiter. Failure of the high-gain antenna to erect for any reason will be detectible by a continued low-level signal and the reduced rate of data transmission. Other direct post-impact failure detection is limited to monitoring the internal thermal environment. The voltage controlled oscillator that controls the data subcarrier and the crystal controlled oscillator that controls the carrier are both temperature sensitive and are calibrated prior to launch. Detection of failure modes other than these must be indirectly deduced from a relative diagnosis of signal magnitude and content.

4.0 PERFORMANCE CHARACTERISTICS

4.1 Flight Control

4.1.1 General

After bus initiation of the terminal sequence the retrosystem assembly, with the aid of those inputs from the bus described in 3.1.3.1, delivers the landing sphere assembly to a nominal altitude of 1,000 feet above the lunar surface at zero descent velocity. There shall be no electrical connections between the landing sphere assembly and the retrosystem assembly.

4.1.2 Altimeter

A radio altimeter is required which radiates energy to and receives its own reflected radiation from the lunar surface for the purpose of determining when the bus has reached the correct altitude for separation of the lunar capsule. The altimeter shall be the only means for initiating this separation from the bus. A means of generating a dc signal which is indicative of the received reflected energy will be provided for the purpose of telemetering this information to earth. The altimeter shall be capable of being deployed from a stowed position to point at the lunar surface along the spacecraft roll axis. Although the altimeter is deployed and activated by command from the bus, it shall contain its own power supply.

4.1.3 Spin Rocket Motor

A solid propellant spin motor assembly is required to develop and deliver axial rotation to stabilize the retromotor/landing sphere assembly. Its exhaust nozzles will be canted to deliver a forward impulse to the assembly as well as torque. Spin motor ignition is initiated by a command from the P&SA.

4.1.4 Retrorocket Motor

A solid propellant retromotor assembly shall be capable of braking the total landing sphere weight from the nominal bus impact velocity. This velocity is completely removed at a nominal altitude of 1,000 feet above the lunar surface. Retromotor ignition is initiated by a command from the P&SA.

4.1.5 Power and Sequencing Assembly (P&SA)

The P&SA is required to initiate and control the timing of sequential events prior to impact. Its operation is initiated by the altimeter fuzing signal. It shall contain its own source of power.

4.1.6 Separation System

Two clamps are used to temporarily mate the landing sphere to the retromotor and the retromotor to its support structure. Lower clamp separation is initiated by the altimeter fuzing signal, and upper clamp separation is initiated by the P&SA.

4.1.7 Support Structure

A support structure capable of supporting the weight of the entire capsule assembly under all prelaunch, boost and transit environmental conditions must be provided. The structure shall also contain all necessary wiring, a mechanism for attachment to and release of the retromotor, and must be compatible with the bus structure.

4.2 Post-Impact Operations

4.2.1 Erection Method

The payload is floated at neutral buoyancy within the impact limiter. Its center of gravity shall be offset from the center of buoyancy so that the payload axis will be aligned with the local vertical after impact.

4.2.2 Shell Cutter Mechanism

Subsequent to erection, a shell cutting mechanism shall remove the upper portion of the flotation shell. This hole shall be of sufficient diameter to allow the high-gain antenna and accelerometer sensor spheres to be deployed through it.

4.2.3 Antenna Deployment Mechanism

Subsequent to shell cutting, the high-gain antenna must be permanently deployed by the deployment mechanism.

4.2.4 Sensor Sphere Deployment Mechanisms

Launcher mechanisms shall be capable of deploying the accelerometer sensor spheres a nominal distance of 150 feet from the payload assembly by way of a high-loft trajectory.

4.2.5 Penetrometer Deployment Mechanism

The penetrometer deployment mechanism shall be capable of driving the penetrometer vertically downward through the flotation shell and into contact with the lunar surface at high velocity. Reaction forces on the payload assembly shall be held to a minimum. The deployment mechanism shall also serve to cage the payload within the flotation shell.

4.3 Communication

4.3.1 Antennas

4.3.1.1 High-Gain Antenna

The inflatable high-gain antenna shall be capable of pneumatic inflation and shall approximate omni-directional coverage over a hemisphere for data transmission.

4.3.1.2 Fixed Antenna

The fixed back-up antenna shall approximate omni-directional coverage over a hemisphere for data transmission.

4.3.2 Transmitter

The L-band transmitter located within the payload operates at approximately 960 mc and shall have a power output of not less than 2 w and an information bandwidth of not less than 85 cps.

4.3.3 Data Storage Unit

The data storage unit shall be capable of sustained retention and repeated readout of a minimum of 1200 bits of data.

4.4 Scientific Experiments

4.4.1 Impact Acceleration Data

The accelerometer sensor spheres shall be capable of obtaining accurate acceleration versus time data during their impact on the lunar surface following launch from the payload assembly. The sensors shall have omni-directional sensing capability. Data of definitive quality shall be obtained for surfaces ranging from very soft unconsolidated material, so that a bearing pressure of 10 psi will allow penetrations up to 1 foot, to consolidated materials having compressive strengths of up to 500 psi. Surface strengths beyond 500 psi shall be indicated but not necessarily measured.

4.4.2 Penetrometer Data

The penetrometer shall be capable of obtaining accurate acceleration versus time data during its penetration of the lunar surface.

The sensing capability need only be unidirectional.

4.4.3 Acoustic Reflection Data

The geophone shall be capable of obtaining amplitude versus time data from the sound transmitted through the lunar surface material from the impacting accelerometer spheres or from detonation of a small charge. The mechanization of this secondary experiment is to be recommended by JPL.

4.5 Environmental Control

4.5.1 Impact Limiter

The impact limiter shall be capable of protecting the payload from damage after a lunar gravity free-fall of nominally 1,000 feet with no initial velocity. The impact limiter shall remain intact after the fall but be capable of explosive removal.

4.5.2 Thermal Controls

Passive temperature control shall be provided to insure mission success under direct solar radiation. A radiation shield shall contribute to this protection during earth-to-moon transit, and a water boil-off thermal control system contained within the payload sphere shall maintain allowable payload temperatures during lunar operation.

SYSTEM DESIGN RESTRAINTS

1.0 ENVIRONMENT

The capsule components must be designed to survive and operate satisfactorily through the environmental stages listed in Table 1-1. These are designated as:

(a) Condition I: ground handling through lunar flight

(b) Condition II: ground handling through spin-up

(c) Condition III: ground handling through retrothrust

(d) Condition IV: ground handling through impact and lunar operation

The expected environmental levels are listed in Tables 1-2 through 1-5.

2.0 VEHICLES

2.1 General

2.1.1 Weight

The total weight of the capsule system shall not exceed 333 pounds.

TABLE 1-1

Condition	Events	Major Equipment
I	Ground handling Launch and Lunar flight	Altimeter and support and deployment mechanism Radiation shield and retraction mechanism Lower separation clamp Retromotor support structure Wiring harness and junction box
II	Condition I plus Spacecraft Separation and Spin-up	Spin motor
III	Condition II plus Retrothrust	P&SA Vibration dampers Upper separation clamp Retromotor
IV	Condition III plus Impact and Lunar Operation	Landing sphere

TABLE 1-2

VIBRATION ENVIRONMENT

(Applies to all Defined Conditions)

	Sinusoidal		White Noise		Combined Sine	Combined Noise
Thrust Axis						
Magnitude	± 3"*	± 2.5g	7.5g**	5g	2.25g	2.25g
Bandwidth, cps	1-2	2-40	15-1500	15-1500	40-1500	15-1500
Duration	8 min; COSR***		6 sec	3 min	3 times, 2 min each; COSR for sinusoid	
Pitch Axis						
Magnitude	± 3"	± 1.25g	3.75g	2.25g	1.125g	1.125g
Bandwidth, cps	1-2	2-40	15-1500	15-1500	40-1500	15-1500
Duration	8 min; COSR***		12 sec	3 min	3 times, 2 min each; COSR for sinusoid	
Yaw Axis						
Magnitude	± 3"	± 1.25g	3.75g	2.25g	1.125g	1.125g
Bandwidth, cps	1-2	2-40	15-1500	15-1500	40-1500	15-1500
Duration	8 min; COSR***		12 sec	3 min	3 times, 2 min each; COSR for sinusoid	

* Where "±" is shown, peak values are implied.

** Where "±" is not shown, rms values are implied.

*** Constant Octave Sweep Rate

TABLE 1-3

THRUST-GENERATED ACCELERATION AND SPIN ENVIRONMENT

	Linear Acceleration (g)	Angular Acceleration (rad/sec^2)	Spin Rate (rpm)
Condition I			
Thrust Axis	+ 7, - 2	-	-
Yaw and Pitch Axes	± 2	-	-
Condition II			
Thrust Axis	+ 7, - 2	30	287
Yaw and Pitch Axes	± 2	-	-
Conditions III, IV			
Thrust Axis	+ 65, - 2	30	287
Yaw and Pitch Axes	± 2	-	-

TABLE 1-4

IMPULSIVE SHOCK ENVIRONMENT

	Amplitude*	Duration
Condition I, II, III		
Thrust Axis	20g peak	3 millisec
Yaw and Pitch Axes	6g peak	3 millisec
Condition IV (any direction)	3,000g peak (Integral up to 200 ft/sec)	4 millisec

* 1/2 sine wave

TABLE 1-5

TEMPERATURE, PRESSURE AND HUMIDITY ENVIRONMENT

	Temperature (°F)	Pressure (mm Hg)	Humidity (% RH)
Condition I, II, III			
Pre-launch	+ 20 to + 125 puls solar radiation	774	100
Space flight	Direct solar radiation where exposed; radiation to 0°R where shaded.	0	-
Condition IV	+ 260 max	10^{12}	

2.1.2 Center of Gravity

The center of gravity of the entire capsule system as installed (altimeter in stowed position) on the bus shall lie within 30 inches of the bus/capsule support structure interface. The misalignment of the thrust axis of the rocket motor and the bus longitudinal axis (as defined by the bolt circle surface) shall not exceed 0.1 degree. The center of gravity of the separated capsule assembly shall not be displaced more than 0.03 inch from the nominal retrothrust axis.

2.2 Power System

2.2.1 Power and Sequencing Assembly

A sealed batter pack is to be used as the sole source of power for the pre-impact sequencing unit and must be small enough to be completely contained with the P&SA unit. It shall provide for an operating period of 16.5 seconds. At no time during operation shall the open circuit voltage be greater than 28 volts nor the terminal voltage less than 14 volts. It shall be capable of providing a continuous current drain of 30 milliamperes plus three (non-simultaneous) current pulses: two 3-ampere pulses each of 1 second duration and one 4-ampere pulse of 100 milliseconds duration. The battery pack should be rechargeable through five cycles.

2.2.2 Altimeter

A power supply, including a sealed battery pack, converters and regulators shall be an integral part of the altimeter system. It shall provide for an operating time of two minutes. At no time during operation shall terminal voltage be less than six volts nor more than nine volts. It shall be capable of providing a maximum peak current drain of five amperes. The battery pack should be rechargeable through five charge/recharge cycles.

2.2.3 Landing Sphere

A sealed battery pack shall be located in and used as the sole source of power for the payload.

2.3 Flight Control

2.3.1 Retrorocket Motor

The retrorocket motor is required to serve as the braking device for a vehicle weighing approximately 308 pounds including the motor weight. The motor with suitable attach devices shall serve as a primary structural member of the capsule system in such a way as to permit separation from the spacecraft structure and separation from the landing sphere assembly. The retromotor shall decelerate the landing sphere in gravity-free vacuum space by approximately 8816 feet per second and shall provide reasonable assurance that burnout will occur at an altitude between 0 and 2000 feet above the lunar surface. The motor shall be of nearly symmetrical configuration so that a condition of dynamic balance may be achieved. The motor shall support the approximately 93-pound weight of the landing sphere plus attachings mounted along the thrust axis on the head end of the motor. The retromotor shall also serve as the structural support for the spin system in such a way as to permit jettisoning of the spin system during retromotor ignition.

2.3.2 Spin Rocket Motor

The spin motor assembly shall be required to develop and deliver to the retromotor/landing sphere assembly a torque to accelerate this assembly to a spin rate of approximately 285 rpm. The spin axis is to be coincident with the retromotor thrust axis. The torque vector shall not be misaligned from the retrorocket centerline by more than 0.010 radians. The spin motor is to be mounted so that the spent motor case can be jettisoned shortly after retromotor ignition. The spin unit ignition shall be sequenced by a signal from the P&SA. The unit must ignite promptly and reliably upon receipt of the signal with a desired minimum probability of ignition of 0.995. It shall be of symmetrical configuration so that a condition of dynamic balance may be achieved.

2.3.3 Support and Separation

The support and separation assembly serves as the primary structural member for transmitting loads from the bus to the capsule. The forward end of the support assembly is attached to the rocket motor

case continuously about the circumference of the case. Separation must occur at this plane on receipt of a command signal from the altimeter assembly. The misalignment of the bus longitudinal axis (as defined by the bolt-circle of the bus) and the thrust axis of the rocket motor shall not exceed 0.1 degree. Exposure to the launch environment shall not produce an additional misalignment which exceeds 0.1 degree. The complete separation process shall not produce a capsule angular rate which exceeds 0.04 radian/sec.

2.3.4 Altimeter

Erection of the altimeter shall be accomplished in no less than 5.2 seconds. The delay between the bus-generated commands for deployment of the altimeter and the omni-antenna shall be no less than 5 seconds. The antenna is to be erected at the beginning of spacecraft terminal maneuver (one hour before landing). The erection mechanism will attach to the bus structure. When the antenna is in the operating position it will project over the side of the bus, and its beam axis must be parallel to the roll axis of the spacecraft. The antenna beam axis shall be within 0.25 degree of normal to a reference plane defined by three points on the antenna structure.

The altimeter is to start operation upon receipt of a command signal and deliver a single output signal (designated "fuzing signal") at a prescribed altitude (designated "fuzing altitude"). The altimeter will not be separated from the bus. The altimeter shall start within 1 second after receiving a start signal voltage step of 18 to 30 volts. The altimeter shall not cause any interference with other r-f equipment on the bus operating in the vicinity of 890 and 960 mc. The altimeter is to be started at a time before bus impact such that warm-up will be complete at an altitude of not less than 180,000 feet. The pulse repetition frequency shall be between 500 and 600 pps, and warm-up time shall not exceed 15 seconds. To prevent false fuzing under these conditions, warm-up shall not begin at an altitude in excess of 820,000 feet. During the time of operation of the altimeter the approach velocity to the moon will be between 8400 and 9400 feet per second. The fuzing altitude shall be set at a point between 61,800 and 81,800 feet. The altimeter shall provide a range resolution accuracy such that the cumulative errors from all effects (range measurement, antenna boresighting errors, switching time, etc.) shall result in a measurement error of no greater than 500 feet at the fuzing altitude. The altimeter shall operate and shall be capable of delivering a fuzing signal for a period of not less than 120 seconds following warm-up. The altimeter shall have a probability of false fuzing, from maximum starting altitude, of not greater than one percent.

2.3.5 Impact Limiter

The impact limiter shall be nominally transparent to radio frequency energy. It shall be adequate to sustain impact normal with the lunar surface at velocities up to 200 feet per second. An interconnect member, adequate to attach the sphere to the retromotor throughout the flight environment shall be attached at one end (along the thrust axis) and shall provide a means of separating the landing sphere from the rocket after rocket motor burnout. A similar clamp device and attach fitting shall be provided on the opposite end, along the thrust axis to support the spacecraft omni-antenna.

2.3.6 P&SA

The P&SA shall consist of equipment and circuitry for sequencing the terminal events just prior to lunar impact. It shall possess a means for isolating the battery supply from the timers and squib circuits until after launch acceleration exceeds a nominal value of 5g for 1.5 seconds. The sequencing unit and the batteries shall be self-contained.

3.0 SCIENTIFIC EXPERIMENTS

Operation of the accelerometer sensor spheres shall be compatible with the surface characteristics listed in Table 3-1.

4.0 COMMUNICATIONS

4.1 Antenna

The data from the experiments are to be transmitted from the moon to DSIF. The antenna shall be compatible with communication angles of from 0 to 45 degrees. (The communication angle is defined as the angle between the earth-moon line and the lunar local vertical.)

4.2 Transmitter

Subsequent to mounting the capsule on the bus the transmitter shall not be operative until after retro-ignition. The carrier shall be 960 mc in the L-band and shall be phase modulated. If subcarriers are employed, they shall be standard IRIG channels.

TABLE 3-1

LUNAR SURFACE CHARACTERISTICS

A. Particle size: Smooth areas of the lunar surface at a scale of the spacecraft or less consists of granular material, perhaps loosely sintered in parts, of grain size range 1-300 microns.

B. Insulation properties: The material is highly insulating ($K P C = 10^{-6}$ in CGS units where K = thermal conductivity, P = density, and C = specific heat of the material).

C. Underlying layer: Underlying the surface material or perhaps exposed on the surface at places will be rock.

D. Bearing Strength: In areas of unconsolidated material, a bearing pressure of ten psi will cause depressions of no more than one foot. Exposed rock will have compressive strengths ranging from 4,000 to 25,000 psi.

E. Hardness: For the purpose of surface penetration, the underlying or exposed rock described in C and D may be assumed to have an indentation hardness as high as seven on the Moh scale.

F. Slopes: Slope conditions averaged over distances on a large scale may be assumed not to exceed 15°. However, local slope conditions, on the scale of the spacecraft, may exceed this value.

G. Protuberances: Surface protuberances in an area of comparable dimensions to the spacecraft may be assumed not to exceed ten centimeters.

5.0 OPERATIONS AND TEST PLAN (EFFECT ON CAPSULE DESIGN)

The landing sphere assembly design shall be based primarily on environments expected from the time of final mating onward through launching and flight. Its components shall not be subjected to environments beyond flight-acceptance levels, and the burden of protection from overexposure shall be on operators and facilities rather than on the landing sphere assembly itself.

High mission reliability must be attained without dependence on checkout instrumentation, control, and correction of deficiencies in the landing sphere assembly after completion of assembly. Subsystems must be designed to maintain operating ability and to hold calibration from the time of assembly to flight.

Except for gross system checkout and tests to verify the compatibility between the capsule and the spacecraft bus, design constraints do not permit testing, trouble shooting nor component replacement beyond final assembly.

All elements of deliverable capsules which can be tested nondestructively must pass acceptance tests. Acceptance tests are environmental and functional tests of the specific components, subsystems and systems which are scheduled for flight. These tests demonstrate that the flight units satisfy the designs and specifications.

6.0 PACKAGING AND WIRING

All electrical, electronic, and electromechanical parts in the capsule will be procured to Minuteman, Space Parts Working Group, or equivalent Aeronutronic-generated high reliability specifications. To the extent practicable modular scheme of packaging of electronic equipment shall be used. The external wiring system for the capsule is used for transmission of electrical signals for controlling terminal events prior to lunar impact. A portion of the system shall also be used to provide telemetry information to the bus telemetry system.

7.0 STERILIZATION

Direct action shall be taken to deliver the capsule system in a bacteriologically sterile condition. To do this, all feasible and reasonable engineering precautions shall be exercised by subjecting the various system elements to one or more of the following:

(a) heat-soaking components and subassemblies at 257 degrees F for 24 hours,

(b) using sporicidal resin systems,

(c) using liquid sterilizing additives to non-metallic components,

(d) using surface sterilizing agents during interfacing operations, or

(e) exposing to ethylene oxide/Freon 12 gas mixture,

and conducting assembly operations, where required, in a sterile environment.

8.0 INTERFACE PROBLEMS

Mechanical mating of the capsule system to the bus is limited to the landing sphere/JPL omni-antenna interface, the retrosupport structure/bus interface, and the altimeter/bus interface. These operations shall be accomplished within tolerances which conform to sections 2.1.2, 2.3.3, and 2.3.4. The design of the capsule should be such that it will not interfere with the shroud envelope.

A junction box capable of exchanging all signals necessary to meet the capsule/bus electrical interface shall be provided.

EVOLUTION OF SYSTEM DESIGN CHARACTERISTICS

1.0 MISSION OBJECTIVES AND GROUND RULES

When the Apollo manned mission to the moon was elevated to a position of high national priority with the ambitious objective of getting a man to the moon and returned during the 1960's, it became strikingly apparent that more detailed information was required on the characteristics of the lunar surface. The predictions of the lunar surface characteristics based on the meager scientific data available varied from flat, smooth surfaces to rocky crags and deep crevasses, and from hard rock-like material to deep layers of fluffy dust. The landing devices of an Apollo vehicle designed for the worst surface condition would easily claim over 50 percent of the allowable payload weight. For a more favorable landing surface, the landing gear could likely be reduced to less than five percent of the payload. Moreover, many millions of dollars and months of delay could be saved by designing to a more definitely known set of lunar surface characteristics rather than for all possible conditions.

In the U. S. space program, the only operation space vehicle system capable of delivering payloads to the moon during the 1961 to 1964 time period is the Ranger system. The Ranger utilizes the well-proved Atlas booster and Agena B upper stage. The Ranger Spacecraft mounted on the Agena B is capable of delivering payloads to the vicinity of the moon on an impact course. By late 1961, the development of a semi-hard-landing capsule capable of placing a payload of instruments on the lunar surface was well advanced to the point of having a high degree of confidence in its successful operation. A sensitive seismometer developed by JPLW as assigned as the first instrument to be landed by this capsule.

The question then raised was whether this same Ranger payload delivery system, already well along in development, could place other instruments on the moon capable of obtaining data in the two categories specified as most urgently needed for the Apollo vehicle design effort:

(1) Detailed surface topography

(2) Surface strength properties

A unique high-resolution facsimile approach to obtaining data in surface topography has evolved and has been designated the Lunar Surface Photo-reconnaissance Capsule (LSPC). The LSPC is completely compatible with the Ranger delivery system and requires modification only to the instrument compartment. The objective which remained was to obtain detailed surface strength properties. This was the mission specified for the Lunar Surface Measurement Capsule (SURMEC).

2.0 DISPERSED SAMPLING

With a payload established safely on the moon via the Ranger system, the problem remains to do meaningful surface testing. To confine such surface testing to that point where the Lunar capsule comes to rest would give very limited, perhaps misleading, information. For example, the capsule could stop on a small localized formation with properties in no way typical of the surrounding terrain. There is also the possibility that the surface characterisitics could be materially influenced by the presence of the capsule itself. Hence, it was concluded that the lunar surface must be tested at a number of locations over as wide an area as possible. A number of studies were initiated of various creeper, crawler, walker, roller, and other types of vehicles for traversing the lunar terrain. Such vehicles did not prove compatible with the rather small allowable payload sphere of less than twelve inches in diameter in the Ranger system. To be capable of traversing any large-scale surface irregularities, such vehicles would have to be unfolded or inflated manyfold. Within the total allowable payload weight of less than 40 pounds all such "expandable" roving vehicle designs appear too flimsy to withstand any of the tumbling or impact which might be encountered while traversing the lunar terrain.

In other areas of locomotion, the "pullers" and "hoppers" indicated improved chances of moving about on almost any type of terrain. The puller vehicle could project an anchor ahead of it and then reel itself toward the anchor. However, such a vehicle still has a fair chance of becoming jammed on a rough and irregular terrain. The rocket-propelled

hopper is probably most independent of the terrain in that its reaction force is completely independent of the nature of the surface and would tend to propel the capsule even though it be burried beneath a layer of dust or lodged in the bottom of a fissure. Preliminary design effort was initiated on such a hopping vehicle, but this effort soon bogged down in rapidly multiplying mechanical design problems. For example, the capsule would have to be erected to the vertical at the end of each hop to properly align the rocket motor or motors for the next firing. The flotation fluid employed in the Seismometer Capsule could not be readily employed as an erection mechanism because of a hole in the outer sphere must be provided to permit exhaust of the rocket jet. Multi-aperture assemblies and roller-bearing devices to permit alignment of the rocket nozzles with apertures in the outer container were all subject to jamming by lunar surface dust and aggregate.

Concurrent effort investigating meaningful experiments and instruments was rapidly indicating that a great deal of quantitative information on the scientific and engineering properties of the lunar surface could be obtained from an analysis of the acceleration profile upon impact of a sphere on the surface. Emphasis on impact acceleration data, rather than radiating, probing, or drilling, led to the concept of not attempting to move the lunar capsule, but rather of projecting small spherical instruments from the main sphere and recording acceleration data from impacts dispersed over a reasonably wide area. This concept promised to achieve the objective of a large sample of surface measurements made in a controlled manner over a reasonably wide representative area, while at the same time maximizing the change of obtaining useful data no matter what type of lunar surface might be encountered. This design concept of a fixed payload assembly and projected sensors was adopted as the basic design approach of the SURMEC system.

3.0 SENSORS

By mid-1960, NASA scientists at the Langley Research Center were well progressed in an investigation of acceleration profiles from impacting spheres as a potential means of determining the lunar surface characteristics. Impacts of spheres of varying weights and diameters over a wide range of velocities on surface materials such as concrete, lead, balsa, soil, sand, peat moss, and various layers of one on another indicated that very distinct acceleration versus time signatures were obtained which clearly characterized one type of surface material from another. Moreover, promising success was achieved in correlating parameters such as the sphere diameter, mass, velocity, acceleration, and depth of penetration to make it possible to apply the results to a wide range of objects, including the landing gear of an Apollo landing vehicle.

Impact sphere sizes tested at Langley ranged from one to three inches in diameter and indicated that this was a satisfactory size range. Piezoelectric crystal sensors were employed at Langley to sense the acceleration within the impacting spheres. Special cable of carefully controlled impedance properties was employed to conduct the data signal to appropriate amplifiers and recording instruments.

While piezoelectric crystal accelerometers are highly accurate and well-proved devices, the handling of their signal output presented problems to the SURMEC design. As the direction of impact of the sensor spheres on the surface is not predictable, an omni-directional acceleration sensing capability is required. This would mean placing three crystal sensors in each sphere, then electronically squaring each output, and adding the sum of the squares. As it was desired to impact the sensors at least 100 feet or more from the payload assembly to obtain an area sample of data, the transmission of the sensor signal to the earth-directed RF transmitter in the payload became a problem. While high miniaturized independent power supplies, amplifiers, and transmitters could probably be developed for packaging within a three-inch diameter sphere, this would require a rather extensive development program consuming valuable time, and would also present a formidable challenge for each of the sensor spheres. Direct wire signal conduction would be preferred, but piezoelectric crystals present attenuation problems when transmitting their output over more than ten to twenty feet of cable. Thus, while a cable is much to be preferred over individual power supplies and transmitters in each sensor sphere, the crystal accelerometers would probably still require a separate amplifier circuit in each sensor sphere. For schedule and reliability reasons, the SURMEC design selected a wire or cable means of transmitting the acceleration data from each impacting sensor sphere to the parent payload assembly for processing and transmission to earth. While the use of three-axis piezoelectric accelerometer sensors with squaring, summing and amplifying circuits in each impacting sphere is undoubtedly feasible, an alternate sensor was recommended for further investigation and feasibility development. This sensor is based on the principle that the hydrostatic pressure developed in a column of fluid is directly proportional to the acceleration imposed on the fluid; thus the pressure at the center of a spherical cavity of fluid within each sensor sphere would be directly proportional to the acceleration of the sphere upon impact with the lunar surface. As the cavity is symmetrical, the acceleration-sensing ability is omni-directional in nature. Placing a pressure transducer at the center of the liquid cavity presents some problem in disrupting the symmetry of the fluid cavity, so that an alternate of placing two transducers on opposite sides of the cavity was proposed. The average of their readings represents the pressure desired

at the center of the fluid cavity. Pressure transducers of small size and high signal strength are desired for this application. Recently developed transducers employing silicon strain gauges directly bonded to diaphragms are uniquely suited to this application, in that they have not only the desired small size and high signal output but are also quite insensitive to shock loading.

Obtaining the maximum number of data points dictates that as many sensor spheres as possible be employed. Within the limited payload size, this requires that the sensor spheres be as small in diameter as possible. Moreover, it is desired to maximize the depth of penetration to obtain surface characteristics down through any possible thin surface crust material, which also dictates spheres of small diameter. The practical lower bound of this diameter is the size required for the sensor elements. The desire to maximize the depth of penetration also dictates that a maximum density be achieved within the sensor sphere.

The resulting sensor spheres, which consist of a minimum-size maximum-density sensor element surrounded by a high-strength metal shell, can minimize the effects of sphere structural deflections on the sensors. An outer coating of a low modulus material, such as epoxy resin, is desired to reduce the peak accelerations and thereby reduce the required range for the accelerometer sensors.

4.0 SENSOR DEPLOYMENT

The experiments at the Langley Research Center produced excellent surface characterization results at sensor sphere impact velocities of from ten to forty feet per second. Impact velocities much higher than this produced no improvement in data while encountering serious cable problems. An impact velocity of approximately thirty feet per second was selected for the SURMEC sensors. Nearly vertical impacts of the sensor spheres are desired from the standpoint of clean data interpretation as well as maximum depth of penetration. However, at the same time it is desired to disperse the sensor impact points as far as possible from the payload assembly, which in turn dictates launch angles approaching 45 degrees. As a compromise, an angle of 20 degrees from the vertical was selected in the initial preliminary design. At this launch angle the altitude attainable is 88 percent of that obtainable from a vertical launch, while the range is still a respectable 65 percent of that obtained from a 45 degree launch. Moreover, the angle is in a range which produces little variation in peak altitude over the possible spread in the launch angle due to misalignment of the payload assembly. Under the foregoing launch conditions, sensor spheres launched along a ballistic path impact nominally 150 feet from

the payload assembly. Later in the preliminary design phase, the additional restriction that the CG of the payload assembly be beneath the center of buoyance to permit erection to the local lunar vertical by flotation techniques required that the launch angle be increased slightly to permit the sensor spheres and their launching mechanisms to be nested lower in the payload structure. The increased launching angle also moved the sensor mechanisms slightly outward within the payload structure, permitting longer strokes for the sensor deployment mechanisms without internal interference between the deployment mechanism housings. The longer stroke is desirable to reduce the peak reaction force on the capsule assembly during sensor ejection.

Of the many energy sources available for projecting the sensor spheres from the payload structure, mechanical springs were employed for their light weight, ease of development, reproducibility, and simplicity. Only the firing of an explosive bolt is required to release the coil spring which ejects the sensor sphere. Providing an individual spring and explosive bolt for each sensor sphere and deployment mechanism maintains independence between the sensors so that the failure of any one does not adversely influence the behavior of the remaining sensors.

The reaction force on the payload section when the spring is released raises the question of whether the payload assembly might be upset or tipped over on the lunar surface. This possibility is minimized by aligning the ejection mechanisms so that the path of reaction passes through the contact point from the payload assembly with the lunar surface. Tipover can then arise only if the assembly should begin to slide along the surface, producing through friction a rolling torque on the capsule. An investigation of static coefficients of friction for typical surfaces indicated that such sliding is not likely, even for launch angles of up to 45 degrees. However, any caging and anchorage provisions which can readily be incorporated in the design will help to insure elimination of this possiblity.

5.0 ACCESS TO SURFACE

The Ranger delivery system requires that the payload assembly be surrounded by a crushable impact limiter to permit survival of the payload upon impact on the moon. Some means must be provided to deploy the sensor spheres through this limiter structure onto the lunar surface. Feasibility tests have indicated that it is practical to explosively propell a "cookie cutter" out through the limiter to produce holes up to at least 3-1/2 inches in diameter. However, launching multiple sensors out of a single such hole would require some means of rotating and pointing

the payload assembly in a fairly precise manner in the desired direction before deploying each sensor. No simple means of doing this was envisioned. An alternative would be to provide a much larger hole, essentially clearing the entire upper hemisphere of the payload assembly to permit launching of the sensor spheres one at a time without reorientation of the payload assembly. A "cookie cutter" to do this would require not only a sizeable explosive charge but would also be prohibitively heavy due to the quite husky barrel required to contain the explosive charge. This then led to the specification of a removable impact limiter for the SURMEC. Experimental results have demonstrated that relatively small amounts of detonating fuse, properly placed, can readily clear the impact limiter material from the outer shell of the payload structure. While the removal can be complete, it is actually desirable to leave enough of the limiter material in a jagged or spiked pattern to promote good seating of the payload assembly upon the lunar surface.

Since electrical connections to a free-floating payload assembly from the impact limiter are difficult to achieve with reliability, it was specified that the removal of the impact limiter be achieved entirely without communication with the payload. Accordingly, an appropriate switch, timer, and detonation mechanism must be located within the limiter structure itself.

6.0 COMMUNICATIONS

To be consistent with the Ranger system and early DSIF capabilities, the SURMEC must employ the 960 megacycle transmitter band. Among the more significant parameters which dictate the amount of information which can be transmitted from the payload on this band are the DSIF gain capabilities, the capsule antenna gain, and the capsule transmitter output. The DSIF capabilities are known for this mission and are essentially fixed. The gain of the capsule antenna can be improved by erecting an antenna structure above the landed payload assembly. The feasibility of such a high-gain antenna capable of pneumatic erection has been demonstrated and adopted for the SURMEC design. The remaining variable is the transmitter output power. A transistorized transmitter is dictated by small volume requirements in the payload as well as the requirement to survive a high "g" initial impact on the lunar surface. The feasibility program on such a transmitter has indicated that as much as five watts might be achieved as a peak output with two watts assured as a minimum value for use in the SURMEC design.

An analysis of the complete communication link performance has indicated that a data band width of up to 93 cycles per second is practical. Direct transmission of the accelerometer data in real time over this band width would limit accurate reproductions of the acceleration profiles to those encountered with relatively soft surfaces of 100 psi or less. Harder limiter surfaces would produce rather sharp peak acceleration pulses which could not be accurately transmitted over the available bandwidth.[1] As surfaces of up to at least 500 psi are of interest to the Apollo vehicle designers, it is desirable to incorporate a data storage unit within the SURMEC payload. While tape recorder units are available which could meet the data capacity, weight and volume requirements, a survey failed to reveal any present or proposed unit capable of surviving the high acceleration of the initial impact on the lunar surface. Solid-state data storage units, on the other hand showed no inherent limitations to survival under such impact conditions, and they also can readily fit within the available weight and volume limitations.

The selected SURMEC communications link accordingly calls for real time transmission of the accelerometer data backed up by repeated transmissions in higher resolution and in delayed time from a solid-state data storage unit.

7.0 SECONDARY EXPERIMENTS

While a majority of selenologists and astronomers believe that the lunar surface can be covered by no more than a few centimeters of dust, there still remains the possibility that a very deep dust layer does exist. Since such a dust layer would greatly complicate the Apollo landing problem, it is highly desirable that the SURMEC return a positive indication if such a layer is encountered. In dust comparable to that found on earth, the impacting capsule should form a crater and be exposed to perform its experiments in the normal fashion. To determine the full depth of the dust layer, a penetrometer has been added to fire vertically downward into the lunar surface with relatively high energy to return an acceleration profile indicating penetration resistance characteristics to a considerably greater depth than possible with the accelerometer sensor spheres.

---

[1] The bandwidth could be extended to approximately 150 cps by utilization of the optional MASER at the DSIF Goldstone Station.

If the dust layer should be extremely fluffy to the extent that the landed capsule is deeply buried, this circumstance can be sensed and preserved by recording in the data storage unit the acceleration profile during the initial lunar impact. Transmission to earth can then be concentrated in a very narrow bandwidth. The obstacle to this is that the high-gain antenna can probably not be erected when covered with a deep dust layer. Accordingly, a slot antenna is provided as a means of transmitting from beneath a lunar dust layer. In this unlikely event of burial, the primary accelerometer experiments cannot be performed, and the entire power capacity of the payload is consumed in transmitting the single set of data from the initial impact on the soft dust layer.

As energy is released into the lunar surface when each of the accelerometer spheres impacts at approximately 150 feet from the payload assembly, there is a good possibility that valuable information on the lunar substructure can be obtained by sensing the acoustic reflections reaching a geophone in the payload assembly. To provide stronger acoustic reflection signals to the geophone pickup, there is available the option of ejecting one or more explosive charges in place of, or as a part of, the accelerometer spheres.

8.0 SUPPORTING SUBSYSTEMS

Other subsystems required in support of the foregoing design features of the SURMEC system are, wherever possible, either identical to or similar in principle to those designs developed for the Ranger Seismometer Capsule. This is consistent with the established ground rule of employing a maximum Ranger development to achieve a capsule operational capability in the minimum time and with the maximum reliability. Thus all subsystems required for delivering the SURMEC payload to the lunar surface are identical to their Seismometer Capsule counterparts. A balsa impact limiter structure is employed, modified only to further increase the survival capability and to permit explosive removal after impact on the lunar surface. The principles of flotation for payload erection and of the caging mechanisms are directly borrowed for the Seismometer Capsule, as is the water thermal control system, and the miscellaneous electrical and mechanical elements required to complete the successful SURMEC mission.

APPENDIX A

SURMEC SENSOR TRADEOFFS

Reference: Aeronutronic Report No. U-1509, "A Lunar Surface Measuring Capsule", January 8, 1962

A.1 SUMMARY AND CONCLUSIONS

(1) The sensor sphere diameter should be minimized. The size of the accelerometer provides a practical lower bound on the diameter.

(2) The stored energy in the spring should be maximized. The size of the spring provides a practical upper bound for this quantity. The spring energy fixes the kinetic energy of the sensor sphere.

(3) For a given sphere diameter the density should be maximized.

(4) The launch angle (measured from the lunar vertical) should be maximized. The coefficient of friction between the capsule outer surface and the lunar surface material provides an upper bound on the angle. In any case, the angle should not exceed 45 degrees.

The effect of (1) and (2) is to maximize the depth of penetration and thereby maximize the data obtained from any one impact. The effect of (3) is to reduce the length of wire for the data link. The effect of (2) and (4) is to maximize the number of sensor spheres.

A.2 INTRODUCTION

The purpose of this memo is to examine, in a general way, the tradeoffs among the hardware quantities;

(a) sensor sphere diameter

(b) sensor sphere density

(c) length of wire

(d) spring size

(e) number of sensor spheres

and the descriptive quantities

(a) launch angle

(b) launch velocity

(c) motion of the capsule

(d) depth of penetration

The original SURMEC system is described in the reference. The pertinent facts are summarized below. Seven sensor spheres are sequentially impacted on the lunar surface in an approximate 300 foot diameter area. The sensor spheres are launched from the erected and anchored capsule (which weighs 38.7 pounds with the spheres and without the balsa wood impact limiter) with an initial velocity of 33.8 ft/sec and a launch angle of 20 degrees measured from the local vertical. A spring with an initial compression force of 500 pounds and a 1 inch stroke (20.8 ft lb energy) is used to launch the sensor sphere. A fine wire (0.05 pounds per 100 feet) serves as the data link between the sensor and the capsule. Each sensor sphere weighs 1.17 pounds and has a 2 inch outside diameter. Each sphere houses an omni-directional accelerometer with a 1 inch cavity of mercury. The largest dimension of the accelerometer is approximately 1.4 inch. The outside cover is stainless steel. Tungsten had been suggested as a possible alternative to steel.

The system described above represents a compromise involving several quantities (notably those mentioned earlier in the introduction.)

A.3 BASIC CRITERION

It seems intuitive that the quantity of data obtained during a single impact is in direct proportion to the depth of penetration of the sphere into the lunar surface. The depth of penetration increases as the kinetic energy (at impact) per cross-sectional area of the sensor sphere is increased. Thus we are led to the basic criterion

for the sensor sphere configuration and launch parameters:

> The kinetic energy per unit area of the sensor sphere should be as large as possible subject to system constraints and design limitations.

A.4 LAUNCH ANGLE

For the system described in the reference, the weight of the wire (less than 300 feet long at 0.05 lbs/100 ft) is an order of magnitude less than the weight of the sensor sphere (1.17 pounds). Thus, the trajectory of the sphere is approximately parabolic with the impact velocity and angle equal to the launch velocity and angle, respectively.

Let x_2 be the horizontal distance between the launch and impact points and let θ_1 be the launch angle as measured from the local vertical. Then

$$\frac{x_2(\theta_1)}{x_2(45^\circ)} = \sin 2\theta_1$$

where

$$x_2(45^\circ) = v_1^{\,2}/g$$

v_1 = launch velocity

g = acceleration due to gravity at the lunar surface

Likewise if y_p is the peak altitude we have

$$\frac{y_p(\theta_1)}{y_p(0^\circ)} = \cos^2 \theta_1$$

where

$$y_p(0^\circ) = v_1^{\,2}/2g$$

For the system described in the reference, θ_1 = 20 deg. and V_1 = 33.8 ft/sec, we obtain

$$x_2(45^\circ) = 216 \text{ ft}, \qquad y_p(0^\circ) = 108 \text{ ft}$$

$$x_2(20^\circ) = 0.766\ (216) \qquad y_p(20^\circ) = 0.883\ (108)$$

$$= 165 \text{ ft}, \qquad = 95 \text{ ft}$$

The radius of the impact area varies as the sin $2\theta_1$. The maximum range occurs when θ_1 = 45 deg. The trajectory of the wire has not been studied, however, it is expected that the length of wire is also maximized at θ_1 = 45 deg.

For a given sensor sphere size the number of spheres N increases as θ_1 approaches 45 deg. N is given by

$$N = \pi(a/r) \sin\theta_1 \left(\cos\theta_1 + \sqrt{\left(1 - \frac{r}{a}\right)^2 - \sin^2\theta_1}\right)$$

where a is the radius of the inner payload sphere and r is the radius of the sensor sphere. This equation is represented graphically in Figure 1. The original system calls for N = 7 at θ_1 = 20 deg

The launch angle is important in yet another regard, rotational disturbance to the capsule during launch. The spring reaction force acts through the contact point. Consider the case when the vertical component of the spring force is resisted by the lunar surface material. A problem arises in this case when the static frictional force is less than the horizontal component of the spring force. Then the capsule will both slide and rotate about the mass center. There exists a critical angle θ_c for any two contact surfaces for which the contact point will commence to move. The system must satisfy the constraint that the launch angle θ_1 be less than θ_c.

It is recommended that θ_1 be set equal to 45 deg or θ_c, whichever is smaller.

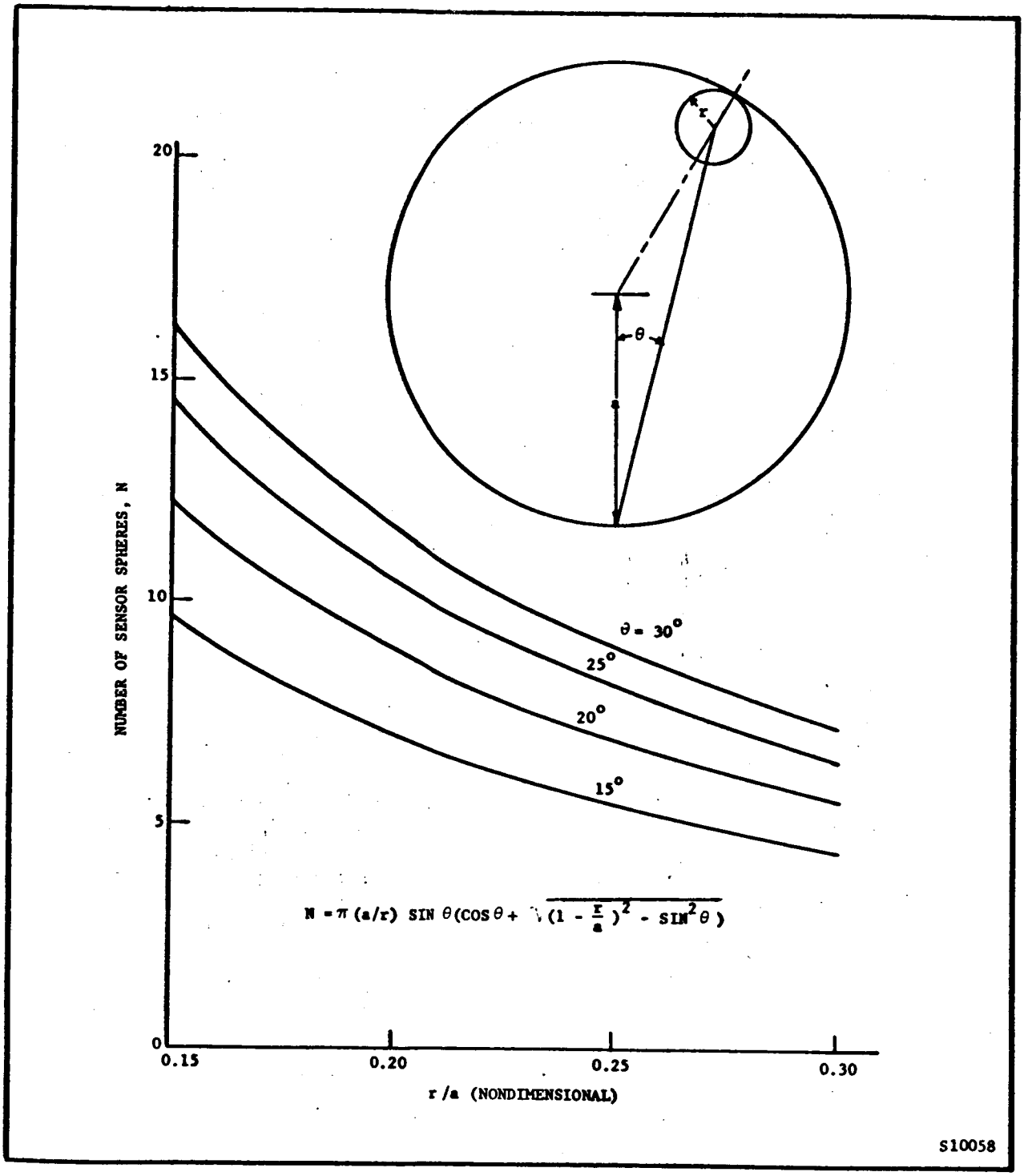

FIGURE 1. NUMBER OF SPHERES VERSUS LAUNCH ANGLE AND SPHERE SIZE

A.5 METHOD OF UNWINDING WIRE

Two schemes are possible; unwind the wire from the capsule, or unwind the wire from the sensor sphere. The first scheme is used in the reference and this scheme is recommended for the following reasons:

(1) The impact velocity is higher for a given launch energy. Here we include the mass of the wire.

(2) Forces are exerted at the fixed end of the wire. Since we choose not to disturb the orientation of the capsule, the first scheme is preferable.

A.6 LAUNCH FORCE AND ENERGY

The differential work done by the spring during extension is

$$dW = Xdx$$

where X is the spring force and dx is the differential stroke. For a linear spring force

$$W = \frac{1}{2} X_o \Delta x$$

where X_o is the maximum compression and Δx is the total stroke. For the system described in the reference

$$X_o = 500 \text{ pounds}, \qquad x = 1 \text{ inch}, \qquad W = 20.8 \text{ ft lbs}$$

W represents the change in potential energy of the spring to kinetic energy of the capsule and the sensor sphere. Clearly it is desirable that the distribution of the kinetic energy be unequal with most of the energy going to the sensor sphere. In the limiting case when the capsule-sensor system is not acted upon by external forces, the energy distribution would be given by

$$T_1 + T_2 = E, \qquad T_1 = \frac{W_2 E}{W_1 + W_2}$$

where T is kinetic energy, W is weight and the subscripts 1 and 2 refer to the capsule and sensor sphere, respectively. For the system described in the reference

$$T_1 = 0.03 E, \qquad T_2 = 0.97 E$$

If motion of the capsule were restricted by the lunar surface material, the energy distribution would be even more onesided.

Since T_1 is much less than the kinetic energy of the capsule at impact ($\sim 3 \times 10^4$ ft lb) the problem of burying the capsule while launching the sensor spheres is somewhat academic. The capsule would be buried during the initial impact if the lunar surface were very soft.

APPENDIX B

LSPC TIP-OVER ANALYSIS

B.1 SUMMARY AND CONCLUSIONS

Due to angular alignment errors in erecting the LSPC payload to a vertical position (typically, $3\sigma_{range}$ = 6 degrees) the explosive hole cutter reaction force can tend to cause tipover or further misalignment of the payload. A general parametric analysis was performed on a simplified tipover model which is believed to be a conservative one involving a hard smooth surface. Typical values based on experimental results were substituted into the generalized solution. On level terrain it was concluded that 1.3 inch diameter flat spots on the impact limiter surface would prevent tipover. On appreciably steeper-slope but smooth surfaces, the landing sphere assembly can only come to rest on one of the deeper flats caused by the initial impact on secondary impacts on the lunar surface. Typical secondary flats would prevent tipover on slopes of up to 32.5 degrees.

B.2 ANALYSIS

If the porting gun in the LSPC survival sphere is not erected to the vertical when it is fired, a net force impulse will be imparted to the survival sphere when the balsa slug and cutter blade are separated from the rest of the survival sphere. Depending upon the manner in which the survival sphere rests on the surface, a turning movement may be generated by this force impulse which is sufficient to overturn the survival sphere. The worst situation would appear to be a case where the survival sphere is resting on a small flat which is in contact with a hard surface. On a soft or dust surface, most of the force impulse energy would go to pushing the survival sphere deeper rather than to overturn it.

In the assumed model (see Figure 1) for the worst case, it is assumed that there is a fixed pivot point, "p", which lies in the plane containing the gravity vector and the porting gun axis (assumed to go through the CG) and is on the circle of intersection of the sphere and lunar surfaces. If "p" is not fixed, some of the force impulse energy will be absorbed in translation of the survival sphere, and this is not objectionable. Figure 1 shows the ball resting on a flat of half angle ϕ with a terrain slope of s. As shown here, s is considered to be a positive

slope which, for the indicated direction of (Fdt), is the worst case. Also, it is tacitly assumed that $(\phi - s) > 0$, otherwise the sphere would not have come to rest.

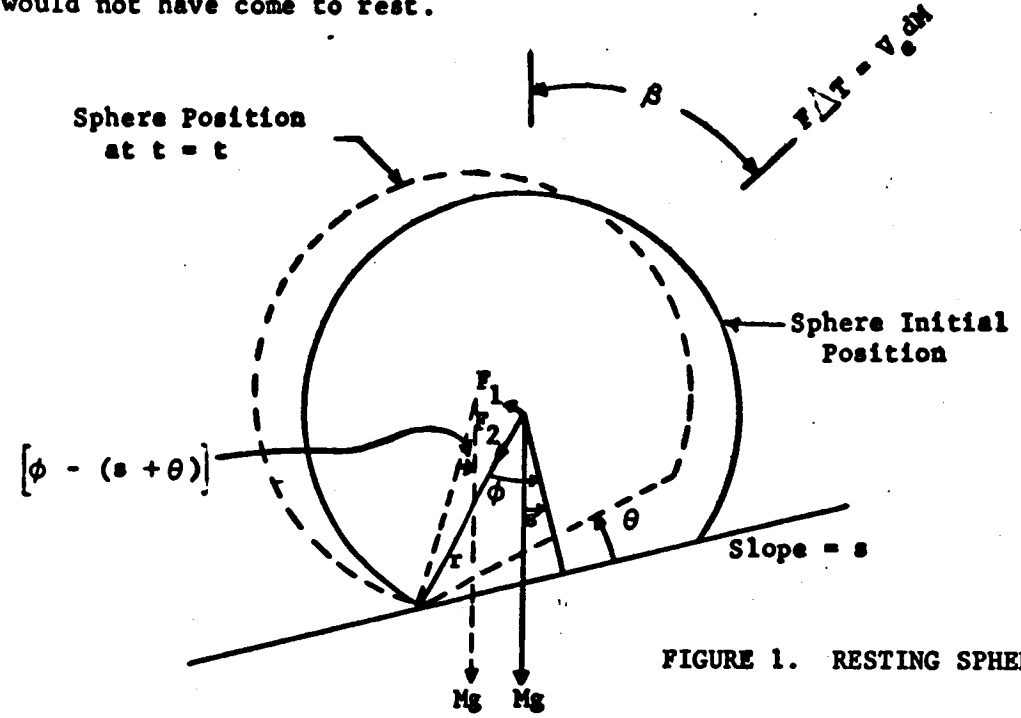

FIGURE 1. RESTING SPHERE GEOMETRY

It is of interest to establish for given values of ϕ and s what values of Fdt and β will cause overturning. Overturning will result when the initial angular velocity of the sphere about point p is sufficiently large that the gravitational torque cannot restrain the buildup in θ to less than the value $(\theta = \phi - s)$ which places the CG over the pivot point p.

Resolving the applied forces along and normal to the line joining the CG and the pivot point, the following torque equation can be written

$$Fr \sin(\beta - \phi + s + \theta) - Mgr \sin\left[\phi - (s+\theta)\right] = I_p \frac{d^2\theta}{dt^2} = I_p \dot{\theta} \frac{d\dot{\theta}}{d\theta} \qquad (1)$$

It is to be noted that F(t) is an impulse function whose magnitude is equal to the momentum represented by the incremental mass having the body at a velocity V_e. That is,

$$\int_0^t F(t)dt = \int_0^{\Delta T} F(t)dt = V_e dM$$

where ΔT is an arbitrarily short time. Integrating equation (1) from $t = 0$ to $t = \Delta T$ which is arbitrarily small yields

$$\int_0^{\Delta T} \left(I_p \frac{d^2\theta}{dt^2}\right) = \int_0^{\Delta T} Fr \sin(\beta - \phi + s + \theta)dt - \int_0^{\Delta T} Mgr \sin\left[\phi - (s+\theta)\right] dt$$

$$I_p \omega_o = r \sin(\beta - \phi + s) \int_0^{\Delta T} Fdt = r \sin(\beta - \phi + s) V_e dM \qquad (2)$$

where ω_o is the sphere's initial angular velocity.

Integrating equation (1) from $t = \Delta T$ to $t = t$ but using the alternate form for $I_p \frac{d^2\theta}{dt^2}$ yields

$$\int_{\dot{\theta}(\Delta T)}^{\dot{\theta}(t)} I_p \dot{\theta} d\dot{\theta} = \int_{\theta(\Delta T)}^{\theta(t)} Fr \sin(\beta - \phi + s + \theta)d\theta - \int_{\theta(\Delta T)}^{\theta(t)} Mgr \sin \phi - (s+\theta) \; d\theta$$

Since F is zero for $T \leq t$

$$\left.\frac{I_p}{2}\dot{\theta}^2\right]_{\omega_o}^{\dot{\theta}(t)} = -Mgr\cos\left[\phi-(s+\theta)\right]\Big]_0^{\theta(t)}$$

Thus,

$$\frac{I_p}{2}\left(\dot{\theta}^2(t) - \omega_o^2\right) = Mgr\left\{\cos(\phi-s) - \cos\left[\phi-(s+\theta(t)\right]\right\} \quad (3)$$

The critical unbalance condition arises when $\theta = (\phi-s)$ at which time $\dot{\theta}$ should be zero or negative. Thus, the requirement on ω_o becomes

$$I_p\frac{\omega_o^2}{2} \leq Mgr\left[1-\cos(\phi-s)\right]$$

or

$$r^2V_e^2dm^2\sin^2(\beta-\phi+s) \leq 2I_pMgr\left[1-\cos(\phi-s)\right]$$

or that

$$V_e \leq \frac{2}{dM}\sqrt{\frac{I_pMg}{r}}\,\frac{\sin\left(\frac{\phi-s}{2}\right)}{\sin\left[\beta-(\phi-s)\right]} \quad (4)$$

Using

$$M = \frac{90}{g}\text{ slugs},\quad dM = \frac{0.6}{g}\text{ slugs},\quad I_p = Mr^2 + 2/5\,Mr^2 + 7/5\,Mr^2$$

$$g = 5.31\text{ ft/sec}^2 \text{ and } r = 1\text{ foot}$$

leads to the following result.

$$V_e \leq 300\sqrt{\frac{7}{5}\,\frac{5.31\text{ ft}^2}{\text{sec}^2}}\,\frac{\sin\left(\frac{\phi-s}{2}\right)}{\sin\left[\beta-(\phi-s)\right]} = 820\,\frac{\text{ft}}{\text{sec}}\,\frac{\sin\left(\frac{\phi-s}{2}\right)}{\sin\left[\beta-(\phi-s)\right]}$$

V_e is plotted in Figure 2 as a function of $\left[\beta - (\phi - s)\right]$ for various values of $(\phi - s)$. These relationships are shown as solid lines. The dashed lines of Figure 2 yield the allowable values of V_e for fixed erection angle errors (β) as a function of the rest condition geometry as reflected in the parameters $(\phi - s)$. As an example, if the sphere has a 4" diameter flat resting on a 5° slope, then

$$\phi = \sin^{-1} 2/12 = 9^\circ\ 35'$$
$$s = 5^\circ$$
$$\phi - s = 4^\circ\ 35'$$

and an erection error β of 15° would permit a value of V_e of up to 179 ft/sec

Discussion with pyrotechnic designers, relative to the porting gun requirements for the LSPC capsule, indicate that a nominal exit velocity of approximately 75 ft/sec would be reasonable and that 3σ variations of $\pm$ 50 ft/sec should be realizable. This tolerance on the exit velocity is subject to the assumption that large pieces of balsa are not removed from the path of the cutter as a result of impact. Using the upper bound value of exit velocity, (125 ft/sec) in conjunction with a 3σ value of 6° for the erection error β, leads to a design point as shown in the Figure 2. Under the assumed model conditions then, tip over would not be experienced if the angle difference $(\phi - s)$ exceeded 1.5°. On level terrain (s=0) this requirement would be satisfyed by the capsules resting upon a flat having a diameter of 1.3 inches. Flats of this size could very reasonably be effected on the outside of the 25" balsa sphere by cementing hemispherical bumps appropriately distributed on the entire outer surface of the limiter cover.

If one assumes that the ball will ultimately come to rest on a flat produced by the impact, relatively large local slope angle could be tolerated. Impact results compiled from seismometer capsule tests PS-1 through PS-13 and tests LTV-1 and LTV-3 through LTV-7 showed that the smallest depression of a major "flat" due to normal impact was about 3.0 inches. The smallest minor "flat" due to a second bounce during an off-normal impact was 2.15 inches. Applied to a 25" diameter ball, these results translate into a tolerance of local slope angles respectively of $40.5^\circ - 1.5^\circ = 39^\circ$ and $34^\circ - 1.5^\circ = 32.5^\circ$ respectively. These would appear to be relatively large slopes compared to the 15° maximum slope (over distances large compared to the surveyor spacecraft) assumed in the J.P.L. model of the lunar surface.

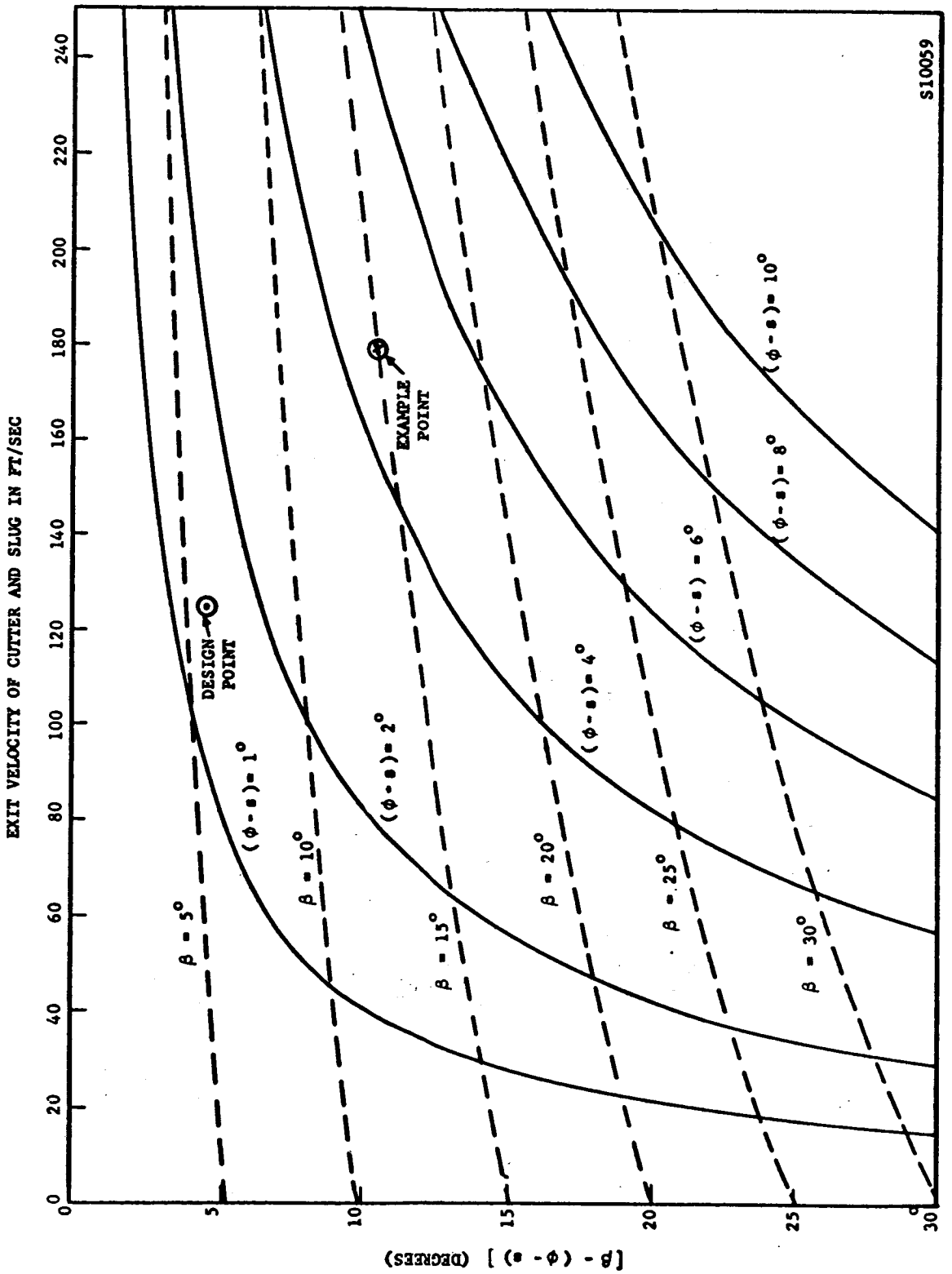

FIGURE 2. ALLOWABLE EXIT VELOCITY AND POINTING ERROR OF PORTING GUN

APPENDIX C

LSPC ILLUMINATION ANALYSIS

Reference: V. A. Fedorets, "Photographic Photometry of Lunar Surface"

C.1 SUMMARY AND CONCLUSIONS

The photometric function Φ for the HRF lunar mission has been obtained (see Figure 1) for all azimuths λ (0° to $\pm 180^\circ$) and three elevation angles ϵ (45°, 60° and 75°) measured from the local vertical. The angle i between the sun-moon line and the local vertical is taken as 60°. The zero azimuth angle λ is defined when the optical axis lies in the plane formed by the sun-moon line and the local vertical, and when the angle between the sun-moon line and the optical axis is less than 90°. Thus, $\Phi(\lambda) = \Phi(-\lambda)$. The geometry is shown in Figure 2. Applying these data to the LSPC system it appears that a relatively high degree of picture contrast can be achieved in a reasonably large fraction of the total picture coverage if the scene possesses contrasting elements.

C.2 ANALYSIS

Based on data obtained from V. A. Fedorets (Reference), D. Willingham of JPL has been able to express Φ as a function of two parameters, g and α, shown in Figure 3. Willingham's two plots are included in this memo as Figures 4 and 5. The spherical angle g is measured from the sun line to the optical axis. The angle α is obtained by finding the line of intersection of the plane containing the optical axis and the sun line with the vertical plane which is normal to the first plane. α is the spherical angle between the optical axis and the line of intersection. Based on the spherical triangles shown in Figure 3 we obtain the following relations

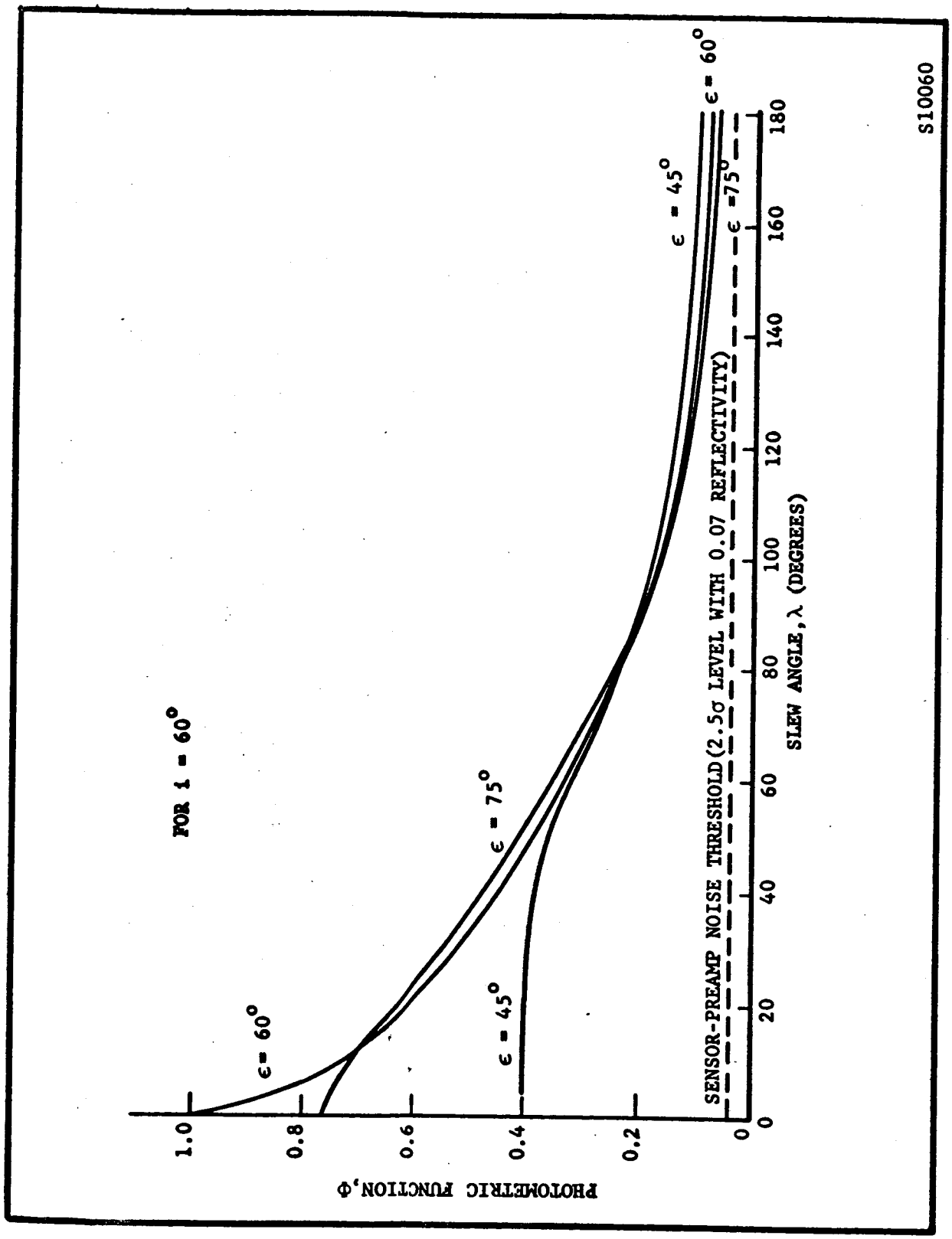

FIGURE 1. PHOTOMETRIC FUNCTION Φ FOR THREE ELEVATION ANGLES

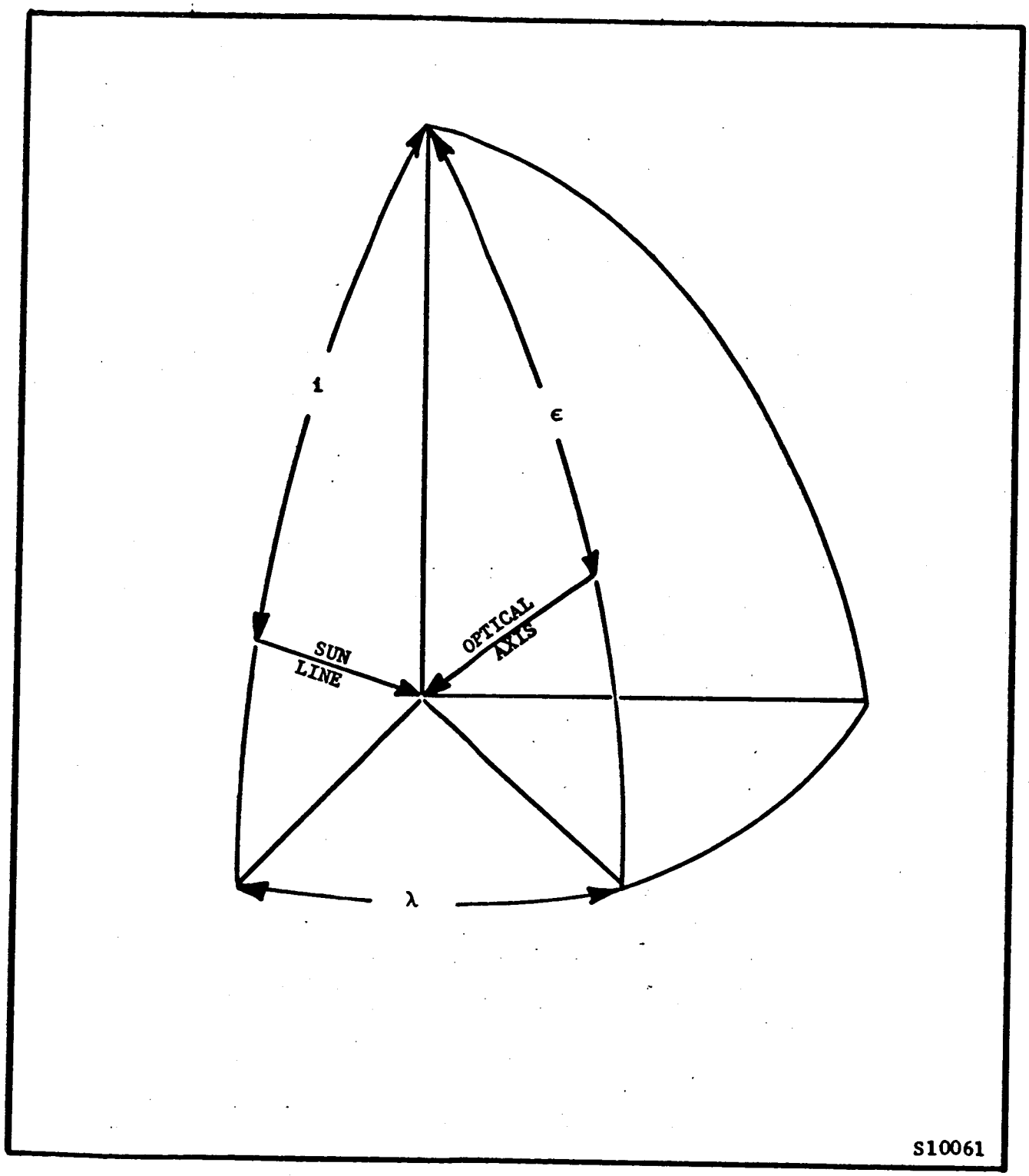

FIGURE 2. GEOMETRY FOR FIGURE 1

$$\cos g = \cos \epsilon \cos i + \sin \epsilon \sin i \cos \lambda \qquad (1)$$

$$\sin \gamma = \frac{\sin i}{\sin g} \sin \phi \qquad (2)$$

$$\tan \alpha = \tan \epsilon \cos \gamma \qquad (3)$$

Now we observe that in Figure 4, g takes on both positive and negative signs, while α is always positive. However, in Figure 5 g is always positive and α takes on positive and negative values. Obviously sign ambiguities are present. We will denote the g and α in Figure 4 with subscripts "4". Likewise g and α in Figure 5 will have subscripts "5". For ϵ between 0 and 90 we have

$\alpha > 0$ if $\gamma < 90^\circ$

$\mu < 0$ if $\gamma > 90^\circ$

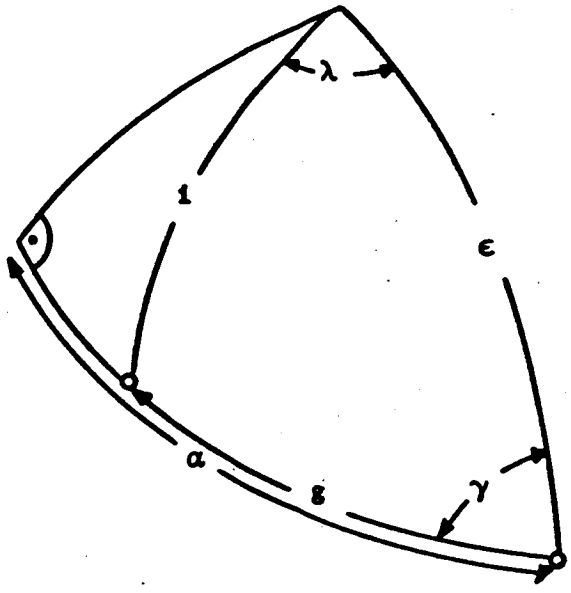

FIGURE 3. GEOMETRY FOR EQUATIONS (1), (2), AND (3)

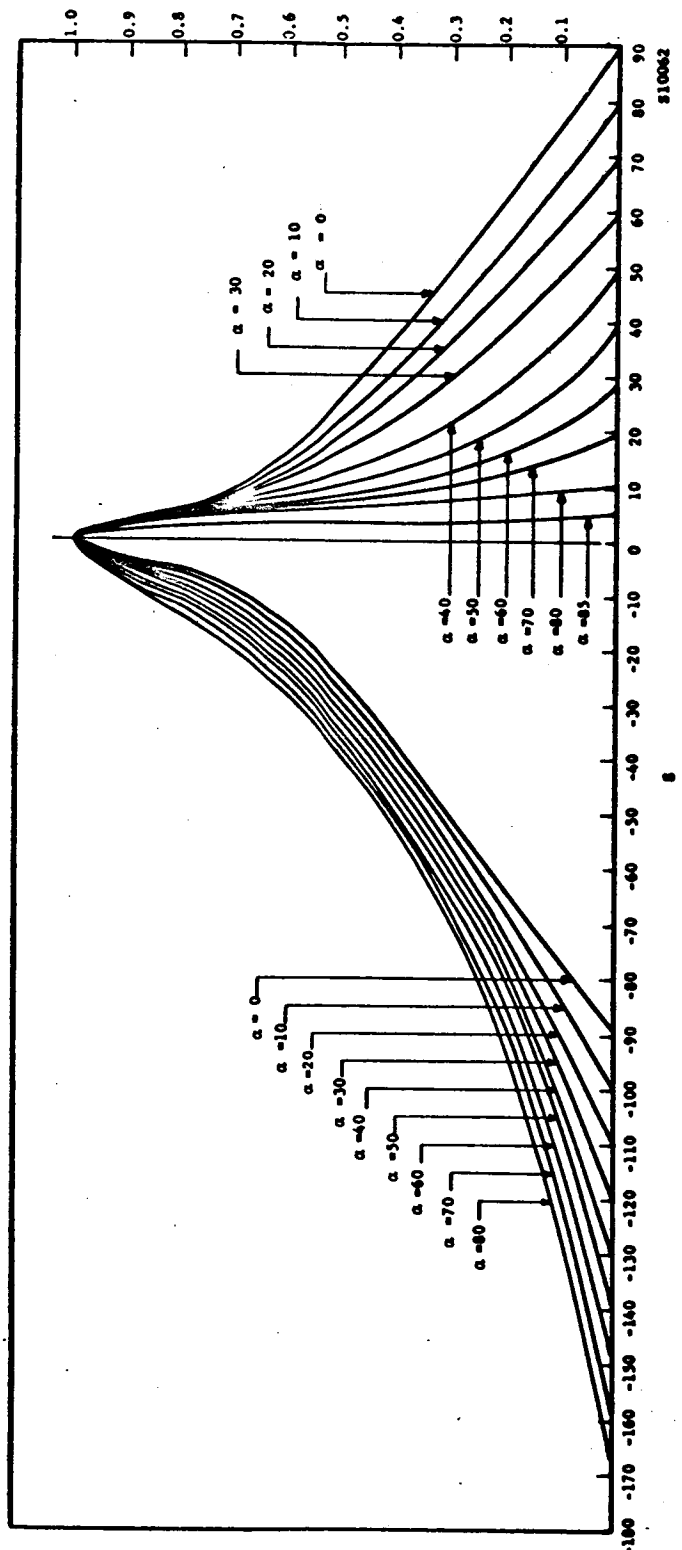

FIGURE 4. PHOTOMETRIC FUNCTION OF LUNAR MARIA USING V. A. FEDORET'S DATA

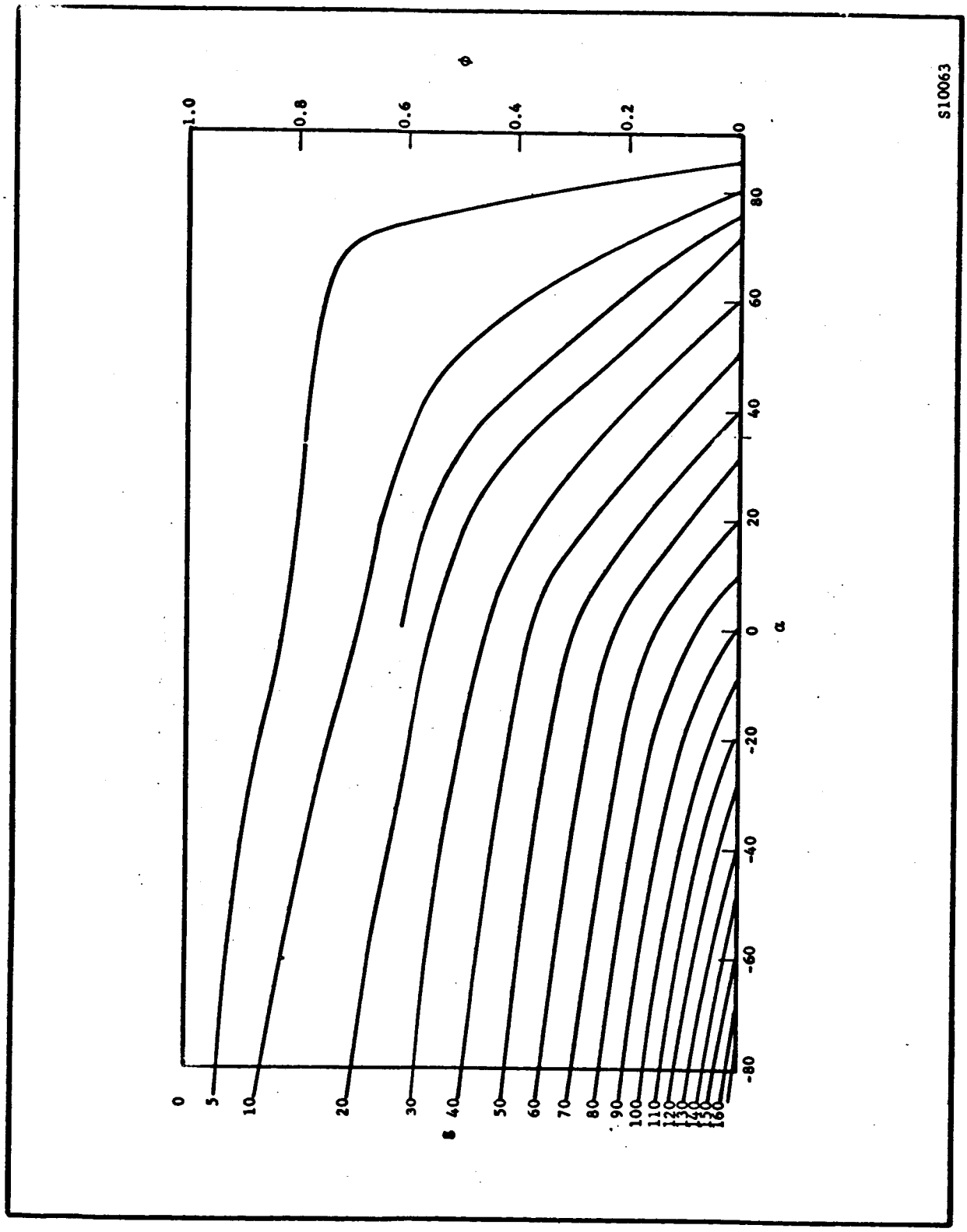

FIGURE 5. PHOTOMETRIC FUNCTION FROM V. A. FEDORET'S DATA

When using Figure 4 we take

$$g_4 = g, \text{ when } \alpha < 0$$

$$g_4 = -g, \text{ when } \alpha > 0$$

$$\alpha_4 = |\alpha|$$

When using Figure 5 we take

$$\alpha_5 = -\alpha$$

$$g_5 = g$$

It is evident from Figures 4 and 5 that Φ is not defined for values of α approaching 90 degrees. From (3) we see that α approaches 90 degrees as ϵ approaches 90 degrees.

To relate these results to their effect on the LSPC capsule consider that measurements made viewing the full moon from the earth, i.e., when $\Phi = 1.00$, resulted in a maximum signal to rms sensor-preamp noise ratio of 187:1. Assuming pessimistically that the maximum signal corresponded to a reflectivity of 0.20, it can be concluded that, when looking at an average reflectivity of 0.07, the 2.5σ level of sensor-preamp noise corresponds to an effective value of 0.038 for the photometric function Φ. This level is shown in Figure 1 as the dashed line. For half of the complete azimuth coverage, i.e., $90^\circ \leq |\lambda| \leq 180^\circ$, the average of the photometric function would be approximately $\frac{0.13}{0.038} = 3.4$ times the 2.5σ noise level which would make illumination highlights (areas of reflectivity equal to 0.20) appear as approximately 10 grey levels above threshold. In the other half of the complete azimuth coverage the photometric function would exceed 0.2 and would make highlights appear as 16 or more grey levels above the 2.5σ noise threshold.

APPENDIX D

IMPACT LIMITER TRADEOFFS

D.1 SUMMARY AND CONCLUSIONS

Relations which exist among the impact limiter parameters (weight, density, strength), payload parameters (weight, density, radius) and the impact parameters (velocity, velocity percentile, acceleration) are documented in this appendix. A general parameter tradeoff chart is presented in Figure 1. This chart is particularly useful if grossly different impact limiter materials are to be compared.

Using Ranger RA-3,4,5 design values for some of the parameters (impact limiter density, impact limiter strength and total weight) in Figure 1 permits development of a chart, Figure 4, which is easier to interpret. The following conclusions may be drawn from Figure 4.

(a) The limiter should not be designed to sustain more than 300 ft/sec since this is, for practical purposes, the 100 percentile velocity (taken for RA-3).

(b) The impact velocity is relatively <u>insensitive</u> to small changes in the payload density (approximately 0.095 ft/sec per % density change) when the nominal density is approximately 140 lb/ft^3.

(c) The impact velocity is relatively <u>sensitive</u> to small changes in the payload weight for all packing densities (approximately 5 ft/sec per pound)

D.2 TRADEOFF CHART (FIGURE 1) AND ITS USE

The mutual relations which exist between each of the parameters:

R_p - radius of payload sphere

y_p - radius of payload sphere radius to impact limiter radius

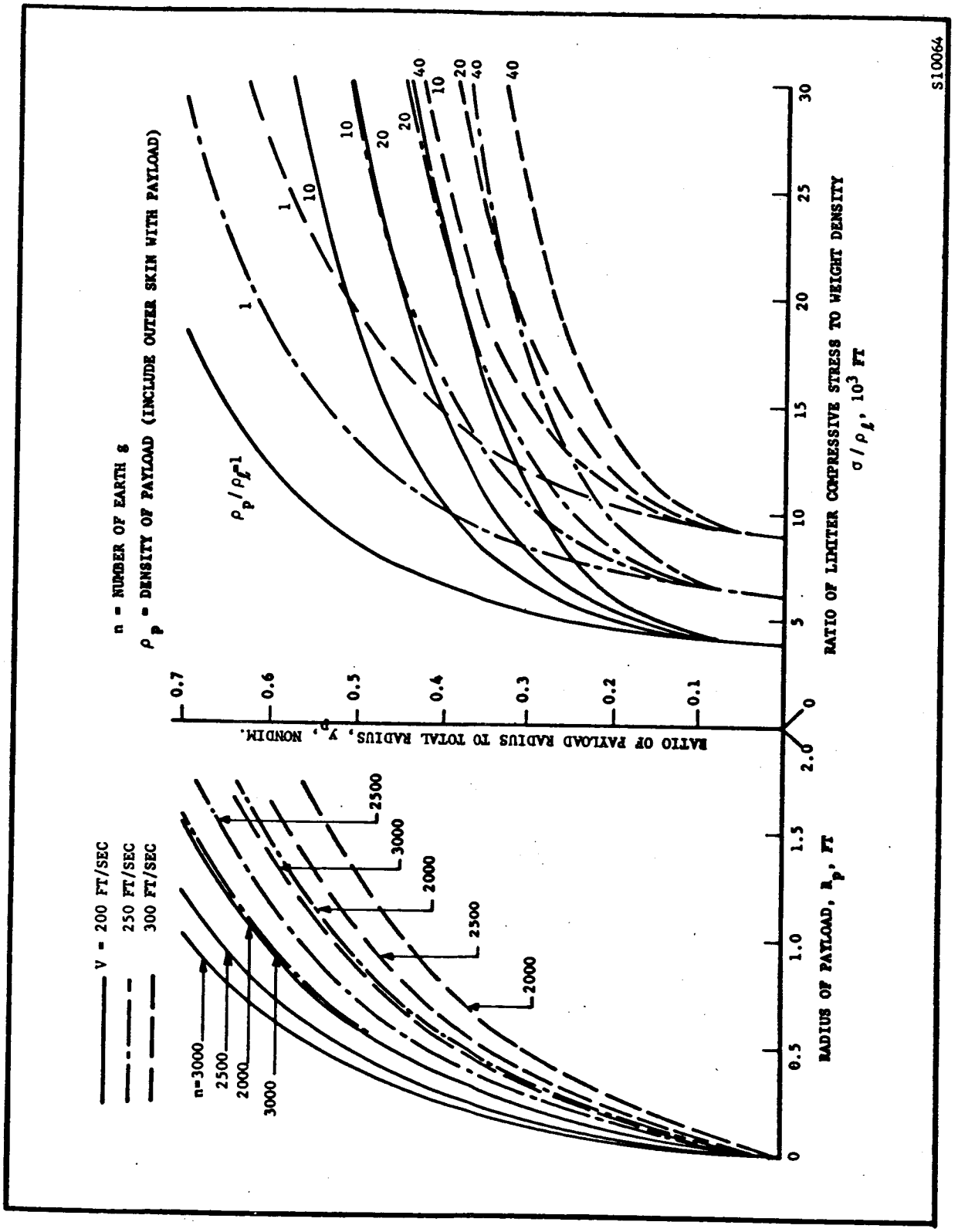

FIGURE 1. IMPACT LIMITER TRADEOFF CHART

ρ_p/ρ_ℓ - ratio of payload density to impact limiter density

σ/ρ_ℓ - ratio of limiter compressive stress to limiter weight density

v - impact velocity

n - number of earth g's at peak acceleration during impact

are presented in Figure 1. The curves are only applicable to spherical payload packages and spherical balsawood impact limiters of the Ranger-type. The equations with which these curves were generated are documented in the succeeding section. The configuration which we are considering is sketched below in a partially crushed situation. The limiting (smallest) value for r is given by

$$r = R_p + \epsilon(R - R_p)$$

where ϵ is the compressibility parameter of the impact limiter material. For balsa wood ϵ is taken as 0.2. The curves in Figure 1 are based on this value.

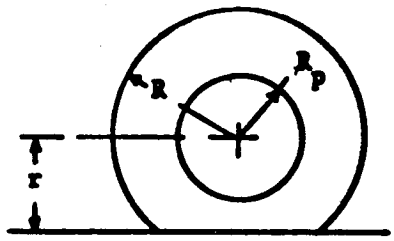

The tradeoff chart says nothing about the problem of sinking into the lunar surface material. Furthermore, we assume that the limiter crushes from the outside only.

The use of Figure 1 depends upon the parameters which are fixed and constraints which may be imposed. Consider the following example.

Given: Impact velocity v = 250 ft/sec

Density and balsa and glue, $\rho_\ell = 6.7$ lb/ft^3

$\sigma/\rho_\ell = 21{,}000$ ft (typical for balsa wood)

Maximum payload density, $\rho_p = 134$ lb/ft^3

Determine: Weights and radii of the payload and limiter as functions of peak acceleration.

Solution: Starting with $\sigma/\rho_\ell = 21{,}000$ in the right half of Figure 1, we move upward until the curve labeled v = 250 ft/sec,

$$\frac{\rho_p}{\rho_\ell} = \frac{134}{6.7} = 20$$

is reached. Moving to the left we find

$$y_p = 0.39$$

Using the left half of Figure 1 we find

$R_p = 0.51$ ft for n = 2000
$= 0.43$ ft for n = 2500 V = 250 ft/sec
$= 0.35$ ft for n = 3000

In Summary

	n = 2000	2500	3000
Radius of Payload R_p	0.51 ft	0.43 ft	0.35 ft
Radius of Limiter R	1.31 ft	1.10 ft	0.90 ft
Weight of Payload	73.2 lb	45.0 lb	24.8 lb
Weight of Limiter	58.2 lb	35.0 lb	19.2 lb
Total Weight	131.4 lb	80.0 lb	44.0 lb

Note: Weight of outer skin cover is to be included as part of the payload weight.

D.3 EQUATIONS FOR GENERATING FIGURE 1

A segment of a crushable balsa wood limiter with radial yield stress σ is shown below. The radial area of the element $d\phi$ at the impact surface is

$$A(r,\phi) = 2\pi^2 \frac{\sin\phi}{\cos^2\phi} \, d\phi$$

The vertical component of force on the element is

$$2\pi r^2 \sigma \tan\phi \, d\phi$$

The total vertical force is

$$F(r) = 2\pi r^2 \sigma \int_0^{\phi_1} \tan\phi \, d\phi = 2\pi r^2 \sigma \ln\left(\frac{R}{r}\right)$$

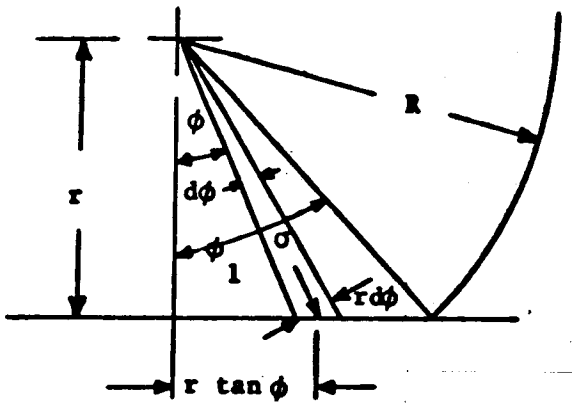

or

$$f(y) \quad \frac{Wn}{\sigma R^2} = 2\pi y^2 \ln\left(\frac{1}{y}\right)$$

where W is the total weight, n is the number of earth g's and y is the ratio r/R. The maximum value for f(y) occurs at $y = e^{-\frac{1}{2}} = 0.607$ and is equal to

$$f(e^{-\frac{1}{2}}) = \frac{\pi}{e} = 1.16$$

The maximum allowable impact velocity is given by

$$v = \sqrt{\frac{2\sigma R^3 \Phi}{m}}$$

where

m = mass of payload and limiter

$$\Phi = \int_1^{y_o} f(y)dy = 2\pi \int_1^{y_o} y^2 \ln\left(\frac{1}{y}\right) dy$$

$$= -\frac{2\pi}{3} y^3 \left[\ln\left(\frac{1}{y}\right) + \frac{1}{3}\right]_1^{y_o} = \frac{2\pi}{9}\left\{1-y_o^3\left[1+3\ln\left(\frac{1}{y_o}\right)\right]\right\}$$

$$y_o = \frac{R_p + \epsilon (R + R_p)}{R_p}$$

ϵ = compressibility factor (for balsa wood, $\epsilon = 0.2$)

The nondimensional parameters f and Φ are plotted in Figures 2 and 3 as functions of $y = r/R_p$. The definitions of f and Φ may be written as

$$f(y_p) = \frac{4\pi n R_p}{3y_p}\left[\left(\frac{\rho_p}{\sigma}\right) y_p^3 + \left(\frac{\rho_\ell}{\sigma}\right)\left[1-y_p^3\right]\right]$$

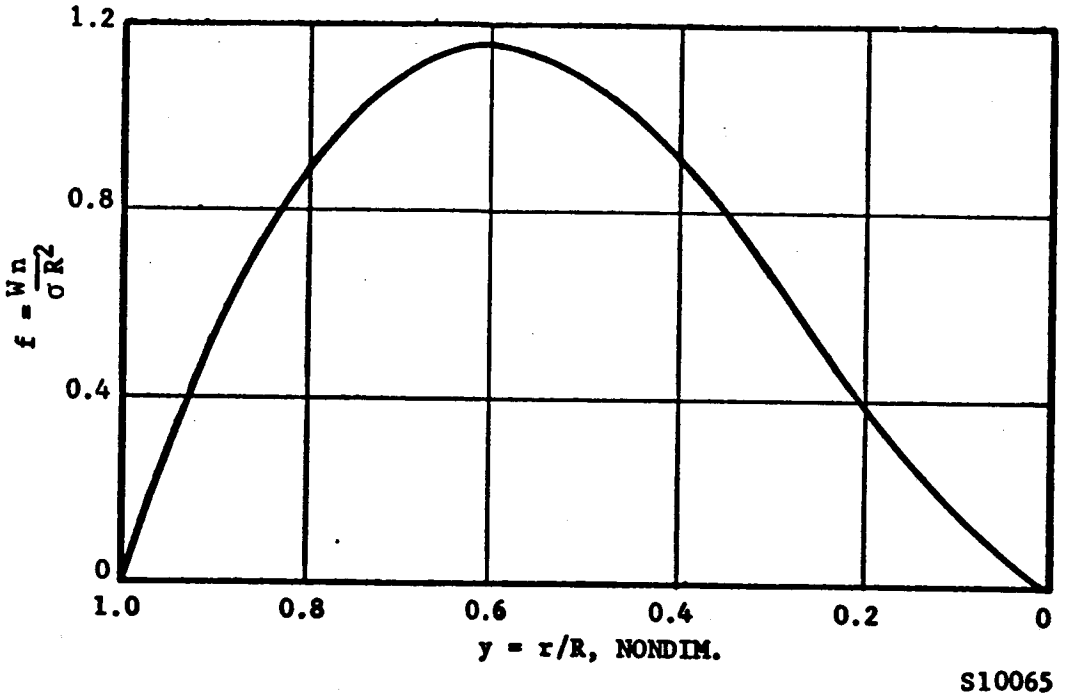

FIGURE 2. NONDIMENSIONAL ACCELERATION CURVE

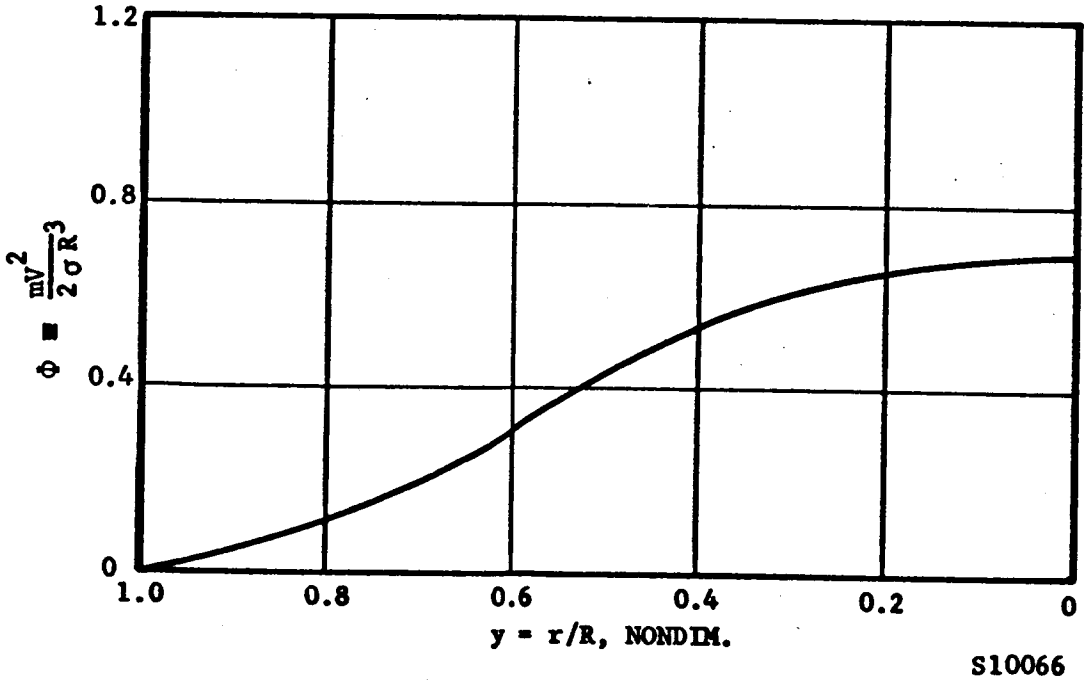

FIGURE 3. NONDIMENSIONAL ENERGY CURVE

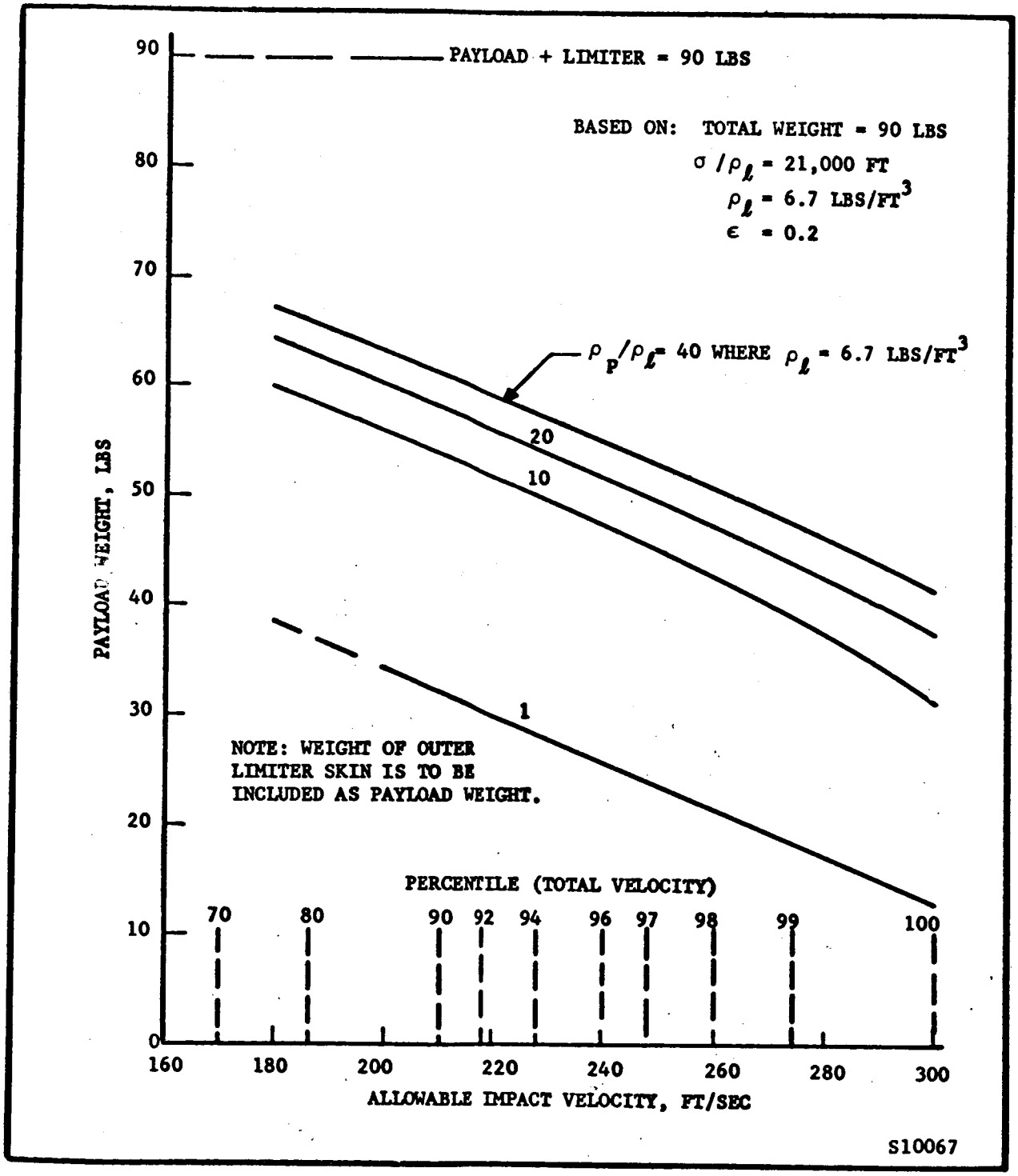

FIGURE 4. PAYLOAD WEIGHT VERSUS IMPACT VELOCITY FOR GIVEN PACKING DENSITIES

$$\Phi(y_p) = \frac{2\pi v^2}{3g}\left[\left(\frac{\rho_p}{\sigma}\right) y_p^3 + \left(\frac{\rho_\ell}{\sigma}\right)\left(1 - y_p^3\right)\right]$$

where

$$y_p = R_p/R$$

σ is the compression yield stress of the balsa

ρ_p is the weight density of the payload

ρ_ℓ is the weight density of the limiter

Then

$$\frac{f}{\Phi} = \frac{2nR_p g}{y_p v^2} \qquad \text{or} \qquad R_p = \frac{v^2 y_p f}{2ng\,\Phi}$$

yields the equation for the left half of the curves in Figure 1. The equation for Φ provides

$$\frac{\sigma}{\rho_\ell} = \frac{2\pi v^2}{3g\Phi}\left[\left(\frac{\rho_p}{\rho_\ell}\right) y_p^3 + \left(1 - y_p^3\right)\right]$$

which is the equation for the right half of the curves in Figure 1.

D.4 SPECIALIZED TRADEOFF CHART

A general impact limiter tradeoff chart was presented in Figure 1. The following parameters are specialized in this section:

(a) Ratio of the impact limiter compression stress to the weight density of the limiter, σ/ρ_ℓ = 21,000 ft.

(b) Density of the balsa wood (including glue), $\rho_\ell = 6.7$ lb/ft^3. This value is approximately the same density used for the RA-3 capsule.

(c) Total weight (payload + limiter) = 90 lb.

Based on these constraints we have generated two figures:

Figure 4: Weight of payload versus impact velocity for different density ratios. Note: ρ_p is the weight density of the payload.

Figure 5: Radii of impact limiter R and payload $y_p R$ are given as functions of the impact velocity for different payload densities.

The percentiles of total and vertical velocities are presented in Figures 6 and 7, respectively. These curves were taken from Aeronutronic Publication No. U-1532 which was developed for the Ranger 3 impact. The total velocity percentiles which appear in Figure 4 were taken from Figure 6. It is conservative to apply these percentiles to Figure 4 in that the total velocity of an off-normal impact is thereby equated to a normal velocity. It would, however, be optimistic to use the vertical velocity percentiles of Figure 7.

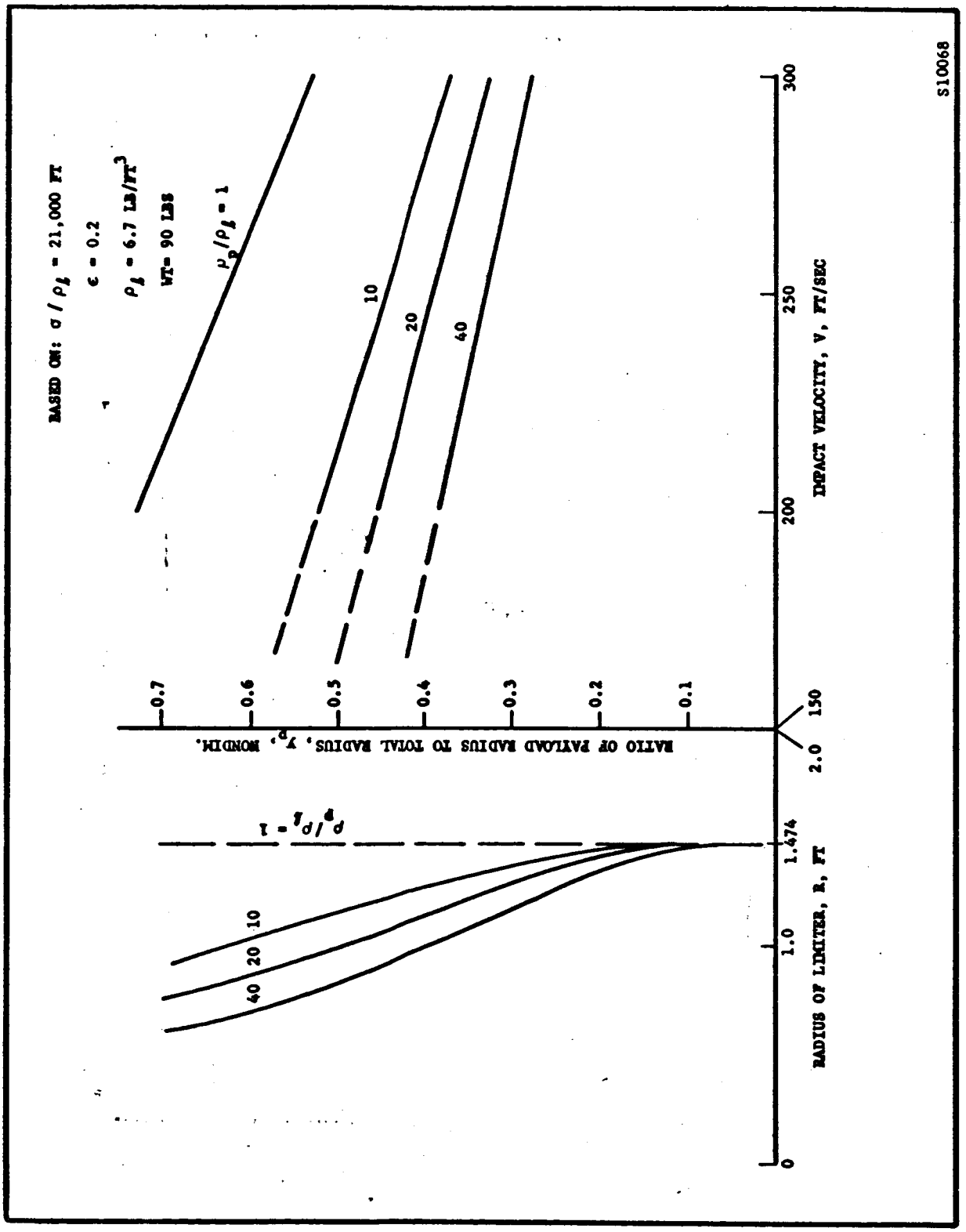

FIGURE 5. RADII OF LIMITER AND PAYLOAD AS A FUNCTION OF IMPACT VELOCITY

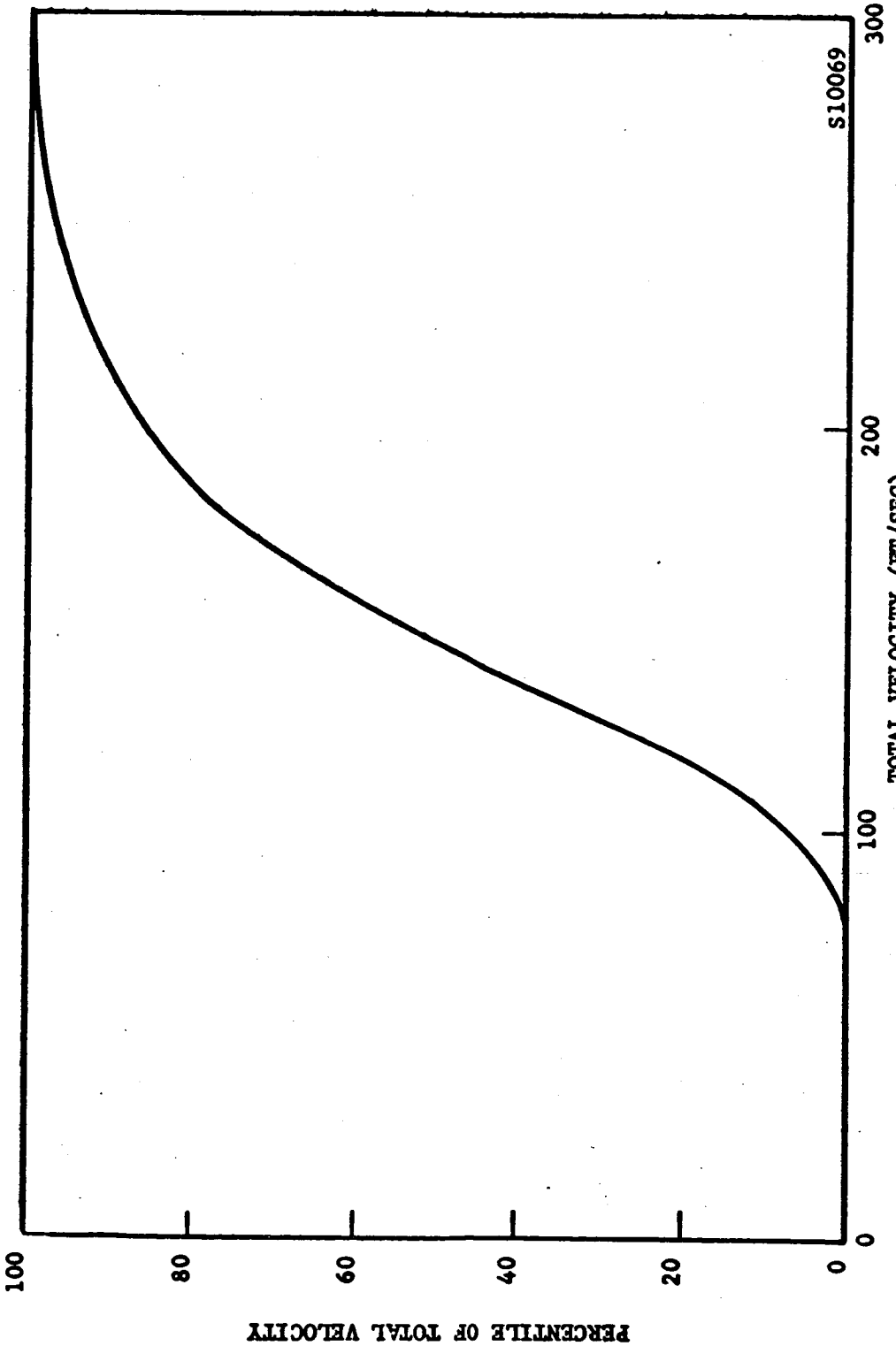

FIGURE 6. PERCENTILE OF TOTAL VELOCITY FOR RA-3 (FROM AERONUTRONIC PUBLICATION U-1532)

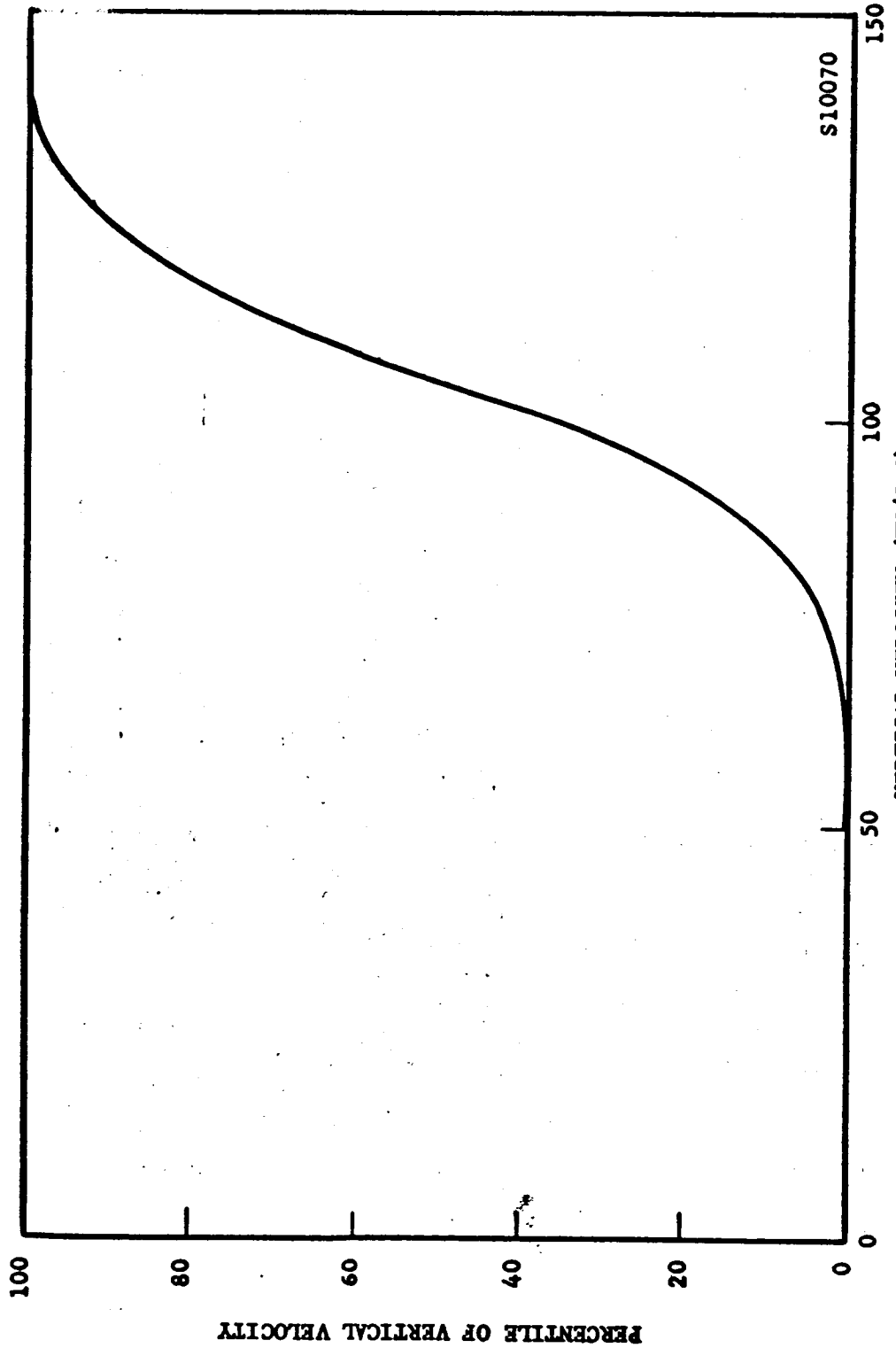

FIGURE 7. PERCENTILE OF VERTICAL VELOCITY FOR RA-3 (FROM AERONUTRONIC PUBLICATION U-1532)

APPENDIX E

COMMUNICATIONS ANALYSIS

E.1 SUMMARY AND CONCLUSIONS

The performance of the lunar payload-to-DSIF communications link was analyzed for both the LSPC and SURMEC applications, assuming functionally identical 2-watt, 960-mc transmitters and inflatable antennas in both payloads. Holding the total normally distributed phase error (from both signal distortion and noise) to less than 90 degrees for 99.0 percent of the time and requiring a minimum output signal-to-noise ratio of 20 db, the allowable data bandwidth is calculated to be 93 cps. This is comfortably in excess of the LSPC requirement of 65 cps and the SURMEC delayed-time transmission requirement, but it is short of the desired minimum of 150 cps for the SURMEC real-time transmission. The 150-cps bandwidth can be just achieved, however, by utilizing the available MASER in the Goldstone receiving system.

E.2 LSPC COMMUNICATION LINK ANALYSIS

As part of the LSPC integration study it is necessary to evaluate the performance of the proposed communication link. This is done to determine what, if any, tradeoffs need be made in the picture coverage to assure reliable reception of the data with the transmitter power which is available. The approach which will be used is to enter into a telecommunication design control table (Table I) all of the pertinent gains and losses in the transmission system. On the basis of these entries, and on the basis of an assumed transmitter power, a received subcarrier power level is obtained. This level, diminished by the accumulated negative tolerances, is then applied to an analysis of the phase-lock receiver (presented in the latter part of this memo) to establish what output signal-to-noise ratio can be obtained with a high probability of remaining in a phase-lock condition. The criterion for lock is taken to be such that the total normally distributed phase error, from both signal distortion and noise, is less than 90° for 99.0% of the time.

The entries on the telecommunication design control table concurrently break into various separate categories, which are discussed below in Sections E.3 and E.4. Section E.5 contains the analysis of the phase-lock receiver characteristics.

TABLE I

TELECOMMUNICATION DESIGN CONTROL TABLE
LSPC CAPSULE TO EARTH (TRACKING FEED (DIPLEXED) PARAMETRIC AMP)

PARAMETER	VALUE	TOLERANCE		COMMENTS
Total Transmitter Power	+ 33.02 dbm	0.0	0.0	
Capsule Transmission Circuit Loss	- 2.64 db	+0.84	-0.99	
Capsule Antenna Gain	+ 5.5 db	+0.50	-0.50	
Capsule Antenna Pointing Loss	- 3.4 db	+0.43	-0.37	87 mi. position error (3σ) 5° erection error (3σ)
Space Loss 960 MC, R = 237,500 St. Mi.	-203.6 db	+0.70	-0.7	AR of Transmitting Antenna = 3.0± 3.0 db AR of Receiving Antenna = 2.6± 0.4 db
Polarization Loss	- 0.46 db	+0.46	-0.68	
Ground Antenna Gain	+ 43.7 db	+0.80	-0.80	
Ground Transmission Circuit Loss	- 0.65 db	+0.13	-0.13	Receiving Line Loss 0.4 ± 0.1 db Diplexer Loss 0.25 ± 0.03 db
Net Circuit Loss	-161.75 db	+3.86	-4.17	
Total Received Power	-128.73 dbm	+3.86	-4.17	
Receiver Noise Spectral Density	-174.61 dbm	+0.60	-0.28	
T system 250.45, + 16.44, - 36.74				
Carrier Modulation Loss δ = 1.4 ± 10%	- 4.93 db	+1.05	-1.27	
Received Carrier Power	-133.66 dbm	+4.91	-5.44	
Carrier APC Noise BW ($2B_{LO}$= 20 cps ± 4 cps	13.01 db	+0.97	-0.79	
CARRIER PERFORMANCE:				
Threshold SNR in $2B_L$	5.6 db	--	--	--
Threshold Carrier Power	-156.00 dbm	+1.57	-1.07	
Performance Margin	+ 22.34 db	+6.48	-6.51	
SUBCARRIER #1 Facsimile Data δ = 1.4 ± 10%				
Modulation Loss	- 2.31 db	+0.33	-0.47	
Received Subcarrier Power	-131.04 dbm	+4.19	-4.64	
Subcarrier APC Noise BW ($2B_{LO}$= 2140)	33.31 db	--	--	Total Mean Square Phase Error = 0.37 RAD^2
Threshold SNR in $2B_L$	5.32 db	--	--	$\left\|\frac{S}{N}\right\|_o$ = 27.9 db
Threshold Subcarrier Power	-135.98 dbm	+0.60	-0.28	
Performance Margin	+ 4.94 db	+4.79	-4.92	

E.3 CAPSULE TRANSMITTER AND ANTENNA SYSTEM

It is assumed for the purposes of the integration study that a total transmitter power of 2 watts at 960 mc will be available for the LSPC mission. As yet no tolerances on the transmitter power output have been established. The 2 watts are entered in Table I as 33.02 dbm. The capsule antenna subsystem is an inflated mylar bifilar conical antenna which is fed with a 4-foot microdot cable. This antenna is circularly polarized and possesses the following characteristics. The nominal parameter values for the antenna subsystem and their tolerances are the result of measurements with the exception of the radiation efficiency, which is estimated.

Parameter	Nominal Value	Maximum Value	Minimum Value
Antenna Gain (on axis)	+ 5.5 db	+ 6.0 db	+ 5.0 db
Antenna Gain (at 45° from the axis)	+ 1.9 db	+ 2.5 db	+ 1.3 db
Transmission Line Loss	-2.0 db	-2.2 db	-1.8 db
VSWR	(1.5 :1)	(2.0 :1)	(1:1)
	(-.18 db)	(- .46 db)	(0 db)
Radiation Efficiency	(90%)	(100%)	(80%)
	(- .46 db)	(0 db)	(- .97 db)
Axial Ratio	3.0 db	6.0 db	0.0 db

The effective db loss associated with a VSWR of 1.5:1 is given by the expression

$$\text{db loss} = 10 \log_{10} \frac{\left((\text{VSWR})^2 + 2 (\text{VSWR}) + 1 \right)}{\left(2 (\text{VSWR})^2 + 2 \right)}$$

For a VSWR of 1.5:1 the loss is

$$10 \log_{10} \frac{6.25}{6.5} = -.18 \text{ db}$$

The radiation efficiency is directly convertible into a db loss of

$$\text{db loss} = 10 \text{ Log}_{10} .90 = -.46 \text{ db}$$

The transmission loss associated with ellipitical polarizations, as reflected in the axial ratio parameter, is dependent also on the axial ratio of the receiving antenna polarization. Given an axial ratio for both the transmitting and receiving antenna, a maximum and minimum transmission link loss can be obtained from the curves in Figure 1. Minimum loss occurs when the semimajor axes of the two ellipitical patterns are coincident and maximum loss occurs when the semimajor axes are normally disposed to each other. The axial ratio for the Goldstone Antenna, when using a tracking feed which is diplexed, is given in a JPL memo as being 2.6 db $\pm$ 0.4 db. From the ensemble of intersection points in Figure 1 which correspond to the various nominal and extreme values for both of the axial ratio parameters, it seems reasonable to assign transmission link polarization losses equivalent to transmission efficiences of 90%, 100% and 77% which represent the nominal, maximum and minimum efficiencies, respectively. The db equivalents of these efficiencies are entered in Table I under polarization loss.

The capsule transmission loss entry in Table I includes the lumped effects of line loss, VSWR loss, and radiation efficiency. In all entries of tolerances in Table I the sign convention is adopted as follows:

If a parameter varies in such a way that transmitter power would have to be increased to overcome the effect of this parameter variation on received power, it is entered as a negative tolerance. For example, a VSWR increased from its nominal value of 1.5 to 1 to its extreme value of 2.0:1 results in introducing a negative tolerance of -0.28 db.

The nominal angle between the earth-moon line and the local vertical, to which the antenna is aligned, is taken to be 45°. The combined effects of impact position error and antenna erection error lead to increased tolerances on the antenna pointing loss which result from using the antenna at an angle of 45° from its axis. Without position and erection errors the antenna gain 45° of the axis is expected to be 1.9 $\pm$ 0.6 db.

The rms variation in the angle between the earth-moon line and the antenna axis is, assuming uniform angular distributions of the position and erection error,

$$\Delta\phi = 1/2\sqrt{\rho_1^2 + \rho_2^2}$$ where ρ_1, and ρ_2 are the

rms angular position and erection errors. Assuming a 3σ error in erection of 5 degrees and a 3σ position error of 87 statute miles from both tracking and midcourse errors, the 3σ value of $\Delta\phi$ is 0.06 radian $\cong 3.5°$. Correcting this to db tolerances using the parabolic relationships

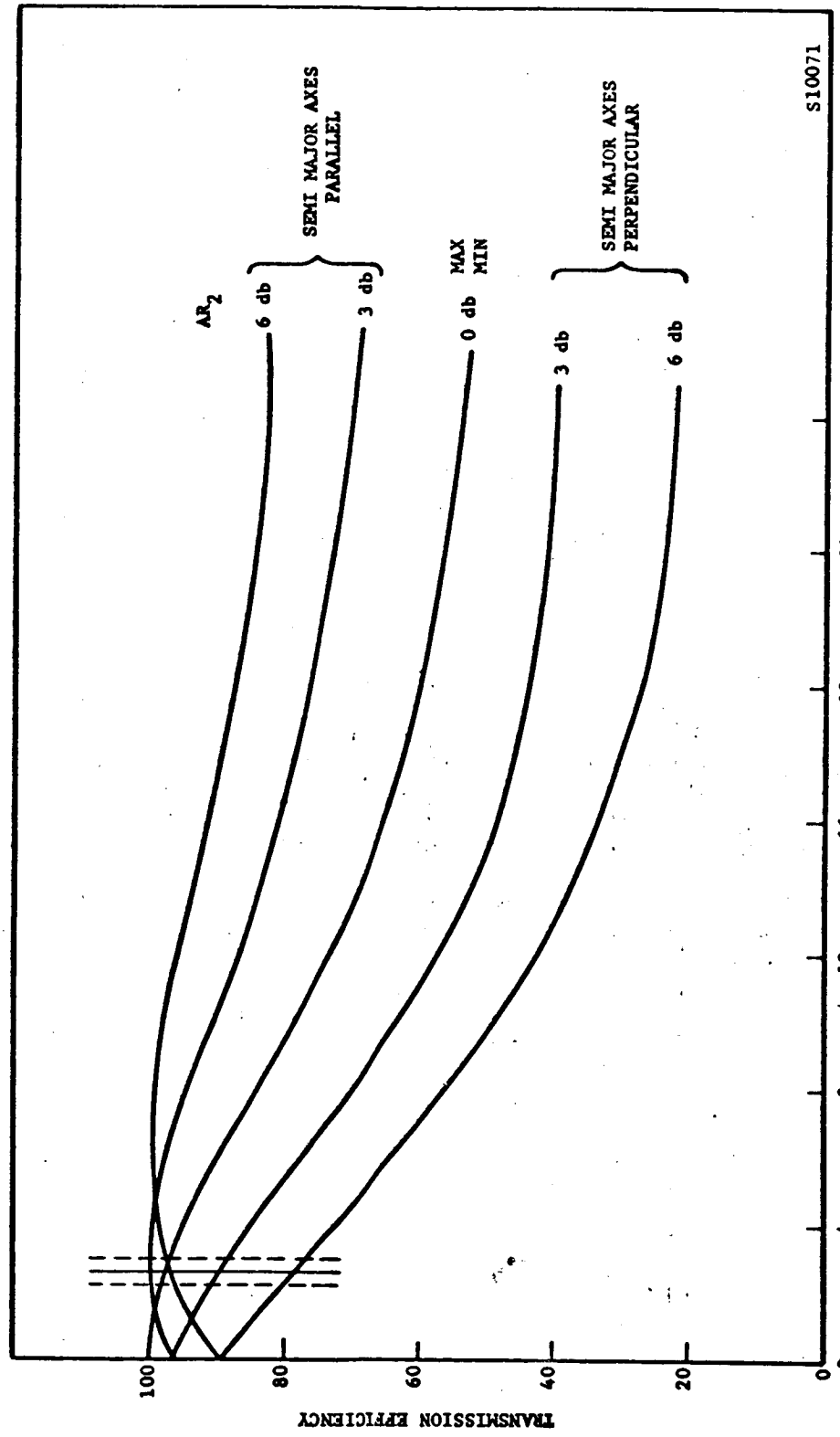

FIGURE 1. TRANSMISSION EFFICIENCY OF TWO ELLIPTICALLY POLARIZED ANTENNAS WITH AXIAL RATIOS A_1 AND A_2, RESPECTIVELY

$$\frac{P_n \text{ (db)}}{P_e \text{ (db)}} = \left(\frac{\phi_e}{\phi_n}\right)^2$$

where P_n and P_e are the nominal and extreme values of power expressed in db and ϕ_n and ϕ_e are the nominal and extreme values of the off-axis angle. Using $P_n = 1.9$ db and $\phi_n = 45^\circ$, the additional tolerances become -.27 db and +.33 db and these must be added to the tolerances on the antenna gain at $\phi = 45^\circ$ to yield the overall tolerance.

The entry for space loss is obtained from the expression L_{FS} (db) = $36.6 + 20 \log_{10} D + 20 \log_{10} f$ where D is the distance in statute miles and f is the frequency in megacycles. The ground antenna gain and ground transmission circuit losses were obtained from JPL-supplied data on the DSIF parameters when the 85-ft reflector is used with a tracking feed and is diplexed to track on 960 mc and transmit on 890 mc.

E.3.1 Receiver Temperature

The effective temperature of the receiver is made up of various contributions from the different sources of loss. In keeping with the idea of using available operational equipment used in its most convenient manner (i.e. accepting something less than a completely optimized transmission link) noise temperatures will be determined for a parametric amplifier using a diplexed antenna with a tracking feed arrangement. The system noise temperature will be referred to the input of the parametric amplifier.

From the JPL data on the DSIF parameters, the antenna temperature is $40^\circ \pm 10^\circ$ K. This temperature is converted into an effective system temperature (i.e. referred to the amplifier input) by the equation

$$\text{Antenna Contribution} = \frac{40^\circ + 10^\circ \text{ K}}{1.162} = 34.4^\circ \text{ K} \pm 8.6^\circ$$

The $\frac{1}{1.162}$ factor arises from the fact that the antenna noise is attenuated by the combined transmission line and diplexer loss of -.65 db = $\frac{1}{1.162}$

The line loss contribution is given by To $(1 - \frac{1}{L})$ where To is the ambient temperature and L is the line loss. Taking To as 290° K and L corresponding to .4 db $\pm$ .1 db we have line loss contribution $= 290^\circ \left(1 - \frac{1}{1 + .23(.4 \pm .1)}\right) =$

$\frac{290\ (.23)\ (.4 \pm 1)}{1.092 \pm .023} = 24.5^\circ\ {}^{+5.96^\circ}_{-6.24^\circ}$.

similarly, the diplexer loss contribution is

Diplexer loss contribution $= 290^\circ \left(1 - \frac{1}{1 + .23\ (.25 \pm .03)}\right) =$

$\frac{290^\circ\ (.23)\ (.25 + .03)}{1 + .23\ (.25 \pm .03)} = 15.75^\circ\ {}^{+\ 1.88^\circ}_{-\ 1.90^\circ}$

Parametric Amplifier Contribution $= 150^\circ\ {}^{+\ 0}_{-\ 20^\circ}$.

Contribution due to pointing antenna at the moon $= \frac{30^\circ \pm 0^\circ}{1.162} = 25.8^\circ \pm 0$

Thus the total system noise temperature is: $250.45^\circ\ {}^{+16.44^\circ}_{-36.74^\circ}$

E.3.2 Carrier Performance

In the interests of facilitating the carrier locking process, a carrier deviation ratio of 1.4 is assumed.

The variation in the deviation ratio due to temperature and voltage variations in the modulating system are taken to be $\pm$ 10 percent. For a δ of 1.4 the relative carrier power is reduced from the total received power in the amount of $J_o^2\ (1.4) = (.567)^2 = .321$. This corresponds to a carrier modulation loss of -4.93 db. The carrier APC noise bandwidth is taken as 20 cps $\pm$ 4 cps which leads to the decibel values shown in Table I. Taking a threshold SNR of 5.6 db in the $2B_{L_o}$ bandwidth, it can be seen that there is a fairly large performance margin in the carrier performance.

E.3.3 Subcarrier Performance

With the assumed deviation ratio of 1.4 the total subcarrier power is reduced from the total received power level in the amount of $2J_1^2\ (1.4) = 2\ (.5419)^2 = .588$. This leads to a modulation loss of -2.31db and yields a total minimum received subcarrier power of -135.68 (including all appropriate accumulated negative tolerance).

With a maximum system temperature of the receiver of 266.9° K the input signal-to-noise ratio in the data bandwidth of 65 cps is $(S/N)_{i\ min}$ = 20.5 db.. The $(S/N)_{i\ min}$ is a parameter used in the phase-look receiver analysis discussed in the next part of this memo which, in conjunction with the total allowable mean square phase error $\sum^2$, determines what the optimum loop bandwidth is and what the minimum output signal-to-noise ratio will be. From the results of the analysis in the next section, the expression for the loop bandwidth B_{LO} in terms of the maximum data frequency f_{max} is given (to a good approximation when $X < 0.5$) by the expression

$$X = \frac{3\pi f_{max}}{2\sqrt{2}\, B_{LO}} \simeq 5/4\ \frac{3\pi}{\sqrt{2}}\ \frac{1}{\left(\frac{S}{N}\right)_{i\ min} \Sigma^2}$$

Using a value of Σ^2 equal to 0.37 rad^2 (the total phase error will be less than $\pm$ 90° for 99 percent of the time) leads to a value of X

$$X = \frac{5}{4}\ \frac{3\pi}{\sqrt{2}}\ \frac{1}{0.37\ (112)} = 0.202$$

This in turn leads to a loop bandwidth

$$2B_{LO} = \frac{3\pi f_{max}}{\sqrt{2}\ (202)} = 2140 \text{ cps}$$

and an output signal-to-noise of

$$\left(\frac{S}{N}\right) = \left(\frac{1}{X^4} + \frac{2}{3X^2} - \frac{1}{5}\right) = 616.1 \text{ or an } \left(\frac{S}{N}\right)_o \text{ of } 27.9 \text{ db.}$$

This minimum value of output S/N is considered as adequate and if the communication link parameters and their tolerances are maintained as shown in Table I the 2-watt transmitter should suffice for the LSPC mission.

Since the $(S/N)_{i\ min}$ is 20.5 db in a bandwidth of f_{max}, the (S/N) in $2B_{LO}$ is 20.5 db - 10 log 10 $\frac{2140}{65}$ = 20.5 db - 15.18 db = 5.37 db.

Under the threshold conditions, with X chosen as 0.202, the mean square noise phase error σ^2_{np} would be

$$\sigma^2_{np} = \frac{\frac{3\pi}{\sqrt{2}}}{\left(\frac{S}{N}\right)_i X} = \frac{\frac{3\pi}{\sqrt{2}}}{(112)(0.202)} = 0.298 \text{ rad}^2$$

Then the signal distortion phase error contribution would be

$$\sigma^2_{sp} = (0.37 - 0.298)\ \text{rad}^2 = 0.072\ \text{rad}^2 \simeq \frac{m_p^2 X^4}{5}$$

or

$$m_p^2 = \frac{0.36}{(0.202)^4} = 216\ \text{rad}^2$$

or

$$m_p^2 = 14.7\ \text{rad}$$

E.4 SURMEC COMMUNICATION LINK ANALYSIS

Applying the above considerations to the SURMEC Capsule, with the recognition that the desired data frequency f_{max} is 150 cps in this case, the additional received subcarrier power needed to maintain the 99% criterion can be determined.

Alternatively, for the same received subcarrier power, the corresponding reduction in "lock probability" can be evaluated, or if transmitter power and "lock probability" are kept fixed, the maximum data frequency can be determined.

In the case of SURMEC the input S/N ratio in the data bandwidth would be

$$(S/N)_{i\ min} = 20.5 - 10 \log_{10} \frac{150\ \text{cps}}{65\ \text{cps}} = 16.36\ \text{db} = 43.2$$

Using the approximation formula for optimum B_{LO} and tentatively keeping the total mean square phase error at the 0.37 rad^2 value (99% criterion)

$$X = \frac{3\pi f_{max}}{2\sqrt{2}\, B_{LO}} \simeq 5/4\ \frac{3\pi}{\sqrt{2}}\ \frac{1}{(S/N)_i\, \Sigma^2} = 0.518$$

Then $$2\, B_{LO} = \frac{3\pi f_{max}}{\sqrt{2}\ X} = 1930\ \text{cps}$$

and $$(S/N)_{i\ min} \simeq \frac{1}{X^4} + \frac{2}{3X^2} - 1/5 \simeq 16.1 = 12.8\ \text{db}$$

The minimum output S/N at the output of the discriminator is consequently below the desired level of 20 db. A value of 20 db is obtained when

$$\Sigma^2 (S/N)_{i\ min} = 25.7$$

Thus, if Σ^2 is kept at 0.37 rad^2, $(S/N)_{i\ min}$ must increase to a value of 69.5. That is, the received subcarrier power must be increased by 2.07 db or the data frequency must be reduced from 150 cps to 93 cps. Alternatively, with the same received subcarrier power the total mean square error Σ^2 must be permitted to increase from 0.37 rad^2 to 0.595 rad^2 if the 150-cps data frequency is retained. This would result in the total phase error being less than $\pm$ 90^o for approximately 95.76% of the time rather than for 99% of the time.

Another alternative to accepting the reduced data frequency capability or "lock probability" discussed above is to consider using a MASER amplifier in conjunction with the parametric amplifier. Using a MASER amplifier reduces the maximum effective system temperature by 106.0^{o}K. This increases the $(S/N)_{i\ min}$ by 2.2 db, which is just enough to permit obtaining an $(S/N)_o$ of 20 db with a two-watt transmitter and a 150-cps data frequency while still using the 99% criterion applied to the total phase error.

E.5 R. F. COMMUNICATION LINK ANALYSIS

E.5.1 Phase Lock Receiver Analysis

The following analysis is concerned with the output signal-to-noise ratio at the output of a phase-lock loop demodulator. This demodulator is taken to be equivalent to the linearized system shown in block diagram form below

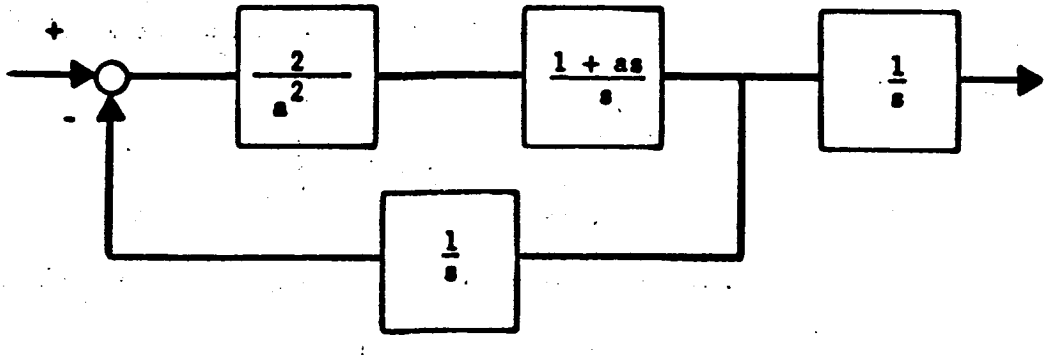

The transfer function for this network is

$$H(s) = \frac{\frac{2}{a^2}\,\frac{1+as}{s^2}}{1+\frac{2}{a^2}\,\frac{1+as}{s^2}} = \frac{(1+as)}{1+as+\frac{a^2s^2}{2}} \qquad (1)$$

The signal input to this network is considered to possess a flat power spectrum over the information bandwidth $-f_{max} \leq f \leq +f_{max}$. The mean square signal distortion at the output of the demodulator is then

$$\sigma_{sp}^2 = \frac{1}{2\pi j}\int_{-j\infty}^{j\infty} \Phi_{sp}(s)\,|1-H(s)|^2\,ds \qquad (2)$$

where $\Phi_{sp}(s)$ is the power density spectum of the signal. If m_p^2 is the mean square phase modulation index, then $\Phi_{sp}(s) = \frac{m_p^2}{2f_{max}}$ rad^2/cps. The mean signal power output S_o^2 is then given by

$$S_o^2 = \frac{1}{2\pi j}\int_{-j\infty}^{j\infty} \Phi_{sp}(s)\,|h(s)|^2\,ds \qquad (3)$$

and the mean square noise output is

$$\sigma_{np}^2 = \frac{1}{2\pi j}\int_{-j\infty}^{j\infty} \Phi_{np}(s)\,|H(s)|\,ds \qquad (4)$$

The output signal-to-noise ratio can be expressed as

$$(S/N)_o = \frac{S_o^2}{\sigma_{np}^2+\sigma_{sp}^2} = \frac{S^2}{\Sigma^2} \quad \text{where } \Sigma^2 = \sigma_{np}^2+\sigma_{sp}^2 \qquad (5)$$

is the total mean square phase error.

Thus,

$$\sigma_{sp}^2 = \frac{1}{2\pi j} \int_{-2\pi j f_{max}}^{2\pi j f_{max}} \frac{m_p^2}{2f_{max}} \frac{\left|\frac{a^2 s^2}{2}\right|^2}{\left|1 + as + \frac{a^2 s^2}{2}\right|^2} ds$$

$$= \frac{m_p^2}{2\pi f_{max}} \int_0^{2\pi f_{max}} \frac{\frac{a^4 \omega^4}{4}}{\left[\left(1 - \frac{a^2 \omega^2}{2}\right)^2 + a^2 \omega^2\right]} d\omega$$

$$= \frac{m_p^2}{2\pi f_{max}} \cdot \frac{\sqrt{2}}{a} \int_0^{\frac{2\pi f_{max} a}{\sqrt{2}}} \left(\frac{y^4}{1 + y^4}\right) dy \qquad (6)$$

where $y = \frac{a\omega}{\sqrt{2}}$

Similarly, $S_o^2 = \frac{1}{2\pi j} \int_{-j\infty}^{j\infty} \frac{m_p^2}{2f_{max}} \frac{|1 + as|^2}{\left|1 + as + \frac{a^2 s^2}{2}\right|^2} ds$

$$S_o^2 = \frac{m_p^2}{2\pi f_{max}} \cdot \frac{\sqrt{2}}{a} \int_0^{\frac{2\pi f_{max} a}{\sqrt{2}}} \frac{(1 + 2y^2)}{(1 + y^4)} dy \qquad (7)$$

The mean sqsure noise output is given, for white noise of constant power spectral density $\Phi_{n(o)}$ as

$$\sigma_{np}^2 = \Phi_n \frac{1}{2\pi j} \int_{-j\infty}^{+j\infty} \frac{|1 + as|^2}{\left|1 + as + \frac{a^2 s^2}{2}\right|} \, ds$$

This can be evaluated by residues to yield the result that

$$\sigma_{np}^2 = \Phi_n \left[\frac{a^2 + a^2/2}{2 \cdot a \cdot a^2/2}\right] = \Phi_n \frac{3}{2a} \tag{8}$$

If the effective noise bandwidth of the phase-lock loop is defined as $2B_L$, then

$$\sigma_{np}^2 = 2B_L \Phi_n = \Phi_n \frac{3}{2a}$$

or

$$a = \frac{3}{4B_L} \tag{9}$$

The output signal-to-noise ratio is now expressible as

$$\left(\frac{S}{N}\right)_o = \frac{S_o^2}{\sigma_{sp}^2 + \sigma_{np}^2} = \frac{1}{\frac{\sigma_{sp}^2}{S_o^2}} \left[1 - \frac{2B_L \Phi_n}{\Sigma^2}\right] \tag{10}$$

$$= G(x) \left[1 - \frac{2B_L\Phi_n}{\Sigma^2}\right] \tag{11}$$

where

$$G(x) = \frac{\int_0^x \left(\frac{1 + 2y^2}{1 + y^4}\right) dy}{\int_0^x \left(\frac{y^4}{1 + y^4}\right) dy} \tag{12}$$

and

$$x = \frac{2\pi f_{max}\, a}{\sqrt{2}} = \frac{3\pi f_{max}}{2\sqrt{2}\, B_L} \tag{13}$$

The integrals in both the numerator and denominator can be evaluated explicitly from Pierce's table of integrals and are of the form

$$\int_0^x \left(\frac{1 + 2y^2}{1 + y^4}\right) dy = \left[3\, v(x) - u(x)\right] \tag{14}$$

and

$$\int_0^x \left(\frac{y^4}{1 + y^4}\right) dy = \left[x - (u(x) + v(x))\right] \tag{15}$$

where

$$u(x) = \frac{1}{4\sqrt{2}} \ln \left(\frac{x^2 + \sqrt{2}\,x + 1}{x^2 - \sqrt{2}\,x + 1} \right) \tag{16}$$

and

$$v(x) = \frac{1}{2\sqrt{2}} \tan^{-1} \frac{\sqrt{2}x}{1 - x^2} \tag{17}$$

Thus, the output signal-to-noise ratio may be expressed as

$$\left(\frac{S}{N}\right)_o = \frac{3v - u}{\left[x - (u + v)\right]} \left(1 - \frac{\Phi_n\, 3\pi f_{max}}{\sqrt{2}\,x\, \sum^2} \right) \tag{18}$$

It can be seen that for a fixed ratio of input signal to input noise in the data bandwidth (which effectively makes the product $\Phi_n f_{max}$ a constant) and a fixed total mean square error $\sum^2$ (which implies the total phase error is less than $\pm 90^\circ$ for same percentage of the time) the $(S/N)_o$ is solely a function of x or equivalently the loop bandwidth B_L. Furthermore, a value of x can be selected which maximizes the $(S/N)_o$.

Analytic manipulation of equation (18) for all values of x is somewhat cumbersome. As it turns out, for $(S/N)_o$ values of interest x is approximately 0.5 or less and, in this region, suitable power series approximations can be obtained for the parameters of interest. A plot of G(x) is shown in Figure 2 along with two plots of

$$\eta(x) = 1 \left(- \frac{\Phi_n\, 3\pi f_{max}}{\sqrt{2}\,x \sum^2} \right) \tag{19}$$

with values of $\frac{\Phi_n f_{max}}{\sum^2}$ corresponding to 0.16 and 0.64.

Φ_n is the resultant spectral density of the phase error where both positive and negative frequencies are integrated to obtain mean-square phase error. When a subcarrier system is used, Φ_n can be determined from a consideration of the mean-square additive noise power density ψ (which is

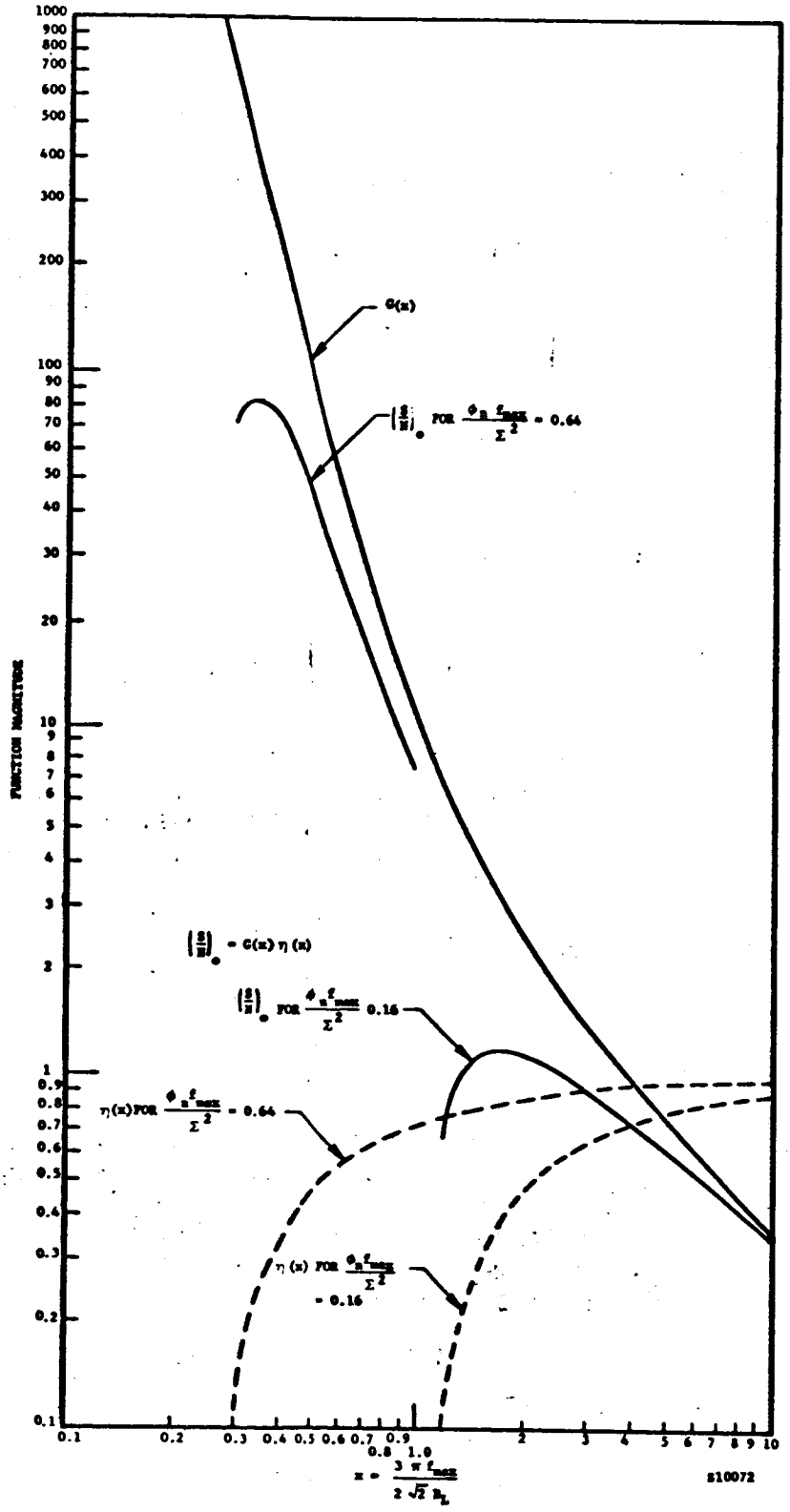

FIGURE 2. COMPONENTS OF OUTPUT SIGNAL-TO-NOISE RATIOS OF PHASE-LOCK DEMODULATOR

constant and equal to a value of $\psi = \frac{KT}{2}$ for all frequencies both positive and negative) and the signal power associated with only one of the four subcarrier components. The additive noise component can be regarded as consisting of two components - a component that is in phase with the subcarrier signal and a component that is in quadrature with this signal. The spectral density of each component is therefore $\frac{KT}{4}$. If the signal is relatively large in magnitude compared to the noise, only the quadrature noise voltage component affects the phase of the signal plus noise resultant and the situation can be represented by the following sketch.

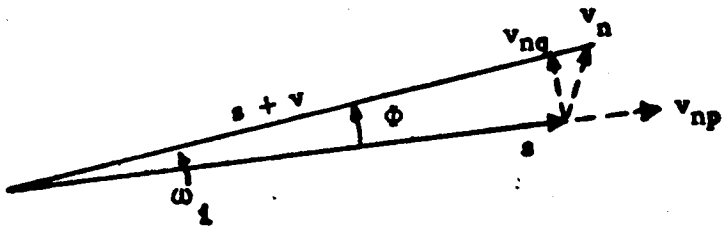

Here S is the rms signal voltage associated with one subcarrier sideband, v_n is the rms additive noise voltage in a 1 cps bandwidth, and Φ is the phase error.

$$\text{For} \quad |S| >> |v_n| \quad \bar{\Phi}^2/\text{cps} \cong \frac{\bar{v}_{nq}^2}{\bar{s}^2} = \frac{\frac{1}{4}KT}{\frac{P_{sc}}{4}} = \frac{KT}{P_{sc}} = \Phi_n \qquad (20)$$

where P_{sc} is the total received subcarrier power. This same result would be obtained if the total received subcarrier power were used, i.e., considered after the frequency folding process of carrier and subcarrier demodulation, since in this case the additive noise spectral density would have to be quadrupled to account for the total bandwidth (at both positive and negative frequencies) surrounding all of the four subcarrier signals. As an example, the curves plotted in Figure 2 for $\frac{\Phi_n f_{max}}{2} = 0.16$ or 0.64 correspond respectively to an input signal to noise (in the data bandwidth of $\left(\frac{S}{N}\right)_1 = \frac{P_{sc}}{KT\, f_{max}} = 25.1 = 14$ db and a total mean square phase error $\sum^2$ of 0.25 rad^2 and 1 rad^2, respectively. That is,

$$\frac{\Phi_n f_{max}}{\Sigma^2} = \frac{1}{\frac{P_{sc}}{KT} \frac{\Sigma^2}{f_{max}}} = \frac{1}{(25.1) \cdot (0.25)} = 0.16$$

The equivalent noise temperature of the system is thus regarded as that which leads to a total noise power contribution of KTB where B is a bandwidth interval only on the positive frequency axis.

Thus, equation (18) can be expressed in terms of an input signal-to-noise ratio $(S/N)_i$ over the data bandwidth

$$\left(\frac{S}{N}\right)_o = \frac{(3v - u)}{\left[x - (v + u)\right]} \left(1 - \frac{\frac{3\pi}{\sqrt{2}} \frac{1}{\Sigma^2}}{\left(\frac{S}{N}\right)_i x}\right) \qquad (21)$$

where

$$\left(\frac{S}{N}\right)_i = \frac{P_{sc}}{KT f_{max}} \qquad (22)$$

E.5.2 Series Expansions of u and v

Since $(S/N)_o \leq G(x)$ for all x and since the area of primary interest is where $(S/N_o \geq 100$ (i.e., 20 db), it is reasonable to expect on the basis of the plot of G(x) in Figure 2 that the most useful range of x is $x \leq 0.5$. For this range of x values it is convenient to consider Taylor expansions of the functions u and v. In this way, a more tractable expression for the $(S/N)_o$ is obtained and optimization is easier. For x in the neighborhood of zero, Taylor's expansion of a function f(x) is

$$f(x) = f(o) + f'(o)x + f''(o)\frac{x^2}{2!} + f'''(o)\frac{x^3}{3!} + .. + f^n\frac{x^n}{n!}$$

Applying this to the function

$$u(x) = \frac{1}{4\sqrt{2}} \ln\left(\frac{x^2 + 2x + 1}{x^2 - 2x + 1}\right)$$

yields

$$u(x) = \frac{1}{2}x - \frac{x^3}{3!} - 12\frac{x^5}{5!} \times 120\ \frac{x^7}{7!}$$

$$= \frac{1}{2}x\left(1 - \frac{x^2}{3} - \frac{x^4}{5} + \frac{x^6}{21}\right) \qquad (23)$$

Applying this to the function $v(x) = \frac{1}{2\sqrt{2}} \tan^{-1}\frac{\sqrt{2x}}{1 - x^2}$

yields the series approximation

$$v(x) \simeq \frac{1}{2}x + \frac{x^3}{3!} - \frac{12x^5}{5!} - \frac{144x^7}{7!}$$

$$= \frac{1}{2}x\left(1 + \frac{x^2}{3} - \frac{x^4}{5} - \frac{2x^6}{35} + ..\right) \qquad (24)$$

Thus

$$x - (v + u) \simeq \frac{x^5}{5} + \frac{x^7}{210} \simeq \frac{x^5}{5} \text{ for } x < 0.5$$

and

$$3v - u = \frac{3}{2}x + \frac{x^3}{2} - \frac{3x^5}{10} - \frac{3}{35}x^7 - \frac{1}{2}x + \frac{x^3}{6} + \frac{x^5}{10} - \frac{x^6}{42}$$

or

$$3v - u \cong x\left[1 + \frac{2}{3}x^2 - x^4/5\right]$$

Hence

$$\left(\frac{S}{N}\right)_o = \frac{5(1 + 2/3x^2 - \frac{x^4}{5})}{x^4}\left(1 - \frac{\frac{3\pi}{\sqrt{2}}}{\left(\frac{S}{N}\right)_i \sum^2 x}\right) \tag{25}$$

The maximum value of $\left(\frac{S}{N}\right)_o$ for a given $\left(\frac{S}{N}\right)_i \sum^2$ product can be approximately obtained by ignoring the x^2 and x^4 terms in the numerator of equation (25) In this case

$$\frac{d}{dx}\left(\frac{S}{N}\right)_o = -\frac{20}{x^5} + \frac{25}{x^6}\,\frac{\frac{3\pi}{\sqrt{2}}}{\left(\frac{S}{N}\right)_i \sum^2} = 0$$

or

$$x \cong 5/4\,\frac{3\pi}{\sqrt{2}}\,\frac{1}{\left(\frac{S}{N}\right)_i \sum^2} \tag{26}$$

Then with x given by equation (26)

$$\left(\frac{S}{N}\right)_{oT} = \left[\frac{1}{x^4} + \frac{2}{3x^2} - \frac{1}{5}\right] \tag{27}$$

The procedure which appears most reasonable is to optimize the $(S/N)_o$ by selection of x, i.e., the loop bandwidth, when the input signal-to-noise ratio $(S/N)_i$ is the minimum it will be. That is, when all the

accumulative negative tolerances in the communication link are used in conjunction with the nominal system gains. Then the nominal performance will be improved over this threshold value in the approximate ratio of

$$\frac{(S/N)_{oN}}{(S/N)_{oT}} = \frac{1 - \frac{4(S/N)_{i\ min}}{5(S/N)_{i\ nominal}}}{1 - \frac{4}{5}} = 5\left[1 - \frac{4}{5}\frac{(S/N)_{i\ min}}{(S/N)_{i\ nominal}}\right] \quad (28)$$

Once a value of x has been chosen on the basis of $(S/N)_{i\ min}$ and the allowable or desired total mean square error $\sum^2$, the mean square noise contribution to $\sum^2$ can be computed as $2B_L KT$ where T is the effective receiving system temperature. The modulation index is then constrained to be that the mean square signal distortion component σ_{sp}^2 is such that from equation (6)

$$\sigma_{sp}^2 = \frac{m_p^2\, 2\sqrt{2\,B_L}}{3\pi f_{max}}\left[x - (u + v)\right] = \sum^2 - 2B_L\Phi_n$$

or

$$\sigma_{sp}^2 \simeq \frac{m_p^2}{x}\left[\frac{x^5}{5}\right] = \sum^2 - 2B_L\Phi_n$$

or

$$m_p = \frac{1}{x^2}\sqrt{5\,(\sum^2 - 2B_L\Phi_n)} \quad (29)$$